Plasma treated, Plasma Polymerized And Spin Coated PMMA Thin Film Based Humidity Sensors -A Comparative Study

A Thesis Submitted To
University Of Pune

For The Degree Of

Doctor of Philosophy (Ph.D)
In
Electronic Science

By
Deshpande Jagdish Dattatraya

Under The Guidance Of

Dr. S.W.Gosavi **(CO-GUIDE)**

Dr. S. A. Gangal **(GUIDE)**

Department Of Electronic Science
University Of Pune
Pune – 411007

September 2011

Plasma treated, Plasma Polymerized And Spin Coated PMMA Thin Film Based Humidity Sensors -A Comparative Study

A Thesis Submitted To
University Of Pune

For The Degree Of

Doctor of Philosophy (Ph.D)
In
Electronic Science

By
Deshpande Jagdish Dattatraya

Under The Guidance Of

Dr. S.W.Gosavi **(CO-GUIDE)**

Dr. S. A. Gangal **(GUIDE)**

Department Of Electronic Science
University Of Pune
Pune – 411007

September 2011

CERTIFICATE

This is to certify that the work incorporated in the present thesis entitled **Plasma treated, Plasma Polymerized And Spin Coated PMMA Thin Film Based Humidity Sensors -A Comparative Study.** submitted by **Deshpande Jagdish Dattatraya** was carried out under our guidance at Department of Electronic Science, University of Pune. The work in this thesis is original and has not been previously reported or submitted for the award of any degree, diploma, fellowship or any other university or institution of higher learning. Any relevant material that has been obtained from the other sources has been duly acknowledged in this thesis.

Dr. S. W. Gosavi
(Research Co Guide)
Dept. of Physics
University of Pune
Pune – 411007

Dr. S. A. Gangal
(Research Guide)
Dept.of Electronic Science
University of Pune
Pune - 411007

Place: PUNE

SELF DECLARATION

I hereby declare that the thesis entitled, **Plasma treated, Plasma Polymerized And Spin Coated PMMA Thin Film Based Humidity Sensors -A Comparative Study.** submitted by me for the degree of Doctorate of Philosophy is the record of the work under the guidance of Dr. (Ms) S. A. Gangal, Department of Electronic Science, University of Pune, Pune and Dr. S. W. Gosavi, Department of Physics, University of Pune, Pune. The work in this thesis is original and has not been previously reported or submitted for the award of any degree, diploma, fellowship or any other university or institution of higher learning. I further declare that the material that obtained from the other sources has been duly acknowledged in this thesis.

Jagdish Deshpande

I, very humbly, dedicate this work to every member of my family.

Acknowledgement

This thesis would not have been possible without the blessings of the Almighty.

It gives me immense pleasure to express my deep gratitude, sincere thankfulness and esteemed regards to Dr. (Ms.) S. A. Gangal, Chair Professor, ISRO, Department of Electronic Science, Pune University, Pune for her scholarly, timely, valuable guidance, continuous encouragement and motivation given to me during the entire progress of this work.

I would like to extend my immense sense of gratitude towards my research co-guide Dr. Suresh Gosavi for guiding me in my research work under his guidance .He was always there to extend his help when needed.

I am also grateful and thankful to Prof. Dr. A. D. Shaligram, Head,Department of Electronic Science, Pune University, Pune for making the laboratory facilities available to me and for creating congenial atmosphere needed for my work.

I am duly thankful to Prof. S. V. Ghaisas, Dr. (Mrs.) D. C. Gharpure, Dr. R. N. Karekar, Dr. R. C. Aiyer for their timely and valuable suggestions. I am also very much thankful to the technical and office staff of the Department of Electronic Science for their kind cooperation.

Since the work presented has been carried out during the tenure of the teacher fellowship awarded to me by the University Grants Commission; WRO, Pune, I offer my sincere thanks also to them.

I am greatly obliged to the Chairman, Secretary and Members of Anekant Education Society, Baramati, the Principal, vice principals and all teaching-non teaching staff members of Tuljaram Chaturchand College, Baramati for their continuous inspiration and motivation.

I also appreciate the help and cooperation that I received from my lab mates and friends Dhananjay, Aditee, Ashok, Abhijeet, Abhay, Bhoopesh, Atul, Sandip, Govind, Ghanasham, Poonam, Madhushree, Abhishek.

I can never forget the sense of tolerance and great patience shown by my loving wife Deepa, my son Devdatta and my daughter Rama without which the completion of this work would have been impossible.

I owe a lot to my family friends/ relatives for their endless support, love and belief over long time.

Let me also thank all those who helped me in one way or the other, directly or indirectly in the completion of my work.

Jagdish Deshpande

Contents

Chapter-II: Experimental Techniques (54-67)

Abstract

The work on comparative study of spin coated, plasma treated and plasma polymerized based capacitive / resistive type humidity sensor is reported in this thesis. PolyMethyl Methacrylate (PMMA) is selected for the study.

The thesis is divided into **5 chapters**.

Chapter 1 introduces the topic of research with necessary background. It also gives the review of Humidity Sensors which consist of basic definitions of humidity (Absolute Humidity, Specific Humidity and Relative Humidity), methods for creating humidity (Use of saturated salts, Divided Flow method, Two Pressure Method, Two Temperature Method etc.), humidity sensing methods (resistive /capacitive) and sensor fabrication technologies (thick film, thin film, dip coating, spin coating etc.).

Ceramic or polymeric materials are used for humidity sensing. Polymer material PMMA was selected for study. Review of the work reported in the literature on relevant topics is carried out and presented. The material was deposited on glass/silicon/glass epoxy (containing interdigited electrodes) substrates using spin coating and plasma polymerization process. The spin coated films were also treated by plasma. These three types of deposited materials were studied for humidity sensing and their performances were compared. Aim of the work and objectives are spelt out at the end of the chapter.

Chapter 2 describes the different experiments carried out for deposition of material (spin coating, plasma polymerization and plasma treatment). Thicknesses of the films were measured by gravimetric method or taly step method. Structural characterization of the material is done by using FTIR and morphological observations were done with SEM. Humidity response of the films is taken using two methods - continuous RH response (resistance measurement) and static step RH response (capacitance measurement). Variation of optical parameters, especially transmission, with humidity was studied using the home made system. Sensor parameters such as sensitivity, response time and recovery time were measured.

In **Chapter 3** results obtained on the humidity response (sensitivity, response time and recovery time) of the spin coated, plasma treated and plasma polymerized thin films of PMMA are given and discussed in the light of basic theory and the results reported in the literature. The response is measured in terms of change in capacitance as a function of humidity.

Spin coated PMMA films of various thicknesses are reported. Spinning speed and viscosity (concentration) of PMMA solution were varied for obtaining films of various thicknesses. FTIR of the deposited films was taken to confirm PMMA deposition. Response time and recovery time were determined for some of the films. The obtained variation in humidity response is discussed on the basis of structure of material and /or basic structure of the sensing device.

Chemical structure of the film has an effect on humidity characteristic of the films especially sensitivity and hysteresis. Attempt was made to modify the structure of the film by

plasma treatment on the surface of the spin coated films. Chapter 3 also describes the results and discussion on the plasma treatment of the spin coated films. Argon gas was used for the treatment. RF power and treatment time were varied. Changes in the structure of the films were found out using FTIR and SEM techniques.

Plasma polymerization is another method of modifying the structure of the film. The effect of change in structure on the sensing characteristics is also studied and reported in this thesis. The plasma polymerization was carried out in homemade system. Thicknesses of the films were measured using taly step method. In this method MMA monomer was used for deposition. The degree of polymerization can be changed by changing the deposition parameters such as gas pressure, monomer flow rate, argon gas flow rate, deposition time and RF power. These parameters were varied to get films of different structure. FTIR spectra were taken to determine the structure of the films. These films were then used to determine their sensitivity, response and recovery time. The results obtained are compared amongst themselves and also with the ones available in the literature.

Chapter 4 describes optical response study of PMMA to humidity. For this study films were obtained by drop casting and spin coating deposition methods. Thicknesses of the films were measured using gravimetric method. The films obtained were used for optical response study. The results on humidity response are given and discussed. It also states the concluding remarks.

Chapter 5 summarizes the work done and proposes the future plans.

List of Figures

Chapter I

Theoretical background and Literature Survey

1.0 Introduction

Humidity sensors have gained increasing applications in industrial processing and environmental control [1, 2, and 3]. For manufacturing highly sophisticated integrated circuits in semiconductor industry, humidity or moisture levels are constantly monitored. There are many domestic applications, such as intelligent control of the living environment in buildings, cooking control for microwave ovens, intelligent control of laundry etc. In automobile industry, humidity sensors are used in rear window defoggers and motor assembly lines. In medical field, humidity sensors are used in respiratory equipment, sterilizers, incubators, pharmaceutical processing, and biological products. In agriculture, humidity sensors are used for green-house air-conditioning, plantation protection (dew prevention), soil moisture monitoring, and cereal storage. In general industry, humidity sensors are used for humidity control in chemical gas purification, dryers, ovens, film desiccation, paper and textile production, and food processing. Other fields of interest are meteorological services, civil engineering and many more. In all these applications there is a strong need for reliable, accurate and low-cost humidity sensors, especially for low relative humidity (RH) conditions.

There are many methods/principles used to measure humidity [4, 5, 6], ranging from mechanical devices, wet-and-dry bulb hygrometry, chemical color change systems, optical fibre systems, dew point hygrometry, infrared absorption and LiCl cell, resonant frequency, thermal conductivity, surface acoustic wave (SAW) and electrical impedance change. As far as electrical impedance change sensors are concerned, which is the topic of this thesis, there are two types of - capacitive type and resistive type.

Resistive-type sensors rely on a change of the electrical resistance of a hygroscopic medium such as a polymer film, sintered ceramic film, salt or treated substrate. Resistive-type sensors exhibit a logarithmic response to humidity (typically 1 kΩ — 10 MΩ between 90 and 10%RH) and require sophisticated electronics to interpret. In addition, resistive-type sensors do not respond well below 20%RH. However, they offer good interchangeability and are generally cheaper to manufacture than capacitive-type sensors.

Capacitive-type humidity sensors rely on a change in permittivity (e) of a ceramic or polymer dielectric with relative humidity. Capacitive-type sensors can be used in aggressive

environments such as the chlorinated air in swimming pools or ammonia present in livestock facilities. Capacitive-type sensors are more expensive to manufacture than resistive type sensors. It is also known that output of a capacitive-type humidity sensor gradually increases with long-term use in a hot and humid atmosphere. However, capacitive type sensors have several key advantages over resistive-type sensors: they exhibit a linear response to humidity, require less complex electronics to interpret and can operate over a wider RH range. The measurement of capacitance is the preferred method, since this property is less influenced by other gases and vapors.

The constructive design of a good humidity sensor is a rather complicated topic because high performance humidity sensors claim many requirements, including linear response, high sensitivity, fast response time, chemical and physical stability, wide operating humidity range, low cost, low hysteresis, and good resistance to chemical agents [5, 7].

A wide variety of ceramic, polymeric and composite sensors are being produced to serve the applications of humidity sensing. Each of these types of sensors however, has limitations, and new sensor concepts continue to emerge. Ceramic sensors [8] are based on adsorption of water molecules in the pores and grain boundaries of porous semiconducting materials such as certain modified spinels or alumina. The internal surface conduction increases with humidity. However, the internal surfaces can become semi permanently changed during prolonged exposure to humid atmosphere or contaminants such as oil vapor or smoke. An internal heater is required to periodically regenerate ceramic sensor and recover the humidity-sensitive properties that characterize the virgin sensor. This adds to complexity and cost. Devices without heaters are useful in low humidity applications or reasonably clean environments and some may require recalibration.

Polymer based humidity sensors present many advantages such as low cost, flexibility and easy processability [5,7]. The resistive-type sensors are fabricated with polymer electrolytes or polymer–salt complexes, while the capacitive-type with hydrophobic polymers. Some polymer–salt complexes have been reported to work as humidity sensors. Typical examples are poly (propargyl alcohol) doped with sulfuric acid, poly (*p*diethynylbenzene- co-propargyl alcohol) doped with iron trichloride and poly(2-acrylamido-2-methylpropane sulfonic acid) doped with alkali salts. It is also reported that the doping of nanometer-size BaTiO3 with

Na_2CO_3 and NaH_2PO_4 can reduce the hysteresis in the RH-dependent impedance characteristics.

In polymer film capacitive-type sensors, the sensing film is often thin (5–25 μm) and produced by casting or extrusion methods [4]. Polymers such as polyimide, cellulose acetate butyrate (CAB), polymethyl methacrylate (PMMA) and polyethylene terephthalate (PET) are some of the materials employed in capacitive-type RH sensors . Poly(methyl methacrylate) (PMMA) is a promising candidate for polymeric sensors due to its processability and mechanical stability. However, water sorption experiments of PMMA revealed that the hydrophilic property of the carbonyl groups contained was not enough for sorption of water molecules.

Different types of polymers play an important role in optical sensors categorized as inorganic and organic e.g. poly(vinyl chloride) (PVC), poly(tetrafluoro ethylene) (PTFE), nafion, nylon, agarose, sol–gels, etc [3]. Conducting polymers are also in use as humidity sensors. Polyaniline is unique among the known conducting polymers because its conductivity is controlled by the doping levels of oxidation and protons. Oxidation states of polyaniline, whose electrical properties are sensitive to water, provide a basis for potential applications in sensors for humidity control. The aqueous environment changes the conductivity due to two reasons:

1. Adsorbed water molecules dissociate at imine nitrogen centers.
2. Positive charge migrates through the polymer.

An earlier study of this problem indicated that one of origins of this drift phenomenon was an irreversible increase in volume of the sensing polymer, presumably caused by swelling of the polymer in a hot and humid atmosphere [6]. The result suggests that the prevention of swelling in the sensing polymer is important in the preparation of stable capacitive-type humidity sensors. Cross-linking the polymer and formation of a rigid film are supposed to be effective for preventing such swelling phenomenon.

Plasma-deposited films have attracted increasing interest as materials for passivation, adhesion promotion, barrier coatings, optical waveguides, and relative- humidity (RH) sensing applications [9]. Plasma deposition of films provides several advantages over the commonly used technique of casting films from resins. Film properties can be varied by adjusting the ratio of feed gases. Also, monomer gases that do not contain reactive sites for polymerization can be polymerized by the production of active species in the plasma. Material properties can also be controlled by adjusting the plasma-processing parameters such as reactor power and pressure.

Both Thin and thick film technologies are used for fabrication of sensors. The benefits of using thick-film technology for a humidity sensor are its inherent advantages of ruggedness and cost, while thin-film sensors offer smaller size and increased sensitivity. Although there are numerous thin-film polymer-based humidity sensors described in the literature and several low-cost commercially available humidity sensors, there are not many reports on comparison of performance. Studies of water uptake in polyimide film using a surface acoustic wave (SAW) sensor have demonstrated the ability of the SAW sensor to detect small changes in water uptake in polyimide. Therefore, the SAW sensor provides an alternative sensor configuration and may also yield information that could be useful for the optimization of a humidity sensor designed for low RH.

Present thesis concentrates on the comparative study of Plasma treated, Plasma Polymerized and Spin Coated PMMA Thin Film Based Humidity Sensors and their performance comparison.

1.1 Basic definitions of humidity [10, 11]

Humidity is a measure of the amount of water vapor dissolved in air (excluding any liquid water or ice falling through the air). The amount of water vapor present in atmosphere varies with time and location. The level of moisture present in the atmospheric air is known as 'Humidity' and specified by number of quantities such as absolute humidity, relative humidity, specific humidity, etc. The definitions for all are given as follows-

1.1.1 Absolute humidity [10,11]

The quantity of water in a particular volume of air at constants temperature is known as absolute humidity. The most common units are grams per cubic meter.

More technically: the mass of water vapor (m_w) per cubic meter of air and (Va) is termed as absolute humidity as given in equation 1

$$AH = \frac{mw}{Va} \quad \ldots\ldots\ldots\ldots\ldots (1)$$

The absolute humidity changes with change in air pressure which leads to problems in calculations where temperatures can vary considerably. Hence , absolute humidity

is generally defined as mass of water vapor per unit mass of dry air, also known as the ‘ mass mixing ratio’ which is much more rigorous for heat and mass balance calculations.

1.1.2 Specific humidity [10,11]

Specific humidity (SH) is a ratio of mass of water vapor to mass of air (including water vapor and dry air) in a particular volume. Specific humidity (equation 2) is expressed as a ratio of kilogram of water vapor (m_w) per kilogram of mixtures ($m_t=m_d+m_w$)

$$SH = \frac{mw}{md+mw} = \frac{mw}{mt} \text{.....(2)}$$

Where,

m_d → mass of dry air(kg)

m_w → mass of water vapor(kg)

m_t → mixture of dry air and water vapor(kg)

1.1.3. Relative humidity [10,11]

Relative humidity (RH) is the ratio of partial pressure of water vapor in a gaseous mixture of air and water vapor to saturated vapor pressure of water at a given temperature. Relative humidity is expressed as the percentage and is calculated by using equation 3:

$$RH=\frac{E(T1)}{E(T2)}\times 100\% \text{.....(3)}$$

Where,

$E(T_1)$- saturated vapor pressure at temperature T1

$E(T_2)$- saturated vapor pressure at temperature T2

RH - Relative humidity of the gas mixture

Relative humidity depends on two factors: the amount of moisture available and the temperature. A change in relative humidity takes place either by adding water vapor available through evaporation or by changing surrounding temperature while holding the water vapor constant.

1.2 Methods for creating humidity:

Humidity sensitive materials have to be subjected to a number of known relative humidity values over the range of 0-100% RH at the given temperature of measurement in order to measure their response and to calibrate them. Hygrometers are used in many fields hence it is

essential to calibrate them for standard humid atmosphere. There are some useful methods to produce relative humidity. Four main methods as described below are used for producing humid atmosphere with varying relative humidity values.

a) Use of saturated salts
b) Divided flow method
c) Two pressure method
d) Two temperature method

1.2.1 Use of saturated salts: [10,11]

Large number of salts such as NaCl, P_2O_5, $(NH_4)_2SO_4$, H_2SO_4, KOH, KCl, LiCl etc. are used for producing relative humidity. These salts are used to produce super saturated solutions by dissolving them in water. The produced mixture is kept in an air tight chamber due to which at different temperatures, for different salts, the equilibrium vapor pressure of water in the chamber varies resulting in different relative humidity values. An air tight chamber is beneficial as the system is very sensitive to the changes in temperature for this the chamber must be thermally isolated from its surrounding. Normally a vertical gradient of water vapor pressure will be present in such a system. Circulating fans are introduced outside the chamber to help to eliminate the pressure gradient and to reduce the time required for equilibrium conditions. The drawbacks of this system are the time required for equilibrium is very long (number of hours or days also) and presence of salts may lead to deterioration of the sensor due to corrosion. The most common example is H_2SO_4 which is avoided in relative humidity control process.

1.2.2 Divided flow method: [10,11]

As suggested by the name the division of flow is useful for measuring relative humidity. An air or nitrogen is used as a carrier gas. Dry and saturated air/N_2 at constant temperature is mixed in different proportions using proportioning values to obtain different values of relative humidity. If X is the volume fraction of gas passing through the saturator or the saturated air then relative humidity is calculated using equation 4,

$$RH = X \times 100\% \quad \ldots\ldots(4)$$

The accuracy of the system depends on the accuracy of designing of the proportioning value or the flow meters or the flow controllers. Only fixed values of relative humidity are possible. The method is quite popular owing to the fastness in varying relative humidity.

1.2.3 Two pressure method: [10,11]

Weaver [12] was the first investigator to use the principle of two pressure method which depends on the assumptions that the water vapor pressure in gas mixture remains the specified fraction of the total pressure when the total pressure changes. For a real 'air-water' mixture a small correction is required at low humidity.

The relative humidity calculation is done by equation 5,

$$\%RH = \frac{E1}{E2} \times 100 = \frac{P1}{P2} \times 100 \ldots\ldots\ldots (5)$$

Where,

P_1-low water vapor pressure

P_2-high water vapor pressure

E_1-saturated water vapor pressure at P_1

E_2-saturated water vapor pressure at P_2

The relation between water vapor and saturated water vapor pressure is given by equation 6,

$$\frac{E1}{P1} = \frac{E2}{P2} \ldots\ldots\ldots\ldots\ldots (6)$$

The advantage of the method is that the relative humidity can be changed faster than the other methods. For example in the two pressure generator, the time required to reach steady state conditions at 20℃ is 30 minutes.

1.2.4 Two temperature method [13,14]

In the 'Two Temperature method' air is saturated with water vapor at lower temperature (T_1) and then heated to required temperature (T_2) so that by varying T_1, different humidity conditions can be obtained. The relative humidity can be calculated with the help of equation 3 (section 1.1.3)

Many researchers tried to improve this method. C.L. cutting [15] gives a simple system which can be used for calibration of small sensors. The time required for steady, stable conditions to be achieved in this type of system is of the order of one hour at room temperatures.

1.3 Principles of Humidity Measurements

Humidity can be measured using a variety of principles. The principles and the corresponding operating mechanism are given in Table-1.2. The selection of the measurement principle is dependent on the material chosen and the application concerned.

Table-1.1: Principles of Humidity measurements

Principle	**Operating mechanism**
Capacitance	Dielectric constant of material varies with H_2O absorbed
Coulometric	Electrolyte is formed by absorption (P_2O_5+H_2O); dc potential dissociates H_2O. Current level is proportional to the moisture content.
Dew point	Temperature corresponding to condensation-evaporation equilibrium at a cooled surface; varies with H_2O.
Gravimetric	A volume of moist air is exposed to a drying agent, subsequently weighed.
Hygroscopic	Length of the fiber varies with H_2O.
Infrared	Absorption at 1.5 to 1.93 μm; split beam to compare sample cell and reference.
Microwave	Attenuation of radiation with H_2O.
Piezoelectric	Hygroscopic coating changes crystal frequency.
RF-Sensor	Radio-frequency current due to dielectric change is a function of H_2O.
Resistance	Conductivity depends on H_2O absorbed.
Saturated salt (LiCl)	Self-heating to temperature of condensation-evaporation equilibrium measures dew point.
Thermal conductivity	Self-heated thermistors in bridge circuit; current imbalance due to difference in heat dissipation between atmosphere and reference cells.

In the present work capacitive type of sensors will be studied. Polymethyl Methacrylate, a hydrophobic polymer is used as a humidity sensitive material.

1.4 Polymers and their Characteristics:

Because of their versatility, their unique properties and ease of processing and fabrication, polymeric materials have found applications as plastics, elastomers, fibers, protective coatings and adhesives. In parallel with these well-established applications, new needs have emerged from technologies, which are still growing, such as microelectronics, optoelectronics, biotechnology and sensor applications.

Progress in organic and polymer chemistry has made possible the synthetic modification of polymer structure and the improvement in polymer properties to fit the desired needs [16].

1.4.1 Overview of Structures of Polymers [17] :

Polymers are large molecules with many (poly) repeatable units (mers). Polymer is a macromolecule. When a polymer contains only small number of structural units it usually is called as an oligomer. Three different types of polymers are shown in Fig-(1.3).

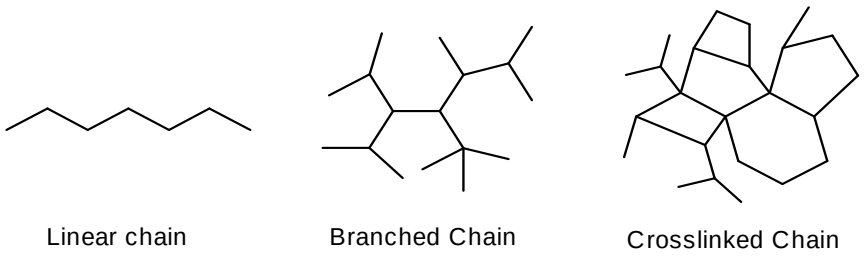

Fig-1.1: Types of Polymers

A linear polymer is a polymer in which the units in each molecule are linked together in a chain-like structure. A branched polymer is a polymer composed of molecules having a branched structure. A cross linked polymer is a polymer composed of macromolecules containing a three-dimensional network structures and for this reason are insoluble. A cross linked product, which is swollen by solvent, is called as a Gel. Cross linked polymers contain several network defects such as unreacted functionality, or chain ends, closed loops, entanglements. These defects influence the elastic properties of the polymer networks.

The polymer shape is considered to have two aspects: The polymeric configuration, which is the polymer shape formed by primary bonding and polymeric conformation, which is the polymer shape due to rotation around primary valence bonds.

1.4.2 The Glass Transition Temperature [17]:

The specific volume of (in mm/g or m^3/kg) an amorphous polymer like PMMA changes linearly with increasing temperature (see Fig-1.2) up to the transition region where a change of the slope occurs (steeper gradient). At certain temperature the rate of change of volume increases and a discontinuity is formed in the specific volume curve. This is known as glass transition temperature (T_g) and is usually defined as the point at which the tangents of the two curves intersect.

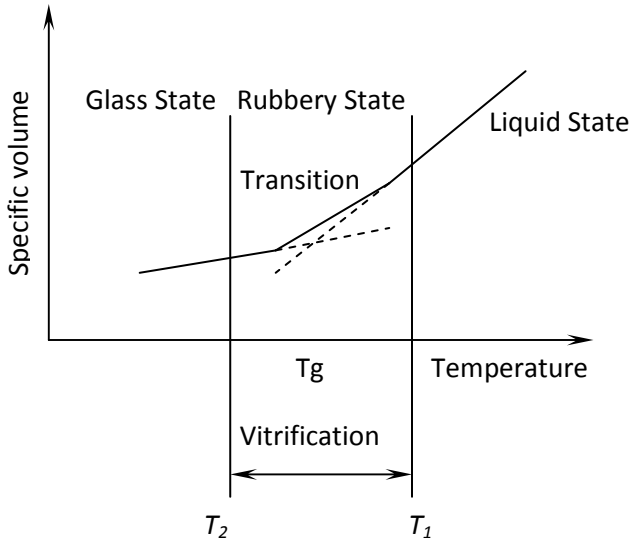

Fig-1.2: The specific volume of polymers as a function of temperature in the transition range

Below T_g, chain segments are frozen in fixed positions in a disordered quasi lattice. Some molecular movements of chain segments take place in the form of vibrations about a fixed position.

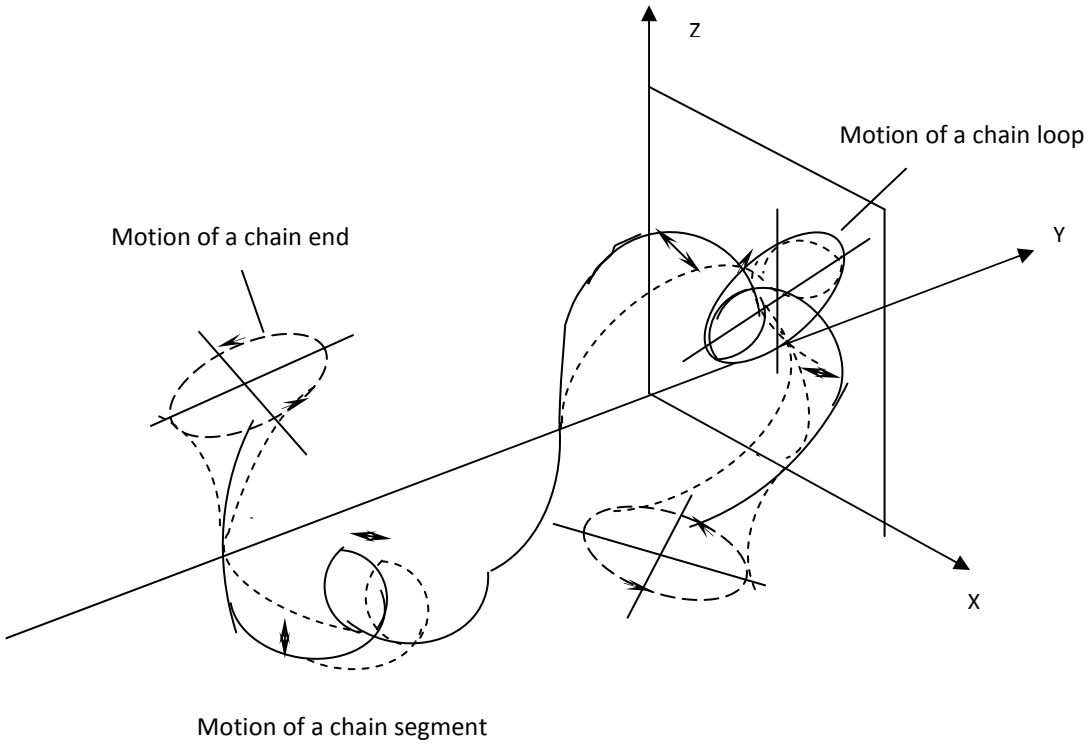

Fig-1.3: Motion of chain loops and chain segments in the transition zone

With increasing temperature, the amplitude of segmental vibrations increases. In the transition state, chain segments have sufficient energy to overcome the secondary intermolecular bonding force. Chain segments or chain loops may perform rotational and transitional motions (see Fig-1.3) which are called as segmental motion or short range diffusional motion.

Chain flexibility and intermolecular packing distances (chain stiffness), bulkiness, flexibility of side chain, and polarity of the chain are major parameters influencing T_g. Chain flexibility is determined by the ease with which rotation occurs about primary valence bonds. A rotation involves an energy barrier that is of the same order as the molecular cohesive forces (1-5 kcal/mol). The decrease in chain flexibility increases the T_g temperatures by increasing steric hindrance. Steric hindrance is dependent on the size, shape and constitution of the backbone group. Rigid and bulky side groups decrease the flexibility of the chain (steric hindrance is increased) and the value of the T_g is reduced. Introducing flexible side groups results in an increase of intermolecular distances; consequently free volume predominates and the T_g is lowered. Other factors influencing T_g are: crystallinity, tacticity, molecular weight, branching and intermolecular bonds.

All polymers exhibit a glass transition at a particular temperature or range of temperatures. Typical glass transition temperatures of various polymers are given in Table-1.1. The value of T_g depends on the experimental time scale and the method of measurement. The values of T_g reported in the literature for any particular polymer however, may vary from 10 to 30 ^oC [17].

Table-1.1: Glass Transition Temperatures (T_g) of some Polymers

Polymer	**T_g (^oC)**
Poly (ethylene)	-80
Poly (isopropene)	-73
Poly (caproamide)	50
Poly (vinyl chloride)	83
Poly (styrene)	100
Poly (methyl methacrylate) PMMA	
Atactic	104 -108
Isotactic	42 – 45
Syndiotactic	105 – 120

1.4.3 Free Volume Theory of Glass Transition:

The free Volume V_f in a polymer is defined by:

$$V_f = V_T - V_o \quad \text{----------(7)}$$

where V_T is the total volume of the polymer at temperature T (in degree Kelvin), V_o is the theoretical molar volume for the most dense packing of the liquid molecules at 0K. The total volume of the polymer V_T is the sum of the free volume V_f and of the occupied volume V_o:

$$V_T = V_f + V_o \quad \text{----------(8)}$$

The occupied volume V_o includes not only the Vander Waals radii but also the fluctuation volume, which is associated with the thermal vibrational motion. Cross linking reduces free volume and increases T_g

1.4.4 Relaxation Process in the region of T_g[17]:

The relaxation process in polymers can be considered as the movement of molecular segments of polymer molecules. For amorphous polymers, in the temperature region on either side of the T_g, three well–defined molecular relaxation processes often labeled with Greek letters α, β and γ [18] are commonly observed.

(i) $\tilde{\alpha}$relaxation is a process above T_g, considered as the primary process and referred to as the glass-rubber transition process. This relaxation process results from large-scale conformational rearrangements of the polymer chain backbone, which occur by a mechanism of hindered rotation around the main chain bonds.

(ii) β–relaxation is the process below T_g, considered as the secondary process and referred to as the glass transition process. This relaxation process results from hindered rotations of side groups independent of the polymer chain backbone.

(iii) $\tilde{\gamma}$relaxation is the process below T_g associated with the disordered regions of the polymer.

The α relaxation is observed at the highest temperature for a given frequency or at the lowest frequency for a given temperature as is usually connected with the glass transition, e.g. with large-scale molecular motions in the main and side chain of the polymer. The secondary relaxation processes, usually connected with limited motions of polar groups in the side chain, are observed in the glassy region of the polymer [19].

1.5 The Plasma State [20]:

At very high temperatures partial molecular dissociation reactions, excitations, and ionization mechanisms are initiated through electron expulsion process. Matter having equal number of simultaneously generated and oppositely charged particles and a different number of unionized neutrals has been recognized as the fourth state of matter and such ionized gases were termed as plasmas. Plasma is therefore an ionized gas.

Plasma contains a mixture of particles with different electric charges and masses. At a first approximation, the plasma may be considered thermally as consisting of two systems: the first containing electrons and the second containing heavy species, i.e. neutral species, ions and neutral molecular fragments.

The mechanisms in the plasma are excitation and relaxation, ionization and recombination. To maintain the steady state of electron and ion densities, the recombination

processes must be compensated by ionization processes, so energy must be continuously supplied to the system to sustain the plasma state.

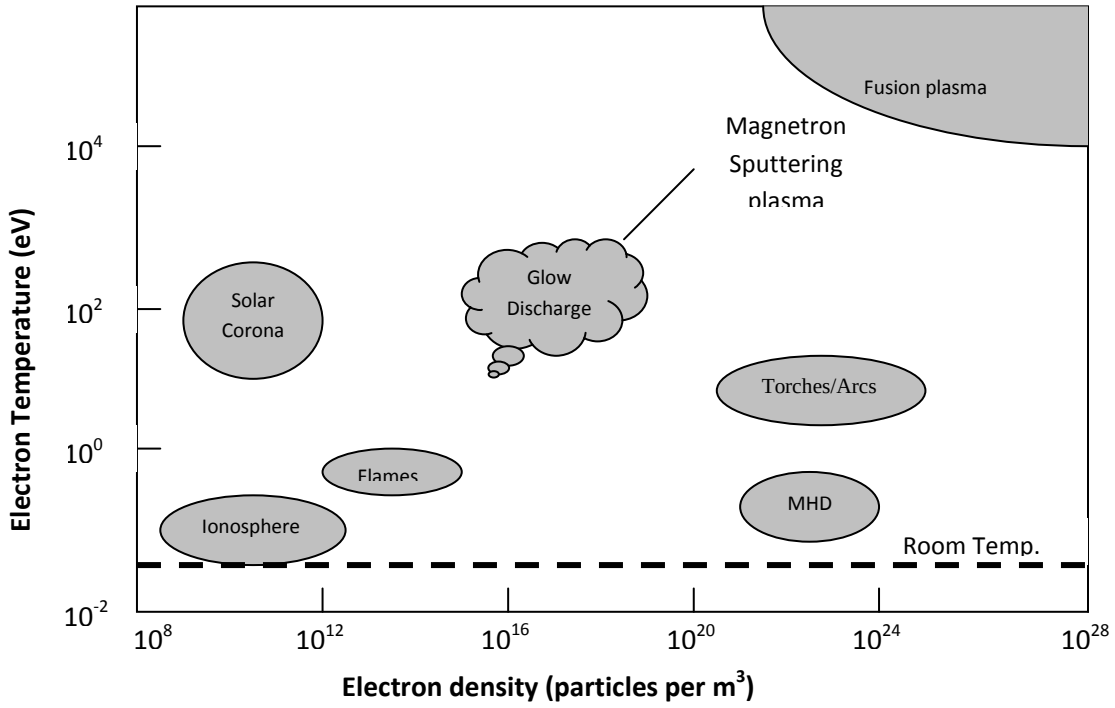

Fig-1.4: Classification of plasmas

1.5.1 Glow Discharge Plasmas (Cold Plasmas) [20]:

On the basis of electron temperatures and electron density the plasmas are classified into various types. Fig-(1.4) gives the classification of plasmas. The plasmas are also classified from the relative temperature of electrons and ions. If the temperature of the electrons is more than that of ions it is known as hot plasma and if the electron temperature is less than that of ions it is known as cold plasma. In the present work concentration is made on the cold plasma. Cold plasmas are also known as glow discharge plasmas.

The glow discharges can be generated by applying DC or RF potential across parallel plates or by inductively coupling the RF power to the gas. These methods are described in this article.

1.5.2 DC Glow Discharges:

A DC glow discharge is created by applying a potential between two parallel plates in a gas. Three important regions are observed in the glow discharge in 50 cm tube filled with neon as shown in Fig-(1.5):

♦ Negative glow – region of bright glow is observed near the cathode. This is a zone of high concentration of positive ions formed by collision with energetic electrons emerging from Crook's dark space. Molecules in excited states are also formed in the negative glow region (thereby giving rise to a bright glow by relaxation to lower states) as well as negative ions and free radicals.

♦ Dark Space – Adjacent to the cathode is the comparatively dark region called as the cathode dark space or the Crook's dark space. This corresponds to the sheath formed in the cathode region. This is the zone where the acceleration of positive ions to the cathode, and acceleration of electrons away from it is observed. A similar sheath is also formed in front of the anode but it is too thin to be seen clearly.

♦ Positive column – it is the region of the discharge which most nearly resembles plasma i.e. a partially ionized gas consisting of equal numbers of positive and negative charges. It can be considered as a channel for carrying current from the negative glow to the anode.

Typical distance between anode and cathode used for the plasma processes like sputtering, plasma treatment is around 5–10 cm. In this case the distance the positive column has negligible length leaving only the negative glow and the dark spaces adjacent to each other.

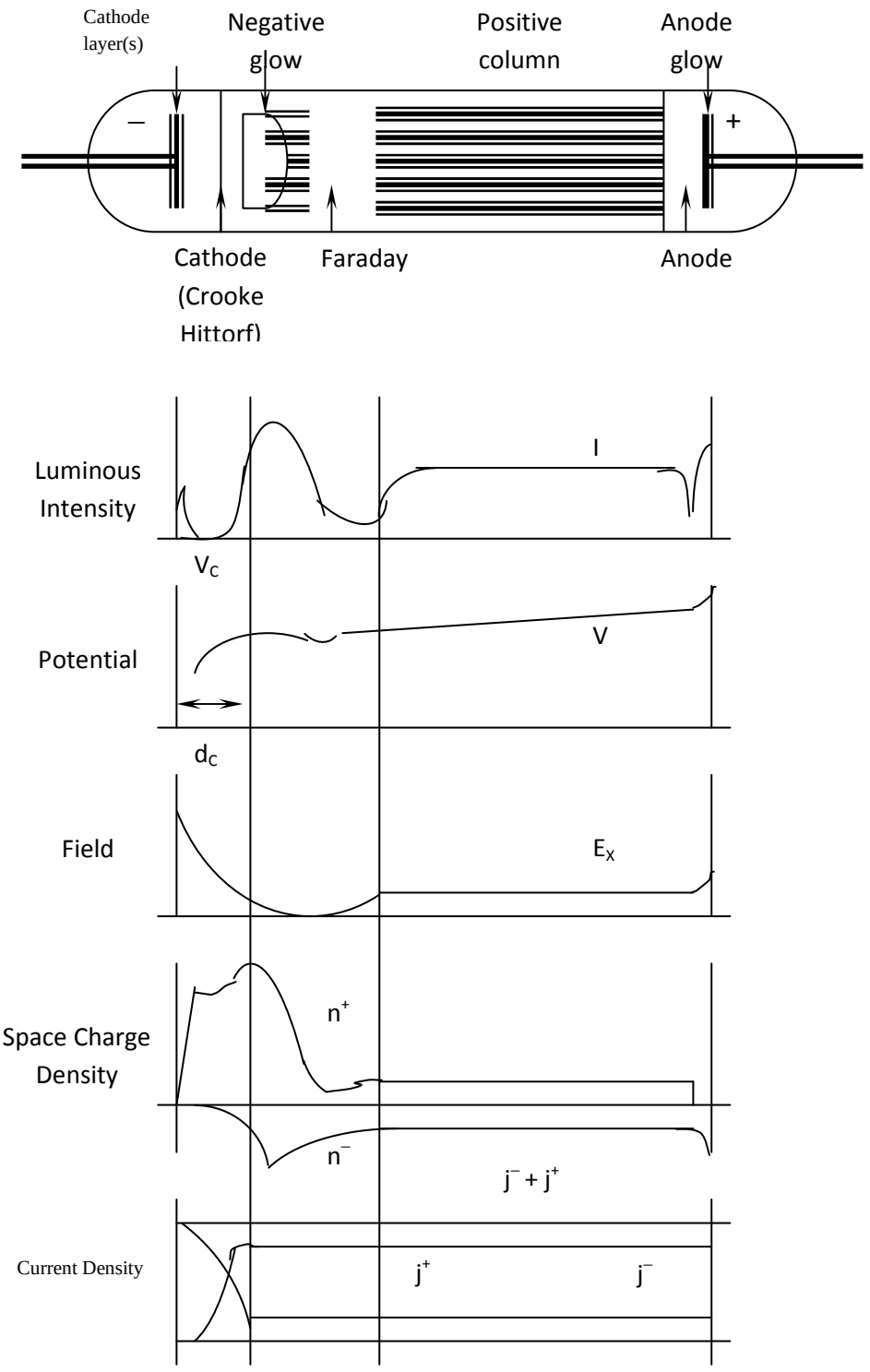

Fig-1.5: The Neon Discharge tube

1.5.3 RF Plasmas:

When the RF field is applied to the capacitively coupled electrode, the electrode surface in contact with the plasma is alternatively polarized positive and negative. When negative it attracts ions, and when positive it repels them. At high operating frequencies, the massive ions cannot follow the temporal variations in the applied potential but the electrons can. Thus a cloud of electrons that constitute the electron component of the negative glow plasma can be pictured as moving back and forth at the applied frequency in a sea of relatively stationary ions on the powered electrode. At radio frequencies (5-30MHz) the electrons oscillating in the glow have sufficient energies to cause ionizing collisions, thus reducing the dependence of the discharge on the secondary electrons and lowering the breakdown voltage.

The RF voltages can be coupled through any kind of impendence it is possible to use reactors without internal electrodes. Two most common techniques for coupling RF power into a glass tube, often refereed to as a tubular or tunnel reactor is by capacitive coupling or inductive coupling.

Most RF apparatus operate at frequency of 13.56 MHz this frequency is normally used for generating plasma. This frequency lies in the 10 to 20 MHz range that has been allocated by the Federal Communications Commissions for industrial use.

1.6 Polymerization:

Before one tries to understand the plasma polymerization process the prior knowledge of different mechanisms of polymerization is essential. In this article the conventional polymerization mechanism is discussed initially and then later the plasma polymerization mechanism is discussed.

1.6.1Conventional Polymerization [21]:

Conventionally, polymers are synthesized via two mechanisms namely stepwise or condensation polymerization and by chain or addition polymerization.

1.6.1.1 Step Growth Polymerization [21]:

This is also called as poly-condensation. Here the polymer is formed by stepwise repetition of the same reaction again and again. For this to occur, the monomers which are capable of undergoing stepwise reactions must possess some active functional groups. If the

monomer is represented by M and the growing molecule by M_1 step–growth polymerization can be represented as:

$$M + M_1 \rightarrow M_2 + H_2O$$
$$M_2 + M \rightarrow M_3 + H_2O$$
$$M_n + M_m \rightarrow M_{n+m} + H_2O$$

1.6.1.2 Chain-Growth Polymerization [21]:

This method of polymerization is also known as the addition polymerization. This is extensively used in industry. In this method a long chain molecule is formed by a series of consecutive steps in seconds and the products are the final polymer.

Addition polymerization can be schematically shown as:

$$Initiation: A^* + M \rightarrow M^*$$
$$\text{Pr}opagation: M^* + M \rightarrow M_2^*; M_n^* + M \rightarrow M_{N+!}^*$$
$$Ter\,\text{min}ation: M_n^* \rightarrow P_n$$

Where, M is the monomer, M* is the reactive species, P_n is the dead polymer and A* is the initiator.

1.6.2 Plasma Polymerization:

Glow discharge polymerization or plasma polymerization has been known for many years; for example, Linder and Davies [22] described the gases and solids formed by some hydrocarbon vapors in a glow discharge in the year 1931. Later, Brick and Knox [23] have described the major features and variables associated with this process. Other articles have been published describing the chemical, physical [24] and electrical [25] properties of glow-discharge polymers.

In a glow discharge polymerization, organic vapors are introduced into a chamber at a pressure of about 1-5 Torr containing two parallel electrodes. An A.C. voltage is applied across the electrodes so as to initiate, and then to sustain, a uniform glow discharge in the intervening space. High energy ions and electrons are produced in the glow and these bombard both the

electrode surfaces and the molecules in the gas phase. These interactions initiate complex chemical reactions which result in the formation of thin (up to about 5 μm) uniform and continuous coatings on the electrode surface [26].

Plasma polymerization is a specific type of plasma chemistry resulting in the deposition of organic film. It refers to the deposition of polymer films through plasma dissociation and excitation of an organic monomer gas and subsequent deposition and polymerization of the excited species on the surface of the substrate. The deposited films are called plasma polymers and are generally chemically and physically different form the conventional polymer. Hydrocarbons, fluorocarbons and compounds containing nitrogen and oxygen and silicon have been used as starting materials for plasma polymerization[27].

The plasma polymers are characterized by the following features[27]:

- The films have thickness between 500 Å to 1 μm
- Such films are highly coherent and adherent to a variety of substrates including conventional polymer, glass and metal surfaces.
- The films are highly cross linked and can be made pinhole-free[27].
- The plasma polymers have no discernable repeating unit as do conventional polymers.
- The properties of the plasma polymer are not determined by the monomer used but by the plasma parameters. A product cannot be defined as the plasma polymer of ethylene; because a variety of products can be obtained from ethylene plasma therefore we can say plasma polymers of ethylene are not polyethylene.
- The monomer used for plasma polymerization does not have to contain a functional group such as double bond for the plasma polymerization to take place[28].

Plasma polymerization is thus a very different process from the conventional polymerization. For this reason, both the generally accepted terms “monomer” for the feed gas and “polymer” to describe the resultant film are strictly not correct since there is no repetition of unique repeat unit along a polymer chain. The real usually very different monomers are the plasma fragments that generate the deposit through homogenous and heterogeneous processes. Plasma polymerization is strongly system dependent process and can be controlled using the various plasma and plasma process parameters available with the experimenter.

1.6.2.1 Plasma Polymerization Mechanism [29]:

It is difficult to define a mechanism of plasma polymerization because of the very large number of elementary processes which must be considered. In order to interpret the kinetics of the polymer deposition in terms of a very simple reaction scheme with only small number steps, the nature of the species which propagate chain growth and the processes involved in initiating polymerization needs to be determined.

The elementary reactions leading to plasma polymerization can be grouped into five generic types-initiation, adsorption, propagation, termination and reinitiation. While in conventional polymerization the termination step interrupts the process, in the case of plasma polymerization chain fragments can be reconverted into radicals by collision with electrons in the gas phase or by impact of energetic particles or photon absorption on the surface of the polymer film. Polymerization in the gas phase and on the surface of the polymer film can be summarized by the reaction proposed by Poll et al[29]. The diagrammatic representation of the process in shown in Fig-(1.6).

Path K-1: Monomer directly polymerized into the growing film: plasma induced polymerization. This is essentially a conventional molecular polymerization process trigged by reactive plasma species. This can take place only if the monomer has polymerizable functional groups.

Path K-2 and K-3: The intermediate reaction products can be ions, excited molecules and free radicals and the monomer need not have polymerizable groups to undergo polymerization.

Ionization of a molecule by collision with an accelerated electron is an essential process for creating and sustaining plasma of the monomer with or without non-polymerizable carrier gas. In case of inert gas, ionization can occur by the elimination of an electron from an electron orbital and requires energy ranging from 12 to 25 eV. Therefore, in the process of ionization of inert gases, electrons having energies lower than ionization potential or off-centered collisions do not contribute to the ionization. In the ionization of organic molecules, the ionization energy required is generally greater than 10 eV, which is far above the bond energies of primary bonds in organic compounds. Therefore, low energy electrons and/or off-center collisions that can not ionize the molecule, can easily break the bonds in the organic molecules or create the exited species (dissociation of molecules) which can trigger the chemical reactions. These side reactions associated with ionization are absent in the plasma of inert and diatomic gases.

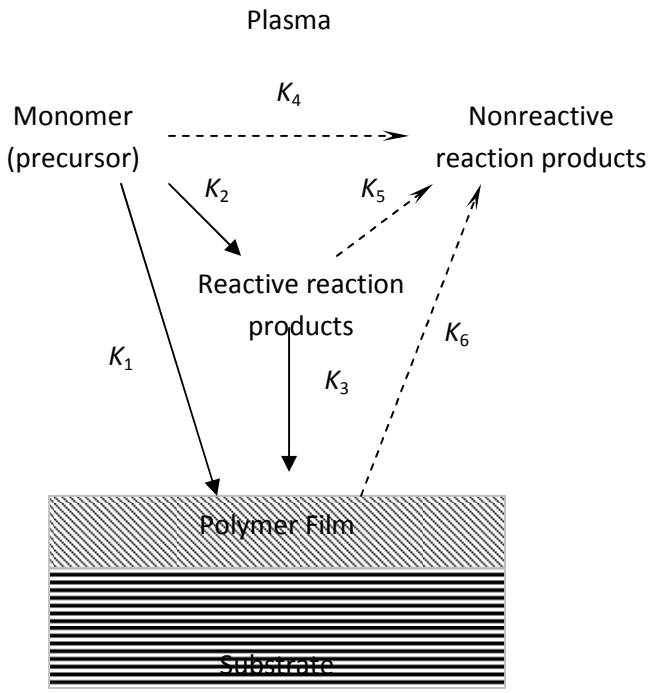

Fig-1.6: Processes in Plasma Polymerization

1.6.2.2 Physical Plasma Process Parameters:

When a monomer is introduced into a glow discharge the rate of plasma polymer deposition and the chemical and physical nature of the plasma polymer is affected by various physical plasma parameters which are at the experimenter's disposal. These are

- f-Frequency of the exciting potential (Hz).
- W- Excitation power (W).
- F-Monomer flow rate (Vol. (STP)/unit time)
- P_g -Plasma pressure (Torr).
- Geometrical factors like volume (cm^3)
- T-Temperature of the deposition site (K).
- n_e-electron density
- f (E)-electron energy distribution
- N-gas density
- τ -residence time (seconds).

The use of composite plasma process parameters is an alternate approach used for controlling the properties of the plasma polymer. One of the most widely used parameter is the W/F, power to flow rate ratio. It is argued that the chemical and physical properties of the plasma polymer will remain constant if the W/F ratio is maintained constant assuming that the pressure, monomer flow and the excitation frequency also remain constant. This is because W and F affect the basic plasma parameters n_e and τ. n_e increases linearly with W and τ is inversely proportional to F. W/F ratio provides only a qualitative understanding of the polymerization process.

1.7 Plasma Treatment of Polymer Surfaces:

It has been known that the interaction of radiation with polymers can lead to the formation of three dimensional network structure, which generally improves the overall physical and chemical properties of the original substrate. This physical and chemical change in the polymer and the mechanism of cross linking and chain scission under exposure to radiation energies has already been established [30-32]. Apart from radiation various other methods of surface modification of polymers have been suggested and used to alter the polymer surface without affecting its bulk properties. These various methods include chemical treatments, flame treatments, coronas, low pressure plasmas, IR, UV, X-ray and γ -ray irradiation, electron and ion beam bombardment, ozone exposure and others [33].

The cold plasma conditions offer a unique route for the polymer modifications as the energies of the active species in the cold plasma conditions are high enough to split the chemical bonds from the organic derivative and consequently, tailored polymeric structures can be created by controlling the plasma conditions. This processing route offers possibilities of achieving unique surface characteristics of polymers for specific applications while the bulk structure and other properties of the polymer are maintained [34].

The surface modification by cold plasma range from simple topographical changes to creation of new chemistries and coatings that are entirely different from the bulk polymer. The surface modification is achieved by: Surface activation, deposition and grafting. The plasma treatments are also environment friendly and economical compared to other forms of treatments.

The effects of plasma treatment on the polymers are [28]:

- Create more reactive surfaces
- Affect wetting properties
- Cross linking

- Change in molecular weight of the surface layers

The main advantages of this technique are [35]:

- It is a clean dry technique and takes only minute to achieve.
- Only the surface properties of the polymer like the permeability, bondability and wettability are profoundly changed while the overall bulk properties of the material for which it was originally chosen remain unchanged.
- The surface characteristics of the polymer is dependent on the plasma parameters i.e. system pressure, gas flow rate, input power, which are under the control of the experimenter.

The processes which take place on the surface of the polymer due to plasma treatment are shown in Fig-(1.7).

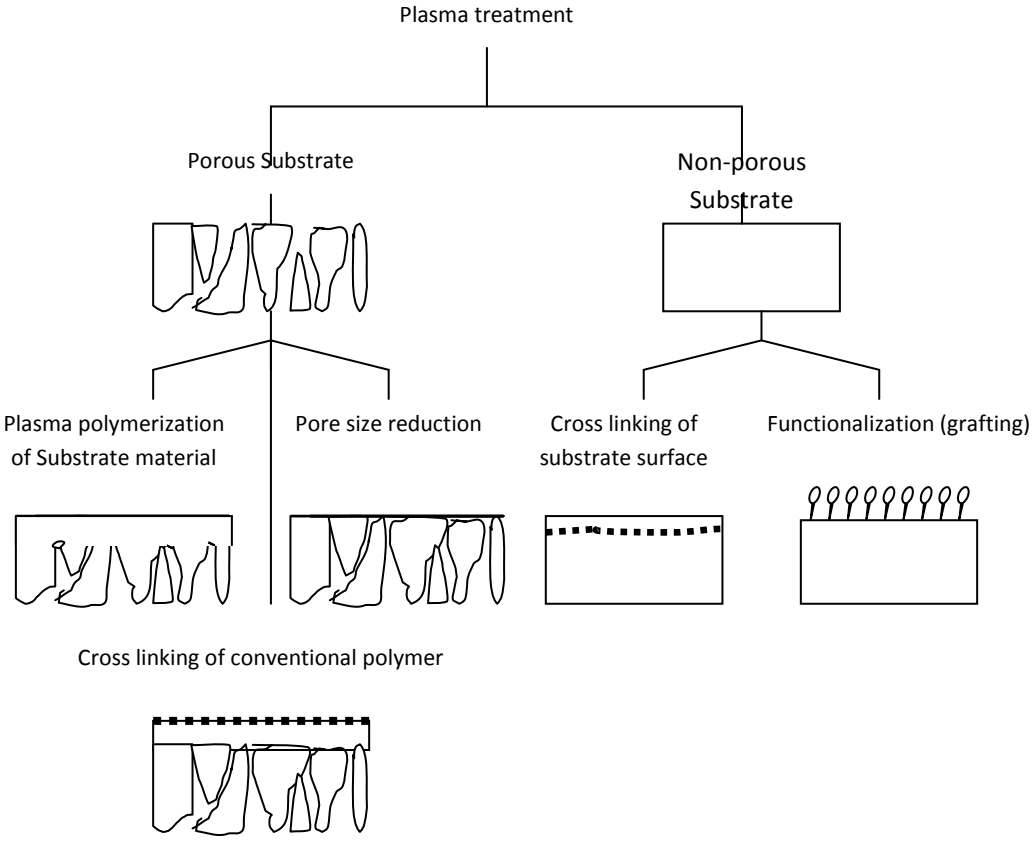

Fig-1.7: Surface Modification of Polymers by Plasma Treatment

1.7.1 Plasma Modification of Polymers:

The modification of polymer surfaces by electrical discharges excited in a variety of gases is a technique widely used as a method to increase the surface free energy or wettability of the material. The major virtues of the technique are: (i) it is a clean reaction and does not take much time and (ii) while making profound changes on the surface properties of the polymer (permeability, bondability and printability) the overall properties of the material for which it was originally chosen for remain unchanged (tensile strength). The thickness of the modified layer has been estimated to be in the range of 0 to 10 μm, depending on the conditions of the discharge (pressure, power, gas flow rate). With the inert gas as the sustaining medium, the reaction initiated in a saturated polymer, via either energy-transfer process, is thought to involve a cross linking mechanism, in which the excited states of the polymer chain undergo homolytic bond cleavage on de-excitation, producing a wide variety of free radicals and unsaturated centers, which by radical additions produce cross links between adjacent polymer chains.

At higher power densities, ablation of small volatile chain fragments form the polymer surface cannot be discounted. However, at relatively low power loading ablation is expected to be minimum.

Clark and Dilks [36] have shown that the nature and effectiveness towards surface modification for each modes of energy transfer available through glow discharge techniques. They have used He, Ne, Ar and Kr as the inert gases for the modification of ethylene-tetrafluoroethylene by RF glow discharge. Their work indicates direct energy transfer as the prominent topmost surface modification parameter, while subsurface restructuring is affected largely through radiative energy transfer process. They have demonstrated that helium is most efficient gas for the cross linking of the outermost few monolayers whereas the cross linking of the subsurface and bulk polymer is best effected by neon.

The surface modification of PMMA films by O_2 and H_2O has been studied by Terrence *et al* [37] whereby they have effectively hydrolyzed a hydrophobic surface of the PMMA by glow discharge.

1.8 Humidity sensing mechanism of PMMA:

The typical water sorption isotherm in glassy polymers such as PMMA are concave in relation to the pressure axis. The dual-sorption model based on both the dissolution of solutes into a polymer and adsorption according to Langmuir's theory in micro voids is effective for analyzing such isotherms [38-41]. However, the amount of sorbed water which was based on milligrams of sorbed water per 1g of dry PMMA , increases with an increase in RH. When this sorption isotherm appears, the swelling of the polymers and the resulting association of sorbed water molecules in the higher humidity region are suggested. Similar water sorption isotherms were observed for all PMMA films with different thicknesses. This is attributed to the water molecule's highly condensable nature because a water molecule has a highly polar and amphiprotic structure. Hysteresis was hardly observed for these sorption isotherms. Consequently, the number of the associated sorbed water molecules seems to be small, arising from PMMA's less hygroscopic nature [42-43] . A decrease in the amount of sorbed water with an increase in film thickness indicates an inhomogeneous water sorption in the PMMA film.

1.8.1 Basic Hypothesis of Diffusion - Mathematical Theory:

Diffusion is a process by which matter is transported from one part of a system to another as a result of random molecular motions. The transfer of heat by conduction is due to random molecular motions, and there is an obvious analogy between the two processes. This was recognized by Fick [44] who first put diffusion on a quantitative basis by adopting the mathematical equation of heat conduction derived some years earlier by Fourier [45]. The mathematical theory of diffusion in isotropic substances is therefore based on the hypothesis that the rate of transfer of diffusion substance through unit area of a section is proportional to the concentration gradient measured normal to the section:

$$F = -D\frac{dc}{dx} \text{----------(9)}$$

Where F is the rate of transfer per unit section, C the concentration of diffusing substance, x the space coordinate measured normal to the section and D is called the diffusion coefficient. In some cases, e.g. diffusion in dilute solutions, D can reasonably be taken as

constant, while in others, e.g. diffusion in high polymers; it depends very markedly on concentration. If F is the amount of material diffusing and C the concentration, both expressed in terms of the same unit of quantity, e.g. grams or gram molecules, then it is clear from the equation that D is independent of this unit and has dimensions cm^2 sec^{-1} the negative sign in the equation arise because diffusion occurs in the direction opposite to that of increasing concentration.

It must be emphasized that the statement expressed mathematically by equation (9) is in general consistent only for an isotropic medium, whose structure and diffusion properties in the neighborhood of any point are the same relative to all directions. Because of this symmetry, the flow of diffusing substance at any point is along the normal to the surface of the constant concentration through the point.

Diffusion in a plane sheet-isotropic-is considered to be one-dimensional diffusion in a medium bounded by two parallel planes. The plane sheet is considered to be so thin that diffusing substance enters through the plane faces and a negligible amount through the edges. The solution to Fick's law for sorption is given by the equation (10). In which M_t and M_∞ are the masses of penetrate at times 't' and infinity, respectively; 2*l* is the thickness of the sheet; D is the diffusion coefficient.

$$\frac{M_t}{M_\infty} = 1 - \frac{8}{\Pi^2}\sum_{n=0}^{n=\infty}\frac{1}{(2n+1)^2}\exp\left\{\frac{-2(2n+1)^2\Pi^2 Dt}{4l^2}\right\} \text{-----(10)}$$

Equation (10) can be simplified using Stefan's approximation to equation (11):

$$\frac{M_t}{M_\infty} = 2\left(\frac{Dt}{\Pi l^2}\right)^{\frac{1}{2}} \text{----------(11)}$$

From the plot of normalized capacitance Vs $t^{1/2}/2l$ the diffusion coefficient can thus be calculated.

1.8.2 Diffusion of H_2O in PMMA:

The water sorption of cross linked glassy polymers such as epoxy [46-51] and melamine-formaldehyde resins has been widely studied [52]. Considerable amount of work has also been done on the water sorption of dimethacrylate networks because of their application as dental materials. Water sorption of PMMA, has also been investigated extensively by Turner D. T. [53-

55], where he has studied the sorption kinetics and volumetric changes together with the effects of molecular weight and cross links on water sorption in PMMA.

According to his observations PMMA of low molecular weight may take up less water than samples of normally higher molecular weight. Further he has noted that due to the addition of cross linking agents, water sorption conforms approximately to Fick's law. The limiting water sorption is also known to increase with increase in cross links.

1.9 Polymer based Humidity Sensing methods:

Polymer sensors have been used longer than ceramic sensors beginning with devices utilizing mechanical output from dilation of hairs to synthetic polymers [56-60]. Various kinds of polymers have been used to prepare humidity sensors like cellulose acetate, polyamide and polymethyl Methacrylate. From the view point of their basic principles, they are classified into two categories. The first one is the resistive type based on the change in the electrical resistance of the material due to sorption of water vapor and the second one is the capacitive type based on the change in the dielectric constant of the material with sorption of water vapor.

These devices suffer from inaccuracy and drift due to creep. However other deficiencies also exist. For example polymers are inherently less robust than ceramics, exhibiting greater sensitivity to both thermal and chemical changes. Applications are therefore limited to lower temperatures. Slow response and hysteresis tend to be more of a problem, since the bulk polymer film must equilibrate with the atmosphere [61]. Temperature compensation is always required, since the change in capacitance with temperature is significant in comparison with its change with humidity. Nevertheless, polymers tend to be more resistant to contamination than porous ceramics, since the sensor mechanism is a bulk rather than a surface phenomenon, and device construction can be simple and less costly.

In order to improve the performance of the humidity sensor modifications in the sensor structure and the sensing material are proposed which include various chemical modifications [60] of the polymers to meet the requirement for use in basically two types of the humidity sensors, i.e. the resistive type and the capacitive type. Some of the relevant ones are described in the following sub articles.

1.9.1 Resistive type Humidity Sensors:

The polymers which are useful for the resistive type humidity sensors have a basic or acidic group such as quaternary ammonium or sulfonate group which sorbs moisture. The amount of sorbed water in the polymer correlates to the environmental humidity. Since, the electrical resistance of the polymer varies with the amount of sorbed water; the humidity can be determined by measuring the resistance or the impedance. Typical impedances recorded in this type of sensors range from 3-7.5 (log Z/Ω) in the RH range of 0–100 % [60].

In the fabrication process of these sensors a pair of gold electrodes are deposited on the polymer films to fabricate a surface type or a sandwich type of a sensor as shown in Fig-(1.8). However these hydrophilic polymers have a serious shortcoming in that they are soluble in water, so they cannot be used at higher humidities. In order to overcome these problem three methods can be used by which the polymer can be modified to make them insoluble in water. These methods are:

(i) preparation of the graft copolymer composed of a hydrophobic trunk polymer and a hydrophilic branch polymer,

(ii) cross linking of a hydrophilic polymer and

(iii) preparation of an interpenetrating polymer network (IPN) between a cross-linked hydrophilic polymer and a cross-linked hydrophobic polymer.

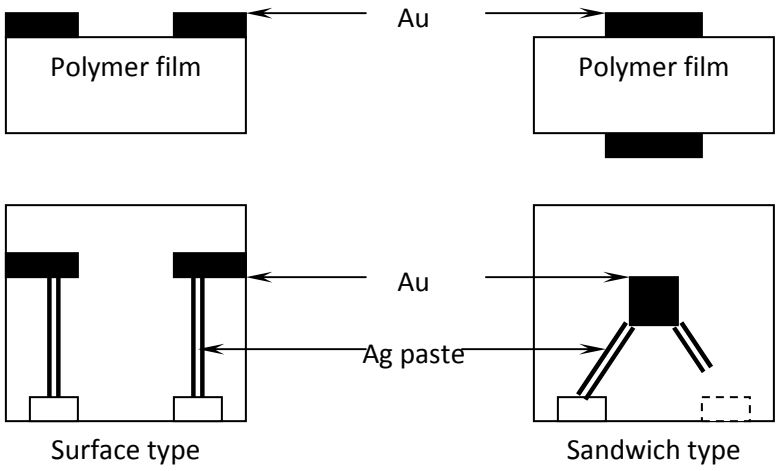

Fig-1.8: Resistive type sensor

When a hydrophilic polymer is chemically bonded on a hydrophobic polymer film by the action of γ-rays or the action of catalysts, the resultant graft polymer film sorbs water vapor but is totally insoluble in water. Such graft polymer films made of poly-tetrafluoroethylene (PTFE) and polystyrene sulfonic acid have ideal properties for humidity sensing [60-61].
When a hydrophilic polymer is cross-linked by an appropriate reaction, the polymer becomes insoluble in water [62-63]. In order to prepare a cross-linked polymer film, a solution of the hydrophilic polymer and the cross linking reagent is mixed and heated to accelerate the cross-linking reaction. After the reaction, the un-reacted materials are washed out with appropriate solvents.

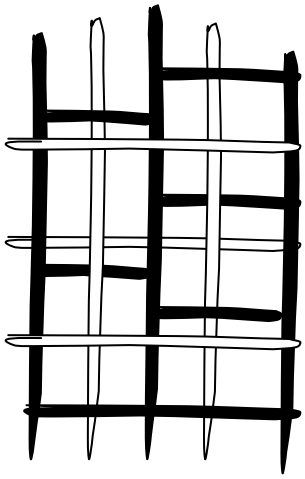

Fig-1.9: Interpenetrating polymer network of a hydrophilic and hydrophobic polymers

An interpenetrating polymer network (IPN) technique has recently been found to be an excellent method for preparing homogeneous polymer alloys. A polymer layer composed of an interpenetrated cross-linked hydrophilic and a hydrophobic polymer can be made using this technique [64-65]. As shown in Fig-(1.9) both of the polymer networks are intermixed together so that it is insoluble in water or in any other solvent.

Y. Sakai *et al* [66] developed water resistant humidity sensor having a long stability by using the technique of graft polymerization. Inside a micro porous polyethylene film, 2-amylamido-2-methylpropane sulfonic acid was graft polymerized by ultraviolet irradiation. Thickness of the film and the porosity was 100 µm and 70% respectively. Gold electrodes

were deposited on both sides of this grafted film to form humidity sensor. The impedance of the sensor was measured with LCZ meter as a function of humidity with the films of various grafting ratios.

The impedance decreased four or five orders of magnitude with the relative humidity increased from 10-90%. Further at all humidities the impedance decreased with the increase in grafting ratio. Response of the sensor to step change in humidity was taken. Sakai *et al*[67] observed that the response time is shortened for acid containing films (< 2 W). The sensors characteristics did not show appreciable change even after 120 days indicating the long term stability.

1.9.2 Capacitive type Humidity Sensors:

In capacitive type humidity sensors hydrophobic polymers (polymers insoluble in water) are used. These polymers should have as few micro voids as possible so that the adsorbed water molecules are isolated in order not to form clusters. In these sensors cross linking is also used to modify the hydrophobic polymer to produce a sensor with small hysteresis, high selectivity and high sensitivity. The materials reported for capacitive type sensor are poly methyl methacrylate, polyvinyl cinnamate, acetylene or terminated polyimide, cellulose acetate butyrate (CAB) and polyamide have been known to be suitable material for capacitive humidity sensors[61-67].

In contrast to the resistive type of humidity sensors already mentioned above, for the capacitive type humidity sensor a thin film of a hydrophobic polymer is sandwiched between the electrodes, in which the upper electrode is usually slotted/grid type or consists of cracks for the diffusion of water vapor into the sensing polymer. The dielectric constants of these hydrophobic polymers are usually very low of about 3, when compared to that of water which is 80. When a small amount of water is sorbed by these polymers the apparent dielectric constant increases, resulting in a linear increase in the capacitance with relative humidity except for the case when the sorbed water molecule form clusters. In addition when the sorbed water forms clusters, hysteresis is observed. Consequently it is desirable to choose polymers in which the sorbed water does not form clusters. It is also required that the apparent dielectric constant is not affected by organic solvent vapors.

Although the hydrophobic polymers are insoluble in water they have some affinity for organic solvents. A capacitive type humidity sensor composed of PMMA cross linked with

divinyl monomers such as ethylene glycol dimethacrylate has been reported [68]and is found to show less hysteresis as it sorbs water much less than the cellulose derivatives. This sensor is also durable in organic solvents.

The humidity sensors have been improved by chemical modification of the polymers such as graft polymerization, cross linking (chemical means) or IPN formation so that the sensor is durable at higher humidities. Recently, plasma deposited polymer films have attracted increasing interest as materials for passivation, adhesion promotion, barrier coatings [23-69] optical waveguides [70] and relative humidity (RH) sensing applications[61,71-74].

Plasma polymerization has been used to deposit unique thin films from a variety of monomers. These monomers may or may not have a formal polymerizable structure such as a double bond, triple bond or a cyclic structure [61]. The monomer primarily acts as a source of elements to build a macromolecular structure [62]. If two monomers having different functions and elements are polymerized by plasma polymerization, the resulting film will generally contain all the elements from both the monomers. Thus, polymer films with a wide range of chemical and physical properties can be obtained easily by mixing two different monomers and plasma polymerizing. There have been several publications on the preparation, characterization and applications of thin films deposited from a single monomer by plasma polymerization [75-78].

Deposition of polymer films by plasma polymerization offers many advantages over commonly used techniques for deposition of polymer films. This is because the polymer film properties can be very easily varied or “tailored” by adjusting the plasma parameters. This technique also allows polymerization of monomer gases which do not contain reactive sites for polymerization. This is achieved by the production of active species in the plasma. The material properties can also be controlled by adjusting the plasma processing parameters like power, pressure and monomer flow rate.

Capacitive humidity sensors using PPMMA as a humidity-sensitive element have been reported by Andrew *et al* [79]. They have reported the role of cross linking density in the performance of the sensor. Four types of materials were basically studied: linear PMMA, PMMA cross linked with ethylene glycol dimethacrylate (EGDM), low-density plasma deposited PMMA and high-density PPMMA. They used a 13.56 MHz capacitively coupled

parallel-plate reactor. The capacitors were fabricated on silicon substrates. The PMMA dielectric lies between a solid lower electrode and a slotted upper electrode. This slotted upper electrode provides a diffusion path for water from the ambient into the PMMA. These sensors measure the changes in the dielectric permittivity of PMMA as a function of moisture content.

1.9.3 Resonant Humidity Sensor:

A third type of humidity sensing device has been recently introduced by Schroth et al [80]. Investigations in this area show that the ambient humidity has a strong influence on both the electrical as well as the mechanical properties of the polyimide polymer. In order to overcome these problems, the use of humidity induced changes of mechanical properties of polyimide have been investigated and the resonant humidity sensor has been introduced.

Schroth A. *et al* [80] have fabricated a resonant humidity sensor based on polyimide. Their sensor consists of an oscillating square membrane, which is covered by a polyimide layer. Under the influence of humidity the layer undergoes a volume extension, which leads to a bending moment and therefore induces tensile stresses in the membrane and therefore induces tensile stresses in the membrane. Additionally, the humidity dependent bonding of hydrogen and hydroxyl molecules increases the mass of the oscillating system. Both these effects act simultaneously and cause a frequency shift.

The sensor chip is fabricated using industrial bipolar technology which allows the integration of the driving and the read-out circuit. The membrane structure is obtained by KOH etching from the back of the wafer in combination with an electrochemical etch stop at the p-n junction between the p-doped substrate and the n-doped epitaxial layer. The detection of the frequency shift as well as the thermal excitation of the oscillation is carried out by piezoresistors located at the edges of the membrane. The polyimide layer is located in the middle of the resonator membrane. It is structured by photolithography to increase the influence of the humidity induced swelling. They have further carried out simulation of the sensor behavior using FEM simulations to predict and optimize the sensitivity of the described structure. They have concluded that this sensing principle is suitable for measuring quantities of RH because it combines the advantages of a frequency measurement and

standard industrial bipolar process manufacturing and the separation between humid environment and sensor electronic.

1.10 Sensor fabrication technologies [11,81]

Sensor fabrication is one of the important tasks and various technologies are used for the same. The sensor deposition technologies affect different parameters of sensors. The advantage in science and technology offered many techniques for sensor fabrication for getting better performance. The three main fabrication technologies given as thick film, pellet and thin film. Every technique has its own merits and demerits.

1.10.1 Thick film technology [82]

Thick film technology was introduced more than 30 years ago. Generally in hybrid microelectronics thick films are preferred in which specially formulated pastes are printed onto a ceramic or insulating substrate in a definite pattern to produce a set of passive components. For formulating thick films, pastes (functional material + permanent blinder) are printed on the substrates by screen printing and fired in the belt driven furnace in air/nitrogen atmosphere by automatic process. This technology offers flexibility by a wide choice of shapes, size of components, choice of substrate material, trimming of components, easy hybridization and mass production which are useful for sensor and transducer implementation. Thickness of thick film is typically in the range of 10-30 μm.

1.10.2 Pellet formation technology [83]

Pellets are having thicknesses in the range of hundreds of µm. For pellet preparation a large amount of paste with binder is needed. The paste of the functional material is added in dye and pressure is applied on it by using hydraulic press. Thus applied pressure allows all the particles of the functional material to combine together resulting in a pellet. The strength of the pellet depends on the pressure applied. To increase the strength of pellet, generally some binders such as poly vinyl alcohol is added. The binders add strength and compactness. Binders are burnt out to neutralize their effect while subjecting the pellets for sintering. Finally electrodes are printed on both the surfaces of pellets to make them ready to use.

1.10.3 Thin film technology [84-85]

If the dimension of materials is less than or equal to mfp of electrons it is defines as thin film. The act of depositing a thin film to surface is known as thin-film deposition. The thin film is deposited atom by atom or molecule by molecule. Thin films are having many applications in industry, research and development and in daily life. The examples are anti reflecting coating, mirrors, interference filters, sun glasses, decorative coating on plastic and textiles, electronic circuits and in research. The thin film deposition is done by several processes such as physical evaporation of material in vacuum, ion plating, sputtering, electroplating, spray pyrolysis, laser ablation, spin coating, dip coating, etc. The methods of depositing thin films are briefly described in the following sub-sections.

1.10.3.1 Dip coating technology [84-85]

This is very simple type of thin film deposition technique, in which the substrate is dipped into the given solution and pulled out a uniform rate and then dried under atmospheric conditions or infrared lamp. Thus dip coated samples become ready to use. Some dip coated films like those of tin oxide have to be subjected for firing at optimized temperature and time. Reproducibility is questionable many times because of non-uniform thickness. If the solution is non-uniform in density as a depth changing then the prepared samples will be having random thickness.

1.10.3.2 Spin coating technology [84-85]

Spin coating is used to get uniform thin films on flat substrate. A predetermined amount of solution is placed on the substrate, which is then rotated at high speed in order to spread the fluid by centrifugal force. Rotation is continued while the fluid spin off the edges of the substrate, until the desired thickness of film is achieved. The applied solvent used is usually volatile, and simultaneously evaporates. Higher angular speed of spinning results in thinner films. The thickness of the film also depends on the concentration of the solution and the solvent.

1.10.4 Deposition technologies [81,84-85]

In CVD chemically reacting volatile compound of a material is deposited in the presence of other gas to produce a nonvolatile solid which deposits on the substrate. The high temperature CVD is having many applications in several many fields.

Physical deposition uses mechanical or thermodynamic means to produce a thin film of solid. An everyday example is the formation of frost. Since most engineering materials are held together by relatively high energies, and chemical reactions are not used to store these energies, commercial physical deposition systems used to require a low-pressure environment to function properly. The material to be deposited is placed in energetic, entropic environment, so that particles of material escape its surface. Facing this source is a cooler surface which draws energy from this particles as they arrive, allowing them to form a solid layer. The whole system is kept in a vacuum deposition chamber, to allow the particles to travel as freely as possible. Since particles tend to follow a straight path, films deposited by physical means are commonly directional, rather than conformal.

Sputtering relies on a plasma (usually a noble gases, such as argon) to knock material from a "target" a few atoms at a time. The target can be kept at relatively low temperatures, since the process is not one of evaporation, making this one of the most flexible deposition techniques. It is especially useful for compounds or mixtures, where different component would otherwise tend to evaporate at different rates. The sputtering step coverage is more or less conformal.

Thermal decomposition of gaseous species such as hydrides, carbonyls and organometallic compounds on temperature control substrate is called spray pyrolysis.

1.11 LiteratureReview

Y. Sakai *et al* [66] developed water resistant humidity sensor having a long stability by using the technique of graft polymerization. Inside a micro porous polyethylene film, 2-amylamido-2-methylpropane sulfonic acid was graft polymerized by ultraviolet irradiation. Thickness of the film and the porosity was 100 µm and 70% respectively. Gold electrodes were deposited on both sides of this grafted film to form humidity sensor. The impedance of the sensor was measured with LCZ meter as a function of humidity with the films of various grafting ratios.

The impedance decreased four or five orders of magnitude with the relative humidity increased from 10-90%. Further at all humidities the impedance decreased with the increase in grafting ratio. Response of the sensor to step change in humidity was taken. Sakai *et al* observed that the response time is shortened for acid containing films (< 2 W). The sensors characteristics did not show appreciable change even after 120 days indicating the long term stability.

Y. Sakai *et al* [66] have reviewed the work of the last 10 years (1986-96) about studies on humidity sensors fabricated with organic polymers. Both the resistive and capacitive type of

sensors are reviewed. They have concluded that in order to fabricate humidity sensors using polymeric materials, one must modify the polymers by chemical reactions to meet the requirements for reliable humidity sensors. Several methods useful for improving the characteristics of humidity sensors are available in the literature. In case of resistive type of sensor one must modify the hydrophilic polymer to be insoluble in water while still maintaining the hydrophilic character to adsorb sufficient water molecules to form an ionic conduction path. Cross linking or graft polymerization is a promising solution to this problem. Sakai *et al* [67] have proposed several one step procedures for this purpose.

T. Maddanimath *et al* [86] have fabricated a resistive type humidity sensor by using surface modified polyethylene (PE) and polypropylene (PP). The surface fictionalization of the polymer was done by dipping the polymer films in oleum for different time intervals at ambient conditions and later washed in de-ionized water. They have shown that controlled sulphonation have promising humidity dependent resistance changes (10^9-$10^6\Omega$ with change in the RH from 30 to 95%) and also other favorable characteristics such as linearity and short response time. They have carried out systematic study of humidity sensing behavior with and without different types of surface fictionalization, where in it is noted that the sensitivity is controlled by surface structure and the extent of functionalization, causing a change in carrier concentration and the mobility of the protons and counter ions.

Y. Li et al [87] have prepared resistive humidity sensors using polymer solid electrolytes. Monolayer and bilayer devices were prepared by filming polymer electrolytes or blends of polymer electrolytes on interdigited gold electrodes. They tested the electrical characteristics of the devices as a function of %RH in a home made cell equipped with a commercial humidity sensor. Different values of %RH were obtained by bubbling dry argon through water. The impedance was measured for corresponding %RH. The logarithm of the impedance modulus or the resistance gave straight lines, as a function of %RH, only for some devices based on copolymers or polymer blends. They have concluded that by utilizing mono or bilayer structures of polymers or copolymers and empirically choosing the more appropriate working frequency, suitable conditions for a good humidity sensing device construction can be found.

Andrew *et al* [79] characterized the frequency dependent response of the films to moisture from 12 Hz to 100 Hz. A β relaxation was identified in the linear and cross linked PMMA films, but was observed to be absent in the plasma-deposited films. This result they have interpreted as

indicating that the high density of cross links in the plasma deposited films inhibits segmental motion in these films. The sensitivity of their PPMMA sensors at 100 Hz was about 60% of the linear and the cross linked PMMA. The hysteresis was found to be low above 1 kHz. The cross linked PMMA however is reported to exhibit significant hysteresis below 1 kHz. The response to moisture at 100 kHz is most linear for the plasma deposited films. The sensitivity measured for these sensors was 2 pF/%RH.

In order to minimize the hysteresis and to increase the sensitivity of humidity sensors, Chan *et al* [88] have used porous polyamide to fabricate capacitive humidity sensor. The polyamide selected contains weak hydrophilic carbonyl group which is suitable for increasing the sensitivity. They deposited the polyamide sensing layer by spin coating polyamic acid onto the lower Ti electrode (1500 Å thick) patterned by e-beam evaporation on an oxidized Si substrate. The coating was cured at a temperature up to 45 ^{o}C in argon environment. In order to avoid shorting Al_2O_3 was deposited on to the lower Ti electrode. To increase the sensitivity, cracks were generated in the top electrode and the polymer layer. To generate cracks on the sensor structure, they deposited the upper chromium electrode in a state of tensile stress using e-beam evaporation. The width and size of the cracks were increased with the thickness of the upper electrode. Chan *et al* [88] have suggested that if the polymer humidity-sensing layer is too dense or hard, the sensor's sensitivity becomes very low and the upper electrode should be porous for water molecules to pass through and reach the sensing layer. The sensor sensitivity they have reported in the 10-90 %RH range is 0.25 pF/%RH, increasing with relative humidity. The hysteresis was observed in the humidity range 3 %RH at 50 %RH. They have attributed this to the hydration and dehydration processes.

Matsuguchi M. *et al* [89] have worked on the stability and reliability of capacitive-type relative humidity sensor using cross linked polyimide films. They have used cross linked polyimide (C-PI) and cross linked fluorinated polyimide (C-FPI) as the sensing material in a sandwich type sensor element. They observed that the electrical capacitance changed linearly over 10-90% RH, their hysteresis was less. Their C-FPI sensor demonstrated long-term stability in harsh environments and the drift was as small as +1.1 pF after 1000 hr of exposure to 40 ^{o}C temperature at 90 %RH atmosphere. The C-PI sensor proved to be resistant to chemicals. The sensor output was not affected even after exposing the sensor elements to saturated acetone

vapor for 20 min. They have concluded that a stable and reliable sensor usable in an office building and in a factory can be achieved by using these sensors properly.

Matsuguchi *et al* [90] have prepared cross linked PVCA on a substrate using photo irradiation technique and have evaluated them as a capacitive humidity sensor. The excitation wavelength is shorter than 325 nm. The effect of irradiation conditions on the degree of cross linking and also on the sensing characteristic was examined. In addition the adsorption behavior of various polar organic vapors was also studied. The device structure in this case is a sandwich type of sensor. Platinum thin film was used as a lower electrode and gold film as an upper electrode. To measure the amount of adsorbed solute the film was prepared on AJ–cut quartz crystal. The electrical properties were measured using an LCZ meter. The humidity was varied by controlling the ratio of dry and water saturated air. The response time was less than 30 sec. in humidification process and was slightly higher in the desiccation process. This also depended on the degree of cross linking. The degree of cross linking was determined from the dielectric loss measurement and the FTIR analysis.

It was found that as the photo irradiation time increases the magnitude of the relaxation peak reduced and shifted to a higher temperature side. It is known that the dielectric relaxation of a polymer arises from the segmental motion of the main chain and the side chain. If the cross linking reaction has taken place then the film becomes rigid and the segmental motion of the main chain is depressed and as a consequence the dielectric loss is lowered. Therefore, lowering of dielectric loss confirms the formation of cross links. In this case, the cross linking reaction proceeded with increase in the irradiation time. The cross linking degree was also confirmed by FTIR analysis 90% cross linking was reached within 4 hrs of irradiation.

The humidity response of the PVCA films was measured at 30 ^{o}C in terms of the ratio of capacitance at certain %RH and capacitance at 0 %RH. The ratio was found to increase linearly with humidity. The sensitivity was seen to have been enhanced with photo irradiation time. The maximum ratio observed was 1.2 at 90% humidity for 4 hr irradiated sample. From the results of the amount of adsorbed water at a particular humidity and the degree of cross linking, the authors postulated that the enhancement of water absorption ability is related to the decomposition of the polymer by exposure to UV light. Reports are also available that the saturation value for water uptake of the cross linked PMMA with dimethylacrylate monomers increases with an increase in the degree of polymerization.

Jose M. *et al* [91] have for the first time developed a capacitive humidity sensor using poly (ethyleneterephthalate)–PETT as the dielectric. They have fabricated a sandwich type of a sensor by cutting 50 μm PETT films in about 1cm diameter circles on which metallic gold thin film (0.1-0.3 nm thick) was deposited by magnetron sputtering. Electrical contacts were made by nickel contacts. This device was incorporated in an oscillator circuit to use it as a humidity sensor. This sensor enabled them to measure the humidity between 10-97 %RH range over saturated salt solutions. They have concluded that the accuracy of their sensor was about ± 2 %RH in the complete measurement range. Its response time was found to be comparable to those of the commercial sensors and has good stability over time.

Li Y. et al [87] have carried out work on capacitive sensors using polymer solid electrolytes. They have used monolayer and bilayer devices prepared by filming polymer electrolytes/blends of polymer electrolytes on interdigited gold electrodes similar to the ones used for resistive type of sensor as mentioned above. They measured the variation of capacitance with %RH at a constant temperature 22 ^{o}C. The measured capacitance in linear or logarithmic scale gave a linear trend with %RH. They have concluded that these devices give fast response and operate over a wide range of %RH.

P.R. Story et. al. [1] reported study of low-cost sensors for measuring low relative humidity. The performance of low-cost commercially available (five different) capacitive and resistive type polymeric humidity sensors has been compared to that of prototype thick- and thin-film polyimide based sensors. Both capacitive and surface acoustic wave (SAW) sensing mechanisms have been studied for the thin-film structure. The prototype sensors were optimized for improved performance at low relative humidity (RH). The commercial capacitive microsensors have a linear response in the range 5-95% RH. The resistive sensors are found to be non linear. The prototype thick-film sensor has a non-linear response, while the response of the thin-film prototype sensor is comparable to that of the commercial capacitive microsensors. The SAW sensor has the potential for higher sensitivity than the commercial capacitive microsensors, but is less linear.

Two prototype capacitive humidity sensors were also studied. They included both thick- and thin-film interdigitated electrode designs as shown in Fig. l(a) and (b). The thick-film sensor was fabricated with 18 (0.65 mm wide) finger pairs spaced 0.65 mm apart on a 2 in **X** 2 in alumina substrate using standard screen-printing processes. The thick-film conductor, which had a final

thickness of 23 μm, was Pd/Ag. The thin-film design was photolithographically patterned aluminum 150 nm thick on a quartz substrate. The pattern consisted of 90 (10 μm wide) finger pairs spaced 10 μm apart. A 2 μm polyimide film (DuPont Pyralin 2555) was spin coated at 5000 rpm for 60 s on both substrates. The samples were softbaked at 120 °C for 10 min and cured at 350 ° C for 30 min in nitrogen.

Authors found that capacitive type thin-film sensor had a fairly linear response with some hysteresis at higher RH. Further they found that the total percentage change in capacitance for the thick-film sensor was greater than that of the thin-film sensor and the thick-film sensor showed no response below 40% RH. They have attributed this to the microscopic structures of these two sensors. The polyimide film is much thicker (2 μm) than the electrodes (150 nm) on the thin-film sensor, therefore the electric field between the electrodes can be considered to be entirely most of the electric field is assumed to be in the air gap between the electrodes. In case of thick electrodes the polyimide (2 μm) is much thinner than the thick film electrodes (23 μm). A smaller overall response would therefore be expected for the thick-film sensor. This only occurred at low RH. The reason for the large capacitance change at high RH is not provided.

Y. Sakai et al [92**]** have presented review on the humidity sensors fabricated with organic polymers. Several useful methods for improving the characteristics of humidity sensors based on polymers are proposed. In the case of a resistive-type sensor, cross-linking of hydrophilic polymers or formation of interpenetrated polymer networks with a hydrophobic polymer makes the hydrophilic polymers durable at high humidities. Graft polymerization is another method of preparing water-resistive humidity sensors. In the case of capacitive-type sensors, cross-linking is also useful to modify the hydrophobic polymer to produce a sensor with small hysteresis, high selectivity and high sensitivity.

Polymers insoluble in water – hydrophobic- have been used to fabricate capacitive-type humidity sensors. Cellulose acetate butyrate (CAB) and polyimide have been known to be suitable materials for capacitive humidity sensors. However, many problems such as hysteresis, stability at high humidity's and at high temperature and durability on exposure to some kinds of organic vapors still remain to be solved. To complete the capacitive-type humidity sensor for practical use, it is important to elucidate the sensing mechanism of this type of sensor. Authors have examined the correlation between the permittivity and the amount of sorbed water for the various cellulose derivatives in one of their previous papers. The hysteresis was confirmed to be

caused by the formation of clusters of sorbed water molecules. It was found that the polymer should have as few microvoids as possible so that the adsorbed water molecules are isolated in order not to form clusters. The formation of clusters leads to appreciable hysteresis. In some cases cross-linking of the polymer chains was found to depress the clustering of water. In addition, the cross-linked polymers are durable in the presence of organic vapors.

Authors reported poly(methyl methacrylate) (PMMA) PMMA sorbs a smaller amount of water than CAB and other cellulose derivatives, resulting in less opportunity to form clusters, The hysteresis for a PMMA capacitive-type humidity sensor is therefore less than ±!% RH, which is smaller than that of the conventional sensors. In addition, cross-linking of PMMA was carried out using divinylbenzene or ethylene glycol dimethacrylate. Authors report that the cross-linking of PMMA reduced the hysteresis and the temperature coefficient. The durability in the presence of organic vapors was also much improved. Authors also have reported Acetylene-terminated polyimide and Poly(vinyl cinnamate) as humidity sensors.

P.M. Harrey et al [4 **]** reported work on Capacitive-type humidity sensors fabricated using the offset lithographic printing process. Authors used polyimide and polyethersulphone (PES) as humidity sensitive materials.

Printed humidity sensors were fabricated via the conductive lithographic film (CLF) process and evaluated. polyimide and polyethersulphone (PES) were investigated as humidity sensor films. A standard sheet-fed lithographic printing press (Heidelberg GTO46) was used to print the electrodes of the sensor structures. Printed sensors were formed on 25 mm PES, and three different thickness grades of polyimide film: HN30, HN50 and HN100 (thicknesses of 7.6, 12.5 and 25 mm, respectively. In addition, sensors with patterned electrode films which incorporate micro-pores were also fabricated and evaluated.

For comparative purposes, a thin film sensor was also formed on polyimide HN film. The sensor was fabricated by sputter coating gold electrode films onto opposing sides of the 7.6 mm polymer film. The calculated thickness of the electrode films was 600 A ° (0.06 μm). This sensor was used to compare the response times of the experimental printed sensors to a more conventional thin-film electrode sensor. Electrical testing of the sensors was accomplished by bonding silver wire test leads to the electrode films of the sensors using a silver loaded conductive adhesive. The effective overlap area of the sensor is 200 mm^2. Humidity tests were performed using a Vaportron H100 humidity test chamber.

The capacitance of the structures was measured using a Fluke PM3606 LCR meter (1 MHz and 1 V test signal). The capacitance response of the sensors was studied over the range of 10–90%RH. Both sensors responded linearly to changes in relative humidity. The results indicate that the sensors exhibited similar nominal capacitances (235 pF). The polyimide sensor exhibited a greater change in capacitance than the PES sensor over the measured range of 10– 90%RH. These findings are in accordance with manufacturers specifications which detail Kapton1 HN film polyimide as having a greater moisture absorption capacity than PES film (2.8% compared to 2.2% ASTM D-570-98).

The capacitance change (pF) and sensitivity (pF/%RH) of the sensors was shown to be inversely proportional to the sensing film thickness. The thin (7.6 μm) polyimide film sensor demonstrated a sensitivity of ~1 pF/% RH, this is 2–3 times greater than contemporary commercial capacitive-type sensors. It has also been shown that the response time of the sensor is inversely proportional to the thickness of the polymer sensing film. Polyimide sensors formed on 25, 12.5 and 7.6 μm film exhibited response times (t_{63}) of 10.5, 5.0 and 1.8 min, respectively. Comparatively, PES sensors were shown to respond more quickly than equivalent film thickness polyimide sensors.

Pi-Guey Su et al **[7]** have worked on resistive type humidity sensors based on PMMA. The ionic conductivity of PMMA was modified by doping with two different salts KOH and K2CO. These dopants are having largely different dissociation constants. The electrical properties of PMMA doped with different amounts of KOH or a mixture of KOH and K2CO3 were examined in detail as a function of relative humidity (RH), to elucidate the contribution of the salts to the sensing properties (linearity and sensitivity).

The sensors were fabricated by dip-coating and subsequent in situ co-polymerization on an alumina substrate with a pair of comb-like electrodes. The precursor solutions were prepared from methyl methacrylate (MMA, 99%, Acros Corp.), KOH (99%, Aldrich) and K2CO3 (99%, Aldrich). The two inorganic salts were mixed into MMA at different compositions together with a small amount of ethanol as an interface modifier. Then, the alumina substrates were coated with the precursor solutions and were in situ co-polymerized in an oven at 90 ◦C for 1 h to give PMMA-based humidity sensors.

Complex impedance of a sensor was measured with an LCR meter (Philips PM6304) in a test chamber at measurement frequency of 1 kHz, an applied voltage of 1V, an ambient

temperature of 25 ◦C and different humidity levels in the range of 30–90%RH. The humidity in the test chamber was controlled by mixing dry and wet air through mass flow controllers. The RH values were measured with a calibrated hygrometer (Rotronic) with an accuracy of ±0.1%RH. Sensitivity is defined as the slope of logarithmic impedance (log *Z*) versus %RH and linearity in terms of correlation coefficient is defined as the *R*-squared value of the linear fitting curve in the range from 30 to 90%RH.

Authors reported that pure PMMA exhibited only a little impedance change in the humidity range studied. They attributed it to its hydrophobic property. When the PMMA was doped with KOH, an inverse sigmoidal humidity dependence of the logarithmic impedance was observed at both low and high dosage. The sensitivity (slope) increased from 0.0012 to 0.0638 with the KOH doping. However, the impedance change was observed at 30–60%RH and more notably at 50–60%RH, and almost no impedance change in the range of 60–90%RH.

The PMMA doped only with KOH had a high sensitivity but low linearity. The poor linearity of the PMMA/KOH complex was improved by further doping of K2CO3. The PMMA doped with a mixture of KOH (0.6%, w/w) and K2CO3 (0.6%, w/w) was optimal in both sensitivity and linearity in the range of 30–90%RH.

With simultaneous doping with KOH and K2CO3, the linearity increased with increasing the dosage of K2CO3. However, the sensitivity decreased with increasing the dosage of K2CO3. The impedance continuously decreased along with the humidity increase in the range of 30–60%RH, though the impedance values increased with increasing the dosage of K2CO3 at 60–90%RH. This behavior is thought to be due to aggregations of ions at high concentrations.

In order to explain the results of the PMMA/KOH/K2CO3 polymer–salts complexes, authors discussed the mechanism for the conductance variation with %RH in the following way. With the absorption of water, a sort of thin liquid layer forms around the polymer chains or fills the openings in the sensing polymer films through capillary condensation or swelling. The sorbed water enhances the electrolytic dissociation of the inorganic salts in the polymer–salts complexes. Finally, the sorbed water acts as a plasticizer which gives rise to an increase in mobility of the ions dissociated.

It is well known that KOH has a very high dissociation constant (6.63×10^{10}) and therefore it is easily and completely dissociated under the conditions of low humidity. Compared with KOH, the dissociation constant (1.50) of K2CO3 is quite low. It means that the K2CO3 can

be dissociated completely only under the conditions of highly humid atmosphere. Thus, it is important to incorporate both KOH and K2CO3 into the PMMA-based composites for the wide-range humidity detection.

In order to get higher sensitivity and better linearity of the PMMA/KOH/K2CO3 materials in a wider humidity range, the optimum doping ratio of KOH to K2CO3 was investigated. It was found that the PMMA doped with a mixture of KOH (0.6%, w/w) and K2CO3 (0.6%, w/w) was optimal in both sensitivity and linearity in the range of 30–90%RH. The sample prepared at optimum conditions was further tested for evaluation of hysteresis and stability. The hysteresis was evaluated by the percent difference in logarithmic impedance between humidification and desiccation processes, that is, by 100×(log *Z*desic −log *Z*humid)/log *Z*desic at 60%RH. The hysteresis was within 4%RH at most. Moreover, the stability test, where a sensor was subjected to repeated humidification and desiccation cycles more than 50 times in the range of 30–90%RH at 25 ◦C, indicated that the present humidity sensors worked normally during the test.

Masanobu Matsuguchi et al [6] reported a capacitive-type humidity sensor based on a poly(methyl methacrylate) (PMMA) cross-linked with divinylbenzene (DVB). They examined the influence of introducing a cross-linked structure in the sensing polymer on the long-term stability of the sensor in a hot and humid atmosphere. As the DVB content increased, the irreversible increase in the water sorption ability of the cross-linked PMMA by long-term aging in a 40°C and 90% RH atmosphere was depressed. This was because the irreversible increase in volume of the sensing polymer caused by swelling in such atmosphere was prevented due to the rigid cross-linked structure. The depression of the drift of the water sorption ability resulted in the depression of the drift of the sensor capacitance.

Sandwich-type devices were prepared for dielectric measurement. Methyl methacrylate (MMA) monomer was mixed with divinylbenzene at various weight ratios and polymerized with benzoyl peroxide until the mixture reached the appropriate viscosity, followed by spin coating on a 4 in. alumina substrate with a Pt lower electrode. The coated thin film was heated to achieve complete polymeriztion at 80 ◦C for 24 h in a N2 atmosphere. The thickness was varied by changing the rotational speed of the spin-coater. Finally, a gold upper electrode was deposited by vacuum evaporation technique. To measure the amount of sorbed water, the cross-linked PMMA film was also coated on a quartz crystal oscillating element (4 MHz) having a silver electrode

plated on both sides. The relative humidity (% RH) of which was controlled by mixing dry and wet air. The measurement was carried out at 100 kHz with an LCZ meter.

The aging test the devices were placed in a humidistat in which the atmosphere was maintained at 40 ◦C and 90% RH. Each device was occasionally removed from the humidistat, and the humidity dependence of the device's characteristics was measured over a humidity cycle of 10–90% RH at 30 ◦C. After the measurement, the device was returned to the humidistat. These procedures were then repeated.

It was found that the depression of a capacitive-type humidity sensor's drift by long-term aging in a hot and humid atmosphere was achieved by introducing a cross-linked structure in the sensing polymer. The sensor's drift was smaller for the cross-linked PMMA having a larger DVB content, corresponding to a smaller change in the water sorption ability. The effect of cross-linking on the drift was explained by the depression of the irreversible increase in volume of the sensing polymer caused by swelling of the PMMA by aging. The cross-linking technique may also improve the chemical resistance of the sensing polymer in wet and humid atmosphere; however, very little information is currently available for such discussion.

In addition, it was shown that the drift of the sensor based on the cross-linked PMMA was observed only in the early aging period. This result means that long-term stability can be achieved in a capacitive humidity sensor, even in a hot and humid atmosphere, by the pretreatment of the present sensor once in such an atmosphere before use.

Zhi Chen and Chi Lu[N2] have reported review of Materials and Mechanisms of Humidity Sensors. The review is based on various materials for both relative and absolute humidity, including ceramic, semiconducting, and polymer materials. Extract of the review on polymer materials, only is reported here.

Most of the polymers are carbon-hydride compounds or their derivatives. The carbon atoms link each other one by one, either by sigma bond (single bond) or sigma bond plus pi bond (double bonds or triple bonds), forming a long chain, which is called the backbone of the polymer. Functional groups are rooted on the backbone, which could be either single atoms (e.g., oxygen or halogen) or molecular groups (e.g., –COOH, –NO2). The functional groups, along with the basic structure of the backbone, determine the chemical and physical properties of the polymers. Polymeric humidity sensors have been widely studied in research and applied in industry for more than 30 years. Most of the sensors are based on porous polymer films thinner

than millimeters and their sensing principle is quite similar to that of ceramic sensors. The film is filled with micro-pores for water vapor condensation and some of the measurable physical properties change due to the water absorption.

The mechanism of protonic conduction inside the adsorbed water layers on the surface of the sensing materials was discovered in study of TiO2 and α-Fe2O3. As shown in Figure 3, at the first stage of adsorption, a water molecule is chemically adsorbed on an activated site (a) to form an adsorption complex (b), which subsequently transfers to surface hydroxyl groups (c). Then, another water molecule comes to be adsorbed through hydrogen bonding on the two neighboring hydroxyl groups as shown in (d). The top water molecule condensed cannot move freely due to the restriction from the two hydrogen bonding (Fig. 3(d)). Thus this layer or the first physically-adsorbed layer is immobile and there are not hydrogen bonds formed between the water molecules in this layer.

As water continues to condense on the surface of the ceramic, an extra layer on top of the first physically adsorbed layer forms (Fig. 4). This layer is less ordered than the first physically-adsorbed. For example, there may be only one hydrogen bond locally. If more layers condense, the ordering from the initial surface may gradually disappear and protons may have more and more freedom to move inside the condensed water through the Grotthuss mechanism. In other words, from the second physisorbed layer, water molecules become mobile and finally almost identical to the bulk liquid water, and the Grotthuss mechanism becomes dominant. This mechanism indicates that sensors based purely on water-phase protonic conduction would not be quite sensitive to low humidity, at which the water vapor could rarely form continuous mobile layers on the sensor surface. The two immobile layers, the chemisorbed and the first physisorbed ones, while cannot contribute to protonconducting activity, could provide electron tunneling between donor water sites. The tunnelling effect, along with the energy induced by the surface anions, facilitates electrons to hop along the surface that is covered by the immobile layers and therefore contributes to the conductivity. This mechanism is quite helpful for detecting low humidity levels, at which there is not effective protonic conduction.

According to sensing mechanisms, polymeric humidity sensors are divided into two fundamental categories: resistive-type and capacitive-type. The former responds to moisture variation by changing its conductivity while the latter responds to water vapor by varying its dielectric constant. Almost all of the humidity sensors based on polymers operate at room

temperature, due to polymers' high sensitivity to heat. Copolymers and mutually reactive copolymers have also been studied for humidity sensing. Polymeric humidity sensors based on piezoresistive, surface wave acoustic (SAW) devices and Optical measurements are also studied. Polymeric resistive humidity sensors are based on two types of materials: polyelectrolytes and conjugated polymers.

Polyelectrolytes are hydrophilic or even water soluble while conjugated polymers are rather hydrophobic and unable to absorb much water.

Polyelectrolytes are polymers with electrolytic groups, which could be salts, acids, and bases. Based on functional groups, humidity-sensitive polyelectrolytes can be fundamentally divided into three major categories: quaternary ammonium salts, sulfonate salts, and phosphonium salts.

Fuke M.V. et al [3] have worked on the evaluation of Co-Polyaniline nanocomposite thin films as humidity sensor. Polyaniline is unique among the known conducting polymers because its conductivity is controlled by the doping levels of oxidation and protons. Oxidation states of polyaniline, whose electrical properties are sensitive to water, provide a basis for potential applications in sensors for humidity control. The aqueous environment changes the conductivity due to two reasons:

1. Adsorbed water molecules dissociate at imine nitrogen centers.
2. Positive charge migrates through the polymer.

Spin coated films of Co-Polyaniline nanocomposite are evaluated for their transmission properties using He–Ne laser for humidity sensing. The thickness (17–29_m) of the films is varied by multiple deposition of Co-Polyaniline nanocomposite on a glass substrate. The samples exhibit typically two to three regions in their sensitivity curve when tested in the relative

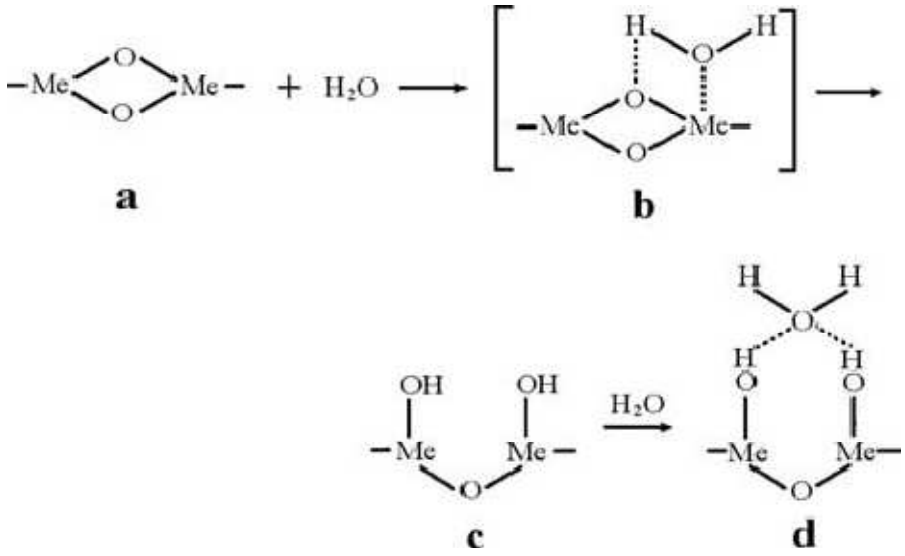

Fig.-1.10. Four stages of the adsorption.

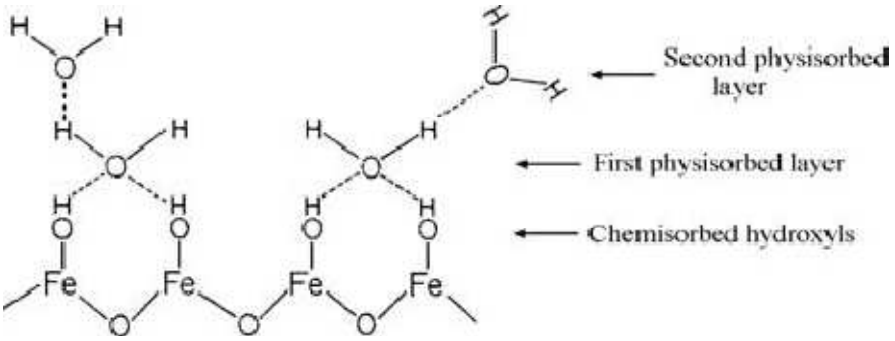

Fig.-1.11. Multi-layer structure of condensed water.

humidity (RH) range of 20–95%. The sensitivity ranges from 0.1mV/%RH to 12.26mV/%RH for lower to higher thickness. The sensors show quick response of 8 s (20–95%RH), and a recovery time of 1 min (95–20%RH) with good repeatability, reproducibility and low hysteresis effect. The sensitivity of the sensor increases with humidity and thickness. Material characterization is done by X-ray diffraction (XRD), scanning electron micrograph (SEM) and Fourier transform infra-red spectroscopy (FTIR).

All the sensors roughly exhibit three regions of sensitivity with very low sensitivity at low humidity levels, increased sensitivity at medium humidity levels and high sensitivity at the high humidity levels. At the thickness of 23.57μm the maximum sensitivity is seen. As the relative

humidity increases the output voltage decreases. At a lower humidity (20 to 40 RH%) the layer of hydroxyl groups is formed [93]. The water vapor molecules are chemisorbed through a dissociative mechanism by which two surface hydroxyl groups per water molecule are formed. This does not change the transmission of light through the film. Therefore at lower relative humidity the sensor response is poor. At a higher humidity (60 to 80 RH%) the water molecules get adsorbed on the wall of the pores. The light through the film gets absorbed in proportion to the deposition of water molecules on the pore walls, in turn the output voltage decreases. For all the samples at higher humidity, around 80%RH, switching behavior is exhibited because of formation of water meniscus on the film, which absorbs the incident light making transmitted intensity to be small.

The variation of humidity response i.e decrease in the output voltage with increase in the relative humidity is also attributed to the mobility of Co ions which are loosely attached to the polymer by weak Van der Waals' forces of attraction. Authors have taken the SEM images of the films. They have reported that lower thicknesses have higher porosity and hence give higher sensitivity. Authors further found out that the hysteresis for 23.57μm thickness is 1%. And the response and recovery time of the sensor is given as 8 s and 1min, respectively. The repeatability and the reproducibility of the optical humidity sensor using Co-Polyaniline nanocomposite was found to be very encouraging for all the concentrations for 23.57μm.

1.11 Aims and objectives :

The main aim of this research was to deposit and/or treat the selected material - polymethyl methacrylate - by plasma processes and compare their performances as capacitive type humidity sensors. .

The main objectives of the study were –

- Study and prepare the experimental set ups for plasma treatment, plasma polymerization and spin coating of thin and thick films.
- Formation of thick/thin film on the substrate using selected material.
- Synthesize the materials by plasma polymerization and plasma treatment of spin coated polymers.
- Structural & physical characterization of synthesized polymers by techniques such as gravimetric method, taly step method, FTIR, SEM…etc.
- Fabrication of capacitive type humidity sensors.

- Determination of sensitivity, response time, recovery time, hysteresis, reproducibility, repeatability of capacitive type sensor.
- Study and specify characteristics of fabricated sensors using above mentioned techniques.
- Study the optical properties of PMMA. For that study drop casted and spin coated films of PMMA were used.
- Compare the characteristics of sensors fabricated using different methods and conclude accordingly.
- Comparison of the obtained results with the ones available in the literature.

References

1) P.R. Story, D.W. Galipeau , R.D. Mileha, Sens. & Actu, B 24-25 (1995) 681.
2) Zhi Chen and Chi Lu, Sensor Letters, 3 (2005) 274–295
3) M. V. Fuke, A Vijayan, M. Kulkarni, R. Hawaldarb, R.C. Aiyer, Talanta, 76 (2008) 1035–1040
4) P.M. Harrey, B.J. Ramsey, P.S.A. Evans, D.J. Harrison, Sens. & Actu., B 87 (2002) 226–232
5) Cecilia Roman , Olimpiu Bodea , Nicolae Prodan , Andrei Levi , Emil Cordos,Ionel Manoviciu, Sens. & Actu., B 24-25 (1995) 710-713
6) Masanobu Matsuguchi , Makoto Yoshida, Takaaki Kuroiwa, Tsutomu Ogura, Sens. & Actu., B 102 (2004) 97–101
7) Pi-Guey Su, Yi-Lu Sun, Chu-Chieh Lin, Sens. & Actu., B 113 (2006) 883–886
8) B. Kulwicki; J. Am. Ceram. Soc.,74 -4 (1991) 697.
9) Andrew R.K. Ralston, Jeffrey A. Tobin, Sateesh S. Bajikar, Denice D. Denton, Sens. & Actu., B 22 (1994) 139-147
10) M. L. Jadhav, Ph. D. Thesis entitled, "Study of some humidity sensitive electrical characteristics of Al_2O_3,H_2O thin films for possible development as, thin film, planar resistive, humidity sensor," submitted to the University of Pune, **(1983).**
11) S.G. Ansari, Ph. D. Thesis entitled,"Development and characterization of Tin oxide based planar film resistors for gas/humidity sensor application," submitted to the University of Pune, **(1996).**
12) E.R. Weaver, R. J. Riley, J RES NBS, 40 **(1948)** 169.
13) Y.Li, M J Yang, Chinese Chemical Letters. 12(8) **(2001)** 701-702.
14) C.L.Dai, Sens. And Actu. B 122(2) **(2007)** 375-380.
15) C. L. Cutting, J. Sci. Inst, 30 **(1953)** 338.
16) P. L. E Barney; Thin Solid Films *152* **(1987)** 99.
17) J. F. Rabek; Experimental methods in Polymer Chemistry;
18) K. Deutsch; E.A. W. Hoff and W. Reddish; J. Polymer Sci. 13 **(1954)** 565.
19) Z. Y. Cheng; S. Yilmaz; W. Wirges; S. B. Gogonea; and S. Bauer; *J. of Appl. Phys.*83-12 **(1998)** 7799.
20) Bharat Bhushan and B. K. Gupta; Handbook of Tribology, Materials Coatings and Surface Treatments; Mc- Graw Hill Inc. New York.
21) M. Zambare; "Plasma Synthesis of electron beam resist, their Characterization and Plasma Diagnostic by

Langmuir probe" Ph.D. Thesis, University of Pune; **(1996)**.

22) Linder and Davis; J. Phys. Chem. 35 **(1931)** 3649.
23) Brick and Knox; Modern Packaging; **(1965)** 123.
24) J. Goodman; J. Polymer Sci. 44 **(1960)** 551.
25) A. Bradley and J. P. Aammes; J. Electrochem. Soc.110 **(1963)** 15.
26) T. Williams, and M.W. Hayes; Nature 19 **(1966)** 769.
27) N. Morosoff; Plasma Deposition, Treatment and Etching of Polymers; ed. R D. Agostino; **(1990)** 1-93.
28) A. Grill; Cold plasma in Materials Fabrication- from Fundamentals to Applications; IEEE Press, New York; **(1994)**.
29) H. U. Poll; M.Artz, K. H. Wicklender; European Polymer Journal 12 **(1976)** 505.
30) E. J. Lawton; A. M. Bueche; and J. S. Balwit; *Nature* 172 **(1953)** 76.
31) A. Chapin; Radiation Chemistry of Polymeric Systems; Wiley-Interscience; New York; **(1962)**.
32) A. Charlesby; Atomic Radiation and Polymers; Pergamon Press, Ltd.; Oxford, UK; **(1960)**.
33) J. O. Choi; and J. C. Corelli; J. P. Silverman; and H. Bakhrun; *J. Vac. Sci. Technol.* B-6 **(1988)** 2286.
34) D. T. Clark and A. Dilks; J. Polymer Sci. 16 (1978) 911.
35) F. Denes; R. A. Young; M. Sarmadi; J. of Photopolymer Sci. and Technol. 10 (1997) 112.
36) Clark; and Dilks; J. of Polym. Sci. Polym Chem. Ed. 16 **(1978)** 911.
37) T. G. Vargo; and J. A. Gardella; J. of Polym. Sci. Polym Chem. *Ed.* 27 **(1989)** 1267.
38) R. Kirchheim, Macromolecules, 25, 6952 , **(1992).**
39) R. M. Barrer, J. A. Barrie, and J. Slater, J. Polym. Sci., **27**, 177, **(1958).**
40) P. Meares, Trans. Faraday, Soc., 54, 40, (**1958).**
41) A. S. Michaels, W. R. Vieth, and J. Barrie, *J.* Appl. Phys., 34, 1, **(1963).**
42) Y. Sadaoka, M. Matsuguchi, Y. Sakai, and K. Takahashi, J. Mater. Sci. Lett., **7**, pp-121-124**, (1988).**
43) M. Matsuguchi, S. Umeda, Y. Sadaoka, and Y. Sakai, Sens. Actuators B**,** 49, pp- 179**, (1998).**
44) A. Fick; *Ann. Phys. Lpz.* 170, 59 **(1955)**.
45) J. Fourier; Theorie analytique de la haleur **(1922)**.
46) M. J. Adamson; J. Mater. Sci. 15 **(1980)** 1736.
47) P. Moy; and F. E. Darasz; Polym. Eng. Sci. 20 **(1980)** 315.
48) D. Y. Marom; and G. Broutman; J. Appl. Polym. Sci. 26 **(1981)** 3015.
49) J.L. Garcia-Fierro; and J.V. Aleman; Macromol. 15 **(1982)** 1145.
50) L.W. Jelinski; J.J. Dumais; R.E. Stark; T.S. Ellis; and F.E. Karasz; Macromol. 16 **(1983)** 1021.
51) M.S. Majerus; D. S. Soong; and J.M. Prausnitz; J. Appl. Polym. Sci. 29 **(1984)** 453.
52) P. M. Smith; and M. M. Fisher; Polym. 25 **(1984)** 84.
53) D. T. Turner; Polym. 23 **(1982)** 197.
54) D. T. Turner; Polym. 28 **(1987)** 293.
55) D. T. Turner; Polym. 28 **(1987)** 297.

56) E. Nelson; and E. J. Amdur; Proceedings of the International Symposium on Humidity and Moisture; Washington DC **(1963)**.

57) W. Smith; *U.S. Pat. No. 3295088* **(1966)**.

58) P. E. Thoma; *U.S. Pat. No. 3582728* **(1971)**.

59) P. E. Thoma; J. O. Colla; and R. Stewart; *IEEE Trans. Compon. Hybrids. Manuf. Technol.* CHMT-2 (3) **(1979)** 321.

60) Y Sakai; Sens. & Actu. B 13-14 **(1993)** 82.

61) Y. Sakai; Y. Sadaoka; and K. Ikeuchi; *Sens. & Actu. B* 9 **(1986)** 125.

62) Y. Sakai; Y. Sadaoka; and H. Fukumoto; *Sens. & Actu. B* 13 **(1988)** 243.

63) Y. Sakai; Y. Sadaoka; and M. Matsuguchi; *J. Electrochem. Soc.* 136 **(1989)** 171.

64) Y. Sakai; Y. Sadaoka; M. Matsuguchi; I. Hiramatsu; and K. Hirayama; Proc. 3rd Int. Meet, Chemical Sensors, ClevelandOH, USA; **(1990)** 273.

65) Y. Sakai; Y. Sadaoka; M. Matsuguchi; and K. Hirayama; Tech. Digest Paper, Int. Conf. Solid-State Sens. & **Actu.;** San Francisco, CA, USA; **(1991)** 562.

66) Y. Sakai; *V*.L. Rao; Sadaoka; and M. Matsuguchi; *Polym. Bull.* **18 (1987)** 501.

67) Y. Sakai; Sadaoka; and M. Matsuguchi; *Sens. & Actu. B* 35-36 **(1996)** 85.

68) H. Yashuda; Plasma Polymerization,; Academic Press; FL; **(1985)**.

69) **J.** Tobin; and D. D. Denton; *Appl. Phys. Lett. 60-21 (***1992)** 2**595.**

70) *N. Ina*gaki**; K. Su**zuki; and K. Nejigaki; *J. Polym. Sci. Polym. Lett. Ed. 2**1*** **(1983) 3**53.

71) Ra**deva; K**. Bobev; and L. Spassov; *Sens. & Actu. B* 8 **(1992)** 21.

72) N. Inagaki; K.Oh-Ishi; and K. Suzuki; *J. Appl. Polym. Sci.* 3*1 **(1986)** 2473.*

73) Takeda; *Vacuum* 41 **(1990)** 1769.

74) J. Sakato; M. Yamamoto; and M. Hirai; *J. Appl. Polym. Sci.* 31 **(1986)** 1999.

75) B.V. Tkachuk; V. V. Bushin; V. M. Kolotyrkin; and N. P. Smetankia; *Vysokomol. Soyed A* 9 (9) **(1967)** 2018.

76) F. Denes; C. Ungurenasu; and I. Haiduc; *J. Eur. Polym.* 6 **(1970)** 1155.

77) N. Inagaki; and K.Ohishi; *J. Polym. Sci. 23 **(1985)** 1445.*

78) R. K. Andrew; Ralston; J. A. Tobin; S. S. Bajikar; D. D. Denton; *Sens. & Actu. B* 22 **(1994)** 139.

79) A. Scroth, K.Sager, G.Gerlash, A.Haberli, bolthauser & Baltes. Sens. Actu. B 34 (1996) 301.

80) Z.A. Ansari, Ph. D. Thesis entitled, "Study of planar optical waveguide sensors with active cladding For gaseous species. N. Inagaki; and K.Ohishi; *J. Polym. Sci.* 23 **(1985)** 1445.

81) J.H. Anderson, G.A. Parks, J. Phys. Chem., 72 **(1968)** 3662.

82) A. D. Garje, Ph. D. Thesis entitled,"Electrical and gas sensing properties of synthesized nanocrystalline SnO_2 based thick film resistors," submitted to the University of Pune, **(2007).**

83) L.I. Maissel and R. Glang, Handbook of thin film technology, McGraw Hill, New York, **(1970)**.

84) H. Nishihara, M. Haruna and T. Suhara, Optical Integrated Circuits, McGraw Hill, New York, **(1989)**.

85) T. Maddanimath; I.S. Mulla, S.R. Sainkar; K. Vijayamohanan; K.I. Shaikh, A.S. Patil and S.P. Vernekar; *Sens. & Actu. B* Communicated **(2002)**.
86) Y. Li; M.J. Yang; N. Camaioni; and G.Casalbore-Miceli; *Sens. & Actu. B* 77 **(2001)** 625.
87) Chan-BokPark; Yonk-Ho Lee; and Sang-Bin Yi; *Sens. & Actu. B* 13-14 **(1993)** 86.
88) M. Matsuguchi; T. Kuroiwa; T. Miyagishi; S. Suzuki; T. Ogura; and Y. Sakai; *Sens. & Actu. B* 52 **(1998)** 53.
89) M. Matsuguchi; M. Shinmoto; Y. Sadaoka; T. Kuroiwa; Y. Sakai; *Sens. & Actu. B* 34 **(1996)** 349.
90) M. Jose; M. Perez; and C. Freyre; *Sens. & Actu. B* 42 **(1997)**27.
91) Y. Sakai*, Y. Sadaoka, M. Matsuguchi Sensors and Actuators B 35-36 (1996) 85-90
92) N. Parvatikar, S. Jain, S.V. Bhoraskar, M.V.N. Ambika Prasad, J. Appl. Polym. Sci.,102 (6) (2006) 5533.

Chapter-II

Experimental Techniques

2.1 Introduction:

In the previous chapter the theoretical background necessary for the work carried out is given. The literature survey gives a bird's eye view of the present scenario of polymer based humidity sensors from which the aims and objectives of the work have been outlined.

The present chapter describes the experiments carried out for fabrication and characterization of humidity sensor. The experimental work includes IDC structure fabrication, monomer distillation, spin coating, plasma treatment, plasma polymerization, structural characterization by FTIR, the response of the material to relative humidity and optical response of the material.

2.2 Sensor Fabrication:

For the sensor fabrication an interdigited capacitive (IDC) type sensor structure was selected. As shown in Fig-(2.1) it consists of planer metal electrodes in the interdigited ID form selected for gathering large value of capacitance and small value of resistance component. The thin film of the sensor material acts as a dielectric between the fingers of the ID structure. The fabrication process is described in following subsections.

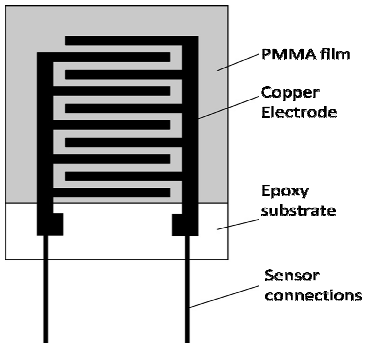

Fig.2.1 Inter-digited capacitor (IDC) pattern

2.2.1 Mask Preparation:

Each finger has length of 8mm and the distance between the successive fingers is 0.3mm. There are total twenty fingers which covered an area of about 0.8 cm^2. The mask pattern was drawn by art work on white paper. The artwork is drawn on the scale which is ten times the original pattern. The final mask was made using photo-reduction technique that reduces the image by 10 times. The mask was made with Kodak high resolution plate (HRP). Mask

preparation depends on the photo resist being used. In this work negative photo resist was used therefore a positive mask was prepared.

2.2.2. Photo Lithography for pattern delineation

Photolithography is a technique of transferring a mask pattern on to the substrate. In this work mask was given to the fabricator. Then using photolithographic techniques, 50 IDCs were fabricated using glass epoxy copper clad substrate.

2.2.3 Cleaning of Glass, epoxy and silicon Substrates:

Prior to PMMA deposition on glass substrates, the glass substrates (borosilicate glass slides) were cleaned in the following manner:

The substrates were boiled in chromic acid (potassium dichromate dissolved in deionized water plus a few drops of sulfuric acid) for a few min and kept soaked in it for an hour. They were then rinsed in DI water and then cleaned in neutral soap (labogen) solution. They were again rinsed in DI water and ultrasonically cleaned in methanol for a few min.

The epoxy substrates were cleaned by putting them in acetone for 10 minutes. Then wash those using DI water. Silicon substrates were cleaned by putting them in hydrofluoric acid (HF) for 10 minutes. Then remove from HF and clean by tissue paper.

2.3. Deposition of the sensing material :

After the ID pattern was transferred onto glass epoxy copper clad, the sensing materials i.e. spin coated PMMA, plasma treated PMMA and plasma polymerized MMA were deposited on the IDCs, glass, and silicon.

2.3.1 PMMA Deposition by spin coating:

Preparation of PMMA solution

Commercially available PMMA granules (Gujpol India Ltd.) were dissolved in AR-grade chloroform and subsequently spin coated onto previously cleaned IDC structures on glass epoxy and glass substrates. In order to vary the viscosity of the liquid 0.1gm, 0.2gm, 0.3gm of PMMA granules were dissolved in 10ml of chloroform.

Fig.2.2: Spin Coater (WS-400-6NPP-LITE)

Spin coating and thickness measurement

For the spin coating of the PMMA, the commercially available PMMA granules (Gujpol India Ltd.) were dissolved in AR-grade chloroform and subsequently spin coated onto previously cleaned IDC structures (where the PMMA got deposited in between the ID fingers) and glass substrates. The thickness of the copper ID is about 34 µm. A Laurell's (WS-400-6NPP-LITE) spin coating system (fig.2.2) was used in this study. Spin coating was achieved by pouring the solution on a clean substrate to fully cover it. After selecting the spin speed of the coater, it was switched on to start spinning. The spin speed used in the experiments was varied between around 500-3000 rpm. The spin coating duration for all samples was 60 seconds. To remove the extra solvent from the layer, the samples were placed in the oven at a temperature of 60 °C for 20 minutes after spin coating.

Several experiments were carried out. Different concentrations of the PMMA solution were prepared by dissolving various amounts of PMMA in chloroform. PMMA solutions prepared were spun on to glass and IDT substrates.

Equation (2.1) is then used to calculate the thickness of the film. (by weight method)

$$\rho = M/V = M/A \times t \text{ ----------(2.1)}$$

Where ρ is the density of the PMMA (1.17gm/cc), M is the mass of the film, V is the total volume of the PMMA film which is product of area 'A' of the film covered and 't' thickness of the PMMA film.

2.3.2. Plasma Treatments of Conventional PMMA:

The spin coated PMMA on copper ID structure, silicon and bare glass substrates were treated in Ar plasma in a tubular plasma system (EMITEK 1050X). The system was initially evacuated to 10^{-2} Torr using a rotary pump. Ar gas was then flushed for ten min before adjusting the pressure to 0.2 Torr. The power was varied between 40 to 60 Watt at the variable time of 5 to 15 minutes.

Fig 2.3: PLASMA SYSTEM (EMITECH, K 1050X, ENGLAND)

Fig. 2.3 shows the schematic of the system used for the experiment. This system is specially used for the surface treatment of polymers. The most important components of this system are a vacuum chamber, a vacuum pump, a high-frequency generator for plasma creation and a gas feeding system.

2.3.3 Monomer (MMA) Distillation:

The commercially available monomer contains an inhibitor added intentionally for preventing polymerization. This has to be removed first before the monomer could be used for polymerization. Distillation under pressure lower than the normal atmospheric pressure is most suitable method for the purification of many organic liquids. For the present work methyl methacrylate (MMA) 99.00% (from Aldrich chemical company Inc.) 86 inhibited with 10 ppm of hydroquinone monomethyl ether/4-methoxy phenol (MEHQ) is purchased.

The thermodynamic properties of MMA and its inhibitor are given below:

	MMA	MEHQ
Boiling point (b.p) at 760 mm of Hg	100 ^{o}C	243 ^{o}C
Melting point (m.p.)	-48 ^{o}C	55-57 ^{o}C
Molecular weight (m.w.)	100.12	124.14

The schematic of the distillation set up is shown in Fig-2.4. The monomer was first washed with 5% NaOH solution to remove the inhibitor such as hydroquinone and later twice with distilled water using a separating funnel to remove the un-reacted NaOH. The monomer is dried using Na_2CO_3, $NaSO_4$ or $MgSO_4$. It is again dried with CaH_2 and kept for one hour.

The distillation is carried out at a pressure of 5-10 Torr in nitrogen atmosphere using the standard procedure. The required pressure is achieved using water pump through low temperature trap. The monomer is then heated at a constant temperature of approximately 45^{o}C throughout the experiment, measured with a mercury thermometer.

Distilled MMA is collected in a flask which is kept at low temperature in an ice-salt bath. The distilled monomer is removed and preserved at low temperature. The purity of the distilled monomer is verified using FTIR spectroscopy.

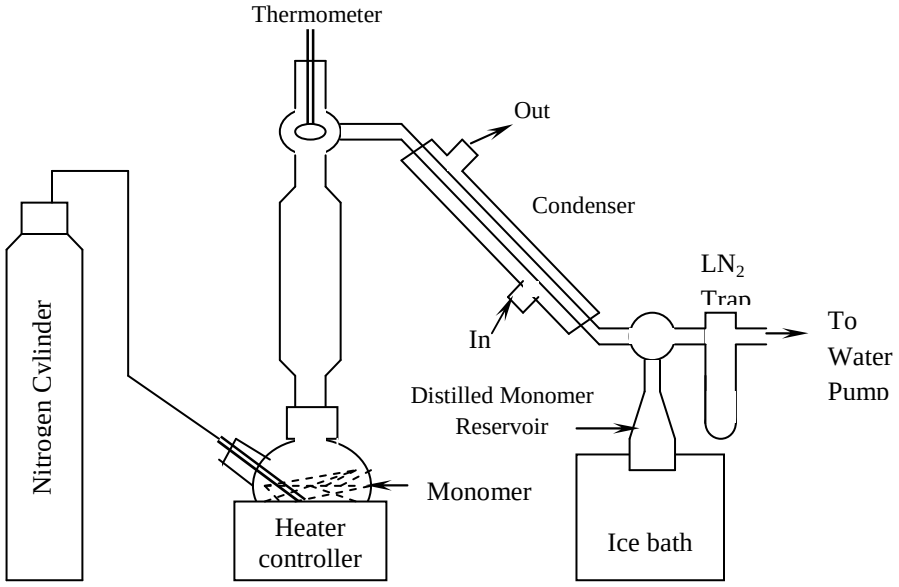

Fig-2.4: Monomer Distillation setup

2.3.4 Plasma Polymerization of MMA (PPMMA deposition):

The ID pattern developed by photolithography together with glass samples (for ESCA analysis) and silicon samples (for FTIR analysis) were used as substrates for plasma polymerization.

The schematic plasma polymerization set up is shown in Fig-(2.5). It consists of an inductively coupled tubular type gas flow reactor, rotary pump; RF generator, an impedance matching unit and liquid nitrogen trap [32]. The substrate holder was water cooled to maintain the substrate below room temperature. It is attached to the chrome-coated mild steel base plate. The system was evacuated using a rotary pump through a liquid nitrogen trap.

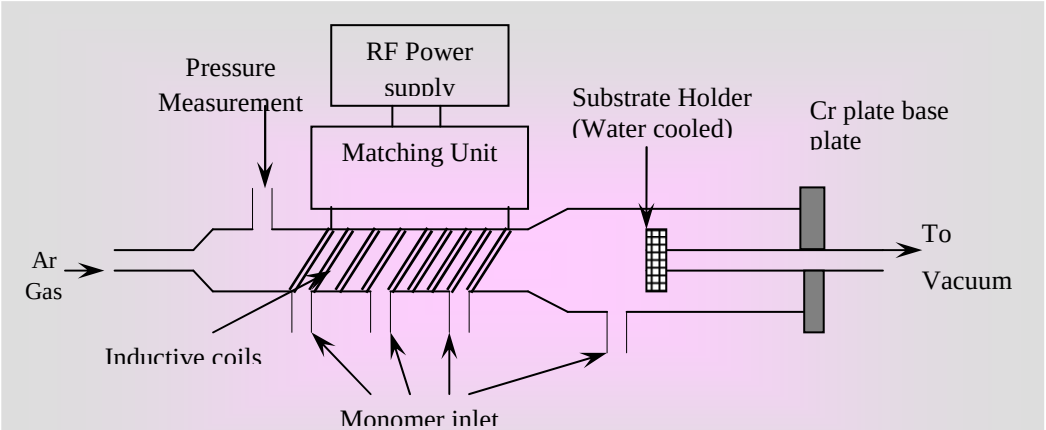

Fig-2.5: RF Plasma Polymerization System

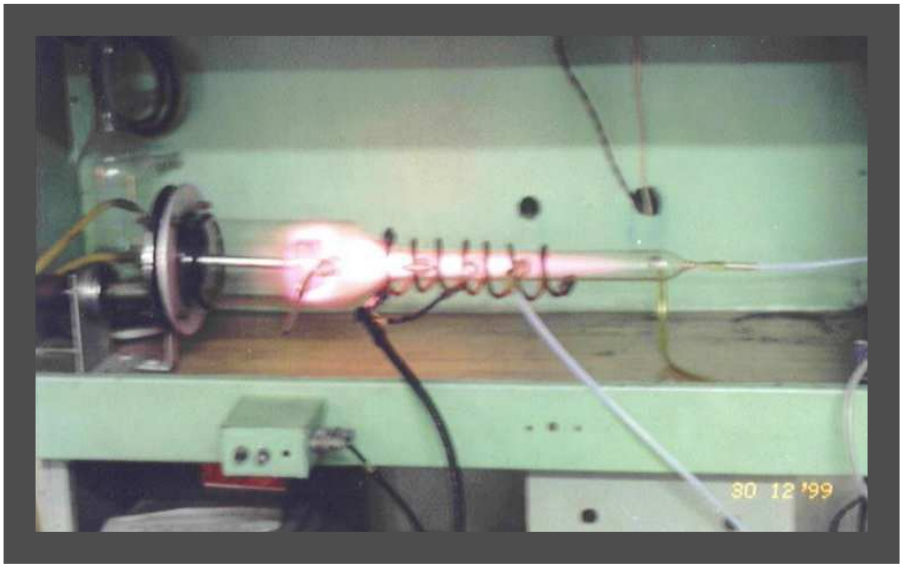

Plate-I: Plasma Polymerization System

The liquid nitrogen trap is used to condense the un-reacted monomer which will otherwise contaminate the rotary pump oil and also the laboratory environment. The reactor is inductively coupled to a RF power supply (RF plasma products, New Jersey model–5S) which operates at a fixed frequency of 13.56 MHz (established by international agreements) with a power output in the range 0 to 555 W.

A pie type impedance matching network (Model MN–500 from RF plasma products) is used to match the impedance of the plasma to the RF generator. The facility of the forward power and reflected power measurements is also provided in this model. The actual power fed to the plasma is the difference between the forward power and the reflected power.

The RF power is fed to an inductive coil, wound on the slim portion of the reactor (Fig-2.5) through a matching unit. The inductive coil has seven turns and is made up of hollow copper tube of 6mm outer diameter, it was tapped to the fourth turn to give an inductance of 0.95 μH.

After feeding the RF power to the coil, the inductor coupled to the reactor acts as an antenna and radiates the RF power outside to an approximate distance of about 2m, which considerably influences the AC mains line and fluctuations are observed on the instrument like DC power supply or MFC's etc. Hence any electronic instruments in the laboratory start malfunctioning. To avoid this, reactor is shielded with mild steel sheet box which is earthed electrically. The shield prevents the radiation coming out from the inductive coil. The reflected power is observed on the RF generator and the actual power coupled to the plasma is calculated by subtracting the reflected power from the input set power.

Mass flow controllers (MFC) of the accuracy of 0.1 sccm are used for the measurements of the carrier gas and the monomer flow rates. The MFC's are equipped with bypass valve so that before starting the actual deposition the air and other impurities from the monomer reservoir can be pumped out.

Flexible teflon tubes are used to introduce the carrier gas and the monomer into the reactor, as teflon does not react with the monomer. The system pressure is measured using digital pirani gauge (Model DHPG–1025), supplied by Hind High Vacuum Co. The system is evacuated using a rotary pump (Hind High Vacuum Co.) and the pumping rate is adjusted using diaphragm valve connected between the liquid nitrogen trap and the rotary pump, this helps in setting the required system pressure during the deposition.

The glass substrates with the ID structure to test the humidity response, Si samples for FTIR analysis and plain glass substrates for thickness measurement were mounted onto water cooled substrate holder after cleaning the substrates and the reactor.(Plate-1)

Initially the reactor is evacuated to a pressure of $1x10^{-2}$ Torr. After evacuating the system the gas line was evacuated [32]. The system was flushed for ten min by introducing argon at high flow rate to flush the system with argon. The argon flow rate is then reduced to get the specified experimental deposition condition. After the pressure is stabilized, argon plasma is initiated for ten min at 40 W.

The intense argon plasma further cleans the substrates. The monomer trap is filled with liquid nitrogen. The monomer is then introduced into the argon glow discharge and the gas flow rates, monomer flow rate, system pressure and the power are all adjusted to the required value. Due to the reaction of the monomer which take place in the glow discharge, as the deposition starts there is slight fluctuation in the system pressure. The deposition parameters were varied in the ranges:

Base pressure	0.01 mbar
Reactor Pressure (at deposition)	0.1 – 0.4 mbar
MMA/Ar flow rate	8-35 cc/min
RF Power	10 – 45 W

A large number of such experiments were carried out by varying the gas and monomer flow rates, system pressure and input power until deposition is finally observed.

2.4 FTIR characterization of PMMA films:

The molecular structure of the conventional plasma treated and the plasma polymerized films has been determined by Fourier Transform infrared (FTIR) spectroscopy [32]. IR measurements of the purified MMA were also taken. The films deposited on silicon substrates were used for IR analysis. IR spectroscopic technique is most widely used technique for structural characterization of polymer films. IR spectrometer from Perkin Elmer 2000 is used in transmission mode and operated between 400 and 4000cm^{-1} in a KBr medium to record the spectra. These spectra are compared with the standard IR spectrum of the MMA. The IR spectra

of MMA, PPMMA and the conventional PMMA as well as the plasma treated PMMA are analyzed. Polymer composition and the structure of PPMMA series polymer films deposited on silicon substrate are evaluated by Fourier Transform Infrared spectroscopy (FTIR).

2.5 Relative Humidity (RH) Measurement of the sensors:

The RH response of all the sensors fabricated was measured using both the continuous and step static mode. In the continuous mode the RH is changing with time where as in the step static mode the sensor is kept at constant RH for one hour each and then moved to the next RH and so on.

2.5.1 Continuous RH Response (Resistance Measurement):

The humidity cell shown in Fig-(2.6) and Plate-II was used for the characterization of the humidity sensor. It consists of a closed flask, half filled with water (Total volume 500ml). The relative humidity of the air in the enclosed system is given by equation (2.2):

$$\%RH = {e_w(T_1)}\Big/{e_w(T_2)} \times 100 \text{ ---------- } (2.2)$$

Where e_w (T_1) is the saturated vapor pressure of water bath at temperature T_1 and e_w (T_2) is the saturated vapor pressure at temperature (T_2) near sensor. The RH is varied by changing the temperature of the system using salt ice mixture. Table-2.1 gives the typical saturated vapor pressure of water with corresponding temperatures.

For the Relative Humidity response of the sensor, resistance Vs RH response was recorded using the above mentioned system. The sensor is kept in the flask 2 cm above the water level with contact leads. These leads are connected to the resistance meter for resistance measurement.

The flask is then surrounded by ice salt mixture for cooling, where as for the warming up process the ice bath is simply removed. From variations in T_1 and T_2 the RH is calculated, the resistance is noted on the digital multimeter from Rish (Model No.-12S) and the plots of resistance Vs RH are drawn. All the measurements were repeated twice to minimize experimental errors.

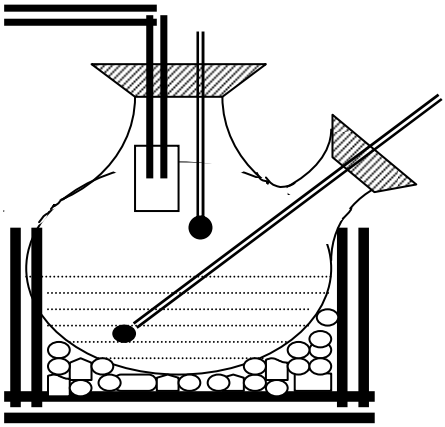

Fig-2.6: RH Measurement apparatus

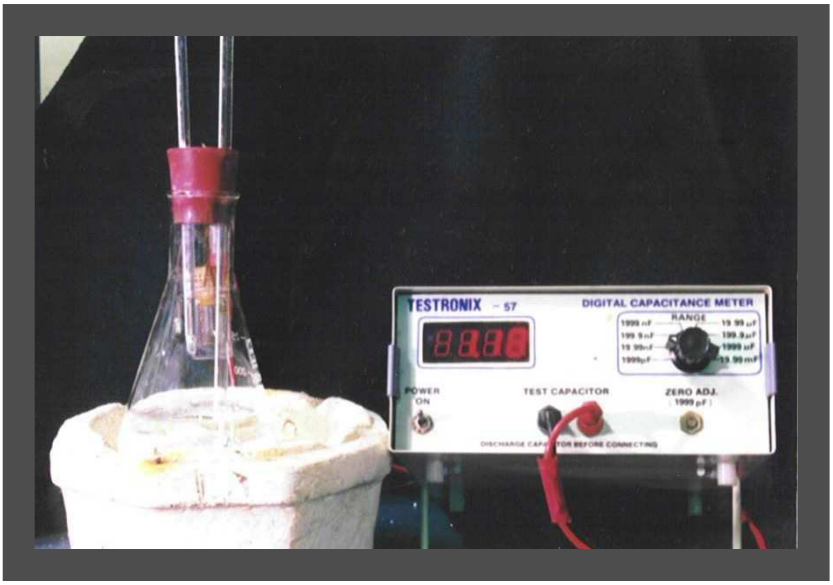

Plate-II: Continuous RH response measurement set up

Table-2.1: Typical saturated vapor pressures of water at different temperatures

Temperature ^{o}C	Saturated Vapor pressure	Temperature ^{o}C	Saturated Vapor pressure
-15	1.436	13	11.231
-14	1.560	14	11.987
-13	1.691	15	12.788
-12	1.834	16	13.634
-11	1.987	17	14.530
-10	2.149	18	15.477
-9	2.326	19	16.477
-8	2.514	20	17.535
-7	2.715	21	18.650
-6	2.931	22	19.827
-5	3.163	23	21.068
-4	3.410	24	22.377
-3	3.673	25	23.756
-2	3.956	26	25.209
-1	4.258	27	26.739
0	4.579	28	28.349

1	4.926	29	30.043
2	5.294	30	31.824
3	5.685	31	33.695
4	6.101	32	35.663
5	6.543	33	37.729
6	7.013	34	39.898
7	7.531	35	41.175
8	8.045	36	44.563
9	8.609	37	47.067
10	9.209	38	49.692
11	9.844	39	52.444
12	10.518	40	55.324

2.5.2 Static Step RH Response (Capacitance Measurement):

For the static step RH response, saturated salt solutions of five different salts were used. Borosilicate glass test tubes (diameter 1.25 in.) were initially cleaned using the procedure described earlier in section (2.3.2). The AR-grade salts were then introduced into the respective test tube using a spatula, the salts were made wet by using de-ionized water using a dropper. Care was taken to just wet the salt completely and not to dissolve the whole salt in water, thus a saturated salt solution was prepared. Table-2.2 shows the saturated salt solutions used and the respective humidities obtained over them. The test tubes were sealed using a greased rubber stopper into which wire leads were inserted.

Table-2.2: Saturated salt solutions used and the respective relative humidities obtained over them.

Saturated Salt solution	% Relative Humidity
Preheated Silica gel	00%
LiCl	12%
$MgCl_2$	33%
$Mg\ (NO_3)_2$	53%
NaCl	75%
K_2SO_4	97%

The sensors were initially placed in silica gel for 1 hr, and the capacitance was recorded. Then it was transferred to each constant RH cell with increasing RH from 0%, 12 %RH to 92%. The sensors were kept in each cell at constant RH for one hour before the capacitance was recorded. The readings were repeated for decreasing in RH i.e. from 92% RH to 0% in a similar fashion. The measurements were repeated twice to minimize errors.

Plate-III: Step static RH measurement set up

2.5.3 Response and recovery Time of the Sensor:

The response time of spin coated , plasma treated and plasma polymerized sensors was measured by first keeping the sensor in dry environment (silica gel) for 24 hrs. Its dry capacitance/resistance was then recorded. The sensor element was then immediately transferred in a static RH environment namely 75% or 92%. The change in capacitance/resistance over time was recorded after every one sec till the capacitance/resistance showed saturation. The graph of capacitance/resistance Vs time was plotted. From this graph the response time was calculated in the linear portion of the curve between 10% and 90 %RH.

The recovery time of plasma treated and plasma polymerized sensors was measured by first keeping the sensor in humid environment (K_2SO_4) for 1 hour. Its humid capacitance/resistance was then recorded. The sensor element was then immediately transferred in a static RH environment namely 12% or 0%. The change in capacitance/resistance over time was recorded after every one sec till the capacitance/resistance showed saturation. The graph of

capacitance/resistance Vs time was plotted. From this graph the recovery time was calculated in the linear portion of the curve between 90% and 10 %RH.

2.6 Optical response of PMMA:

The PMMA solution (Concentration 0.1gm in 10 ml of chloroform) was then used to form the films of PMMA by drop casting (5µL of solution by a micropipette) on the borosilicate glass substrate having fixed area of 1cm×1cm. Drop was spread on the substrate neatly which were used as samples. The thicknesses of the films were varied by changing number of drops of PMMA solution. The thicknesses of the films were measured by using gravimetric method.

A simple optical method was used to test the prepared films for their sensitivity towards humidity. Closed humidity system for testing the humidity responses of the films was fabricated as shown in Fig. 2.7. It consists of a closed glass chamber (volume: 6 L), with a neck for inserting a sample under test and a probe of the standard Vaisala humidity meter (humidity range: 0–100% RH with an accuracy of 1–5% RH for different humidity ranges). The chamber was kept on an aluminum plate and was sealed from outside by modeling clay to make the system air tight. The relative humidity was created inside the chamber by keeping hot water in the beaker and simultaneously monitoring the humidity to get maximum(85%)RH at room temperature (30–35°C) as measured by the standard Vaisala humidity meter. After achieving 85% RH the beaker was removed. The 85% RH was kept for 5 min. The chamber was gently lifted and the saturated vapors were wiped by tissue papers and the chamber was kept at its original position. Humidity was decreased by putting dehumidifying material like phosphorous pentoxide (P_2O_5) in an appropriate amount in a pettry dish. While humidifying and dehumidifying the chamber, the 2–5°C change in the temperature was observed.

A He–Ne laser beam, incident perpendicular to the plane of the film, is allowed to pass through the sample (films) and the transmitted output is measured using a simple photovoltaic detector. The samples were mounted in the chamber and were exposed to the highest humidity. The related output in the form of voltage was measured by Digital Multimeter (DMM) (Agilent U1241A).

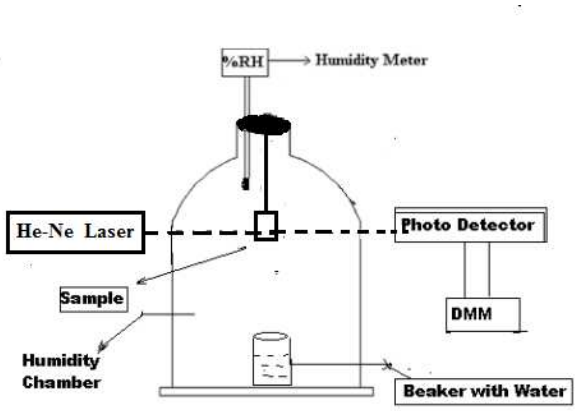

Fig.2.7: Experimental set up for the measurement of relative humidity.

Keeping dehumidifying material (Thomas Baker's P_2O_5 LR grade) in the chamber, relative humidity was decreased to the lowest value and related voltage was also noted. The change in relative humidity is related to the change in the output voltage of the sample. Normalized output with respect to the lowest relative humidity is plotted. Output is normalized with respect to voltage at lower humidity i.e.

$$\% \text{ Normalized Output} = [(V_{lh}-V_{hh})/(V_{lh})]*100$$

Where V_{lh} is output voltage at low humidity and V_{hh} is output voltage at high humidity.

The sensitivity is defined as the change in transmitted output (mV) per unit change in RH%, i.e. δ (mV)/ δ (RH%) [6]. As there are four samples (one, two, three and four drop) having different thicknesses, sensitivity is calculated for each sample.

We noted optical response of drop casted as well as spin coated PMMA samples.

Measurement of moisture in the samples-

For the measurement of moisture, the samples were exposed to 100% RH for around 10 min. and then immediately weighted (Wx) on electronic balance (Citizen CX165) Then these samples are vacuum dried and weighted again at room humidity (35%RH). The percentage moisture content is calculated using following equation [19]

$$\text{Moisture}(\%)=[Wx-W_0]/W_0$$

Chapter III

Results and Discussion on humidity sensing characteristics

Results on humidity sensing characteristics of spin coated, plasma treated and plasma polymerized PMMA films are described in this chapter and discussed. Further they are compared amongst themselves and with the ones available in the literature.

3.1: Spin Coated PMMA as humidity sensor- Results and Discussion

3.1.1 Introduction

The process of applying a solution to a horizontal rotating disc, resulting in ejection and evaporation of the solvent and leaving a liquid or solid film, is called spin coating. Spin coating is a unique technique in the sense that it is possible to apply a highly uniform film to a planar substrate over a large area (30 cm) with a highly controllable and reproducible film thickness. The spin-coating technique applies to inorganic, organic and mixtures of inorganic/organic solution.

Because of its ability to produce uniform layers, transparency in visible wavelengths and its suitable glass transition temperature, PMMA (Poly (methyl methacrylate)) is used as host in many opto-electronic applications. In thin film humidity sensing applications, achieving the required thickness with desirable surface quality is very important. To produce a coating with such thickness, dilute solutions of polymer are necessary. Generally, thickness of layer in this method is dependent on spin speed, primary concentration, viscosity of solution and solvent vaporizability [1, 2]. The nature of this dependency varies across different materials and solutions.

Depositing a viscous fluid on a horizontal rotating disc produces a uniform liquid film. During deposition the disc should either be static or be rotating at a low spin speed, where after the disc is rapidly accelerated to a high spin speed. The adhesive forces at the liquid/substrate interface and the centrifugal forces acting on the rotating liquid result in strong sheering of the liquid which causes a radial flow in which most of the polymer solution is rapidly ejected from the disc. This process combined with subsequent evaporation of the liquid causes the thickness of the remaining liquid film to decrease. For a solution, e.g. a polymer solution, the evaporation process causes the polymer concentration to increase (and thus the viscosity) at the liquid/vapor interface, i.e. a concentration gradient is formed through the liquid film, which, after evaporation of most of the remaining solvent, consequently results in the formation of a uniform practically solid polymer film.

It is thus known that spin speed and solution concentration significantly affect the film thickness, while the amount of solution initially deposited on the disc, the rate at which it is deposited, the history of rotational acceleration prior to the final acceleration, and the total spin time have limited or no effects.

3.1.2: Sample preparation by spin-coating process

Spin coating of PMMA on to silicon substrate was carried out at various conditions. The concentrations of PMMA were taken as 0.1g, 0.2g and 0.3g / 10cc of $CHCl_3$. The baking temperature of the sample after spinning was kept at 50^{o}C. This temperature range was selected as the T_g of PMMA is 105^{o}C. Above this temperature PMMA may degrade. Moreover baking of the photoresists, which are basically polymer/resins is also done in the similar temperature range. The baking time was kept at 20 min. At this time the film becomes completely dry and nonsticky. Due to baking the film becomes dry and its adhesion with substrates also get improved. The spinning was carried out at different spin speed of 500, 1000 and 1500 rpm for a constant time of 1 min. The FTIR spectra were taken on one sample for each condition.

As described above, total 27 samples were prepared. The baking temperature was 60 ℃ and baking time was 20 minutes. The spin speed, concentration and obtained thicknesses are tabulated in table 1 below.

Table-3.1: Thickness (μm) variation at different Spin speed and PMMA concentration.

Conc. (gm) / Spin speed (rpm)	0.1	0.1	0.1	0.2	0.2	0.2	0.3	0.3	0.3
500	5.25	5.19	5.27	5.70	5.64	5.72	5.98	6.09	6.11
1000	3.40	3.22	3.30	3.61	3.70	3.69	4.36	4.40	4.47
1500	2.84	2.79	2.80	3.10	3.01	3.08	3.28	3.34	3.29

As can be seen from the table for particular concentration the thickness of the film decreases with increase in the spin speed. This is indicated in the following table 3.2 and Fig 3.1.

Table-3.2 Thickness variation w.r.t. speed and concentration.

Speed (RPM)	Average Thickness(µm)		
	Concentration(gm)		
	0.1	0.2	0.3
500	5.23	5.7	6.09
1000	3.22	3.61	4.4
1500	2.85	3.01	3.29

Fig-3.1-Schematic of the relation between film thickness, speed and concentration in the spin-coating process.

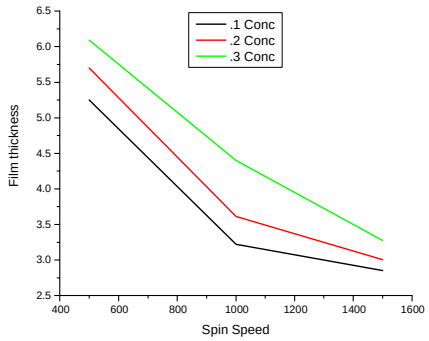

For particular spin speed the thickness is larger for larger concentration (larger viscosity). These results are as per expectations [2-6]. It can also be seen that for particular concentration the change in the thickness is not greater than 5%. This indicates the reproducibility of the results. The thicknesses obtained are in the range of 2.79µm to 6.11 µm.

3.1.3: FTIR Characterization of the spin coated films:

In order to confirm the deposition of PMMA, FTIR absorption spectra of the deposited films on silicon substrate was taken (Fig.3.2).

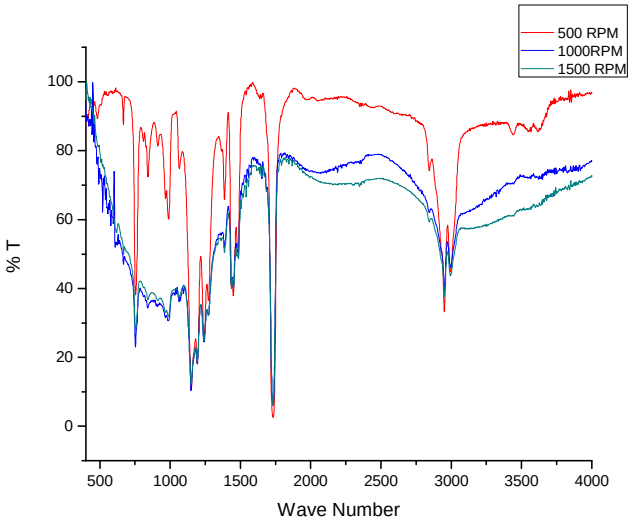

Fig-3.2: **IR spectra of spin coated PMMA samples**

Fig.3.2 shows the representative IR spectra of the untreated PMMA films spin coated by 500, 1000, 1500 RPM on to silicon substrates. The peak values observed at 2995, 2946, 1731, 1447, 1240, 1149, 986, 610 $cm^{-1}$are attributed to CH_2 asymmetric stretch, CH_2 symmetric stretch, carbonyl group (C=O), CCH_3, C-O, CH bend in ester group, O-CH_3 rocking and silicon respectively. These peaks match with the standard reported FTIR spectra of PMMA [7, 8] indicating confirmation of PMMA films**.** A broad –OH feature in the spectrum between 3600-3900 cm^{-1} is due to chemisorbed H_2O [8]. This shows all the expected peaks of PMMA confirming the material.

3.1.4: SEM of spin coated film:

Scanning electron microscopy was carried on all the spin coated samples. The typical micrograph is shown in fig.3.3

The films coated with 1000 and 1500 RPM of 0.1, 0.2 and 0.3gm concentration showed smooth, uniform surface with no cracks or micro-pores at all magnifications and also at high resolutions hence they were not photographed.

Typical SEM photographs of the film spin coated at 500 RPM and the other at 1000RPM with the concentration of 0.3gm on silicon substrate are shown in Fig.3.3(a and b) respectively. The topography is different in the two films.

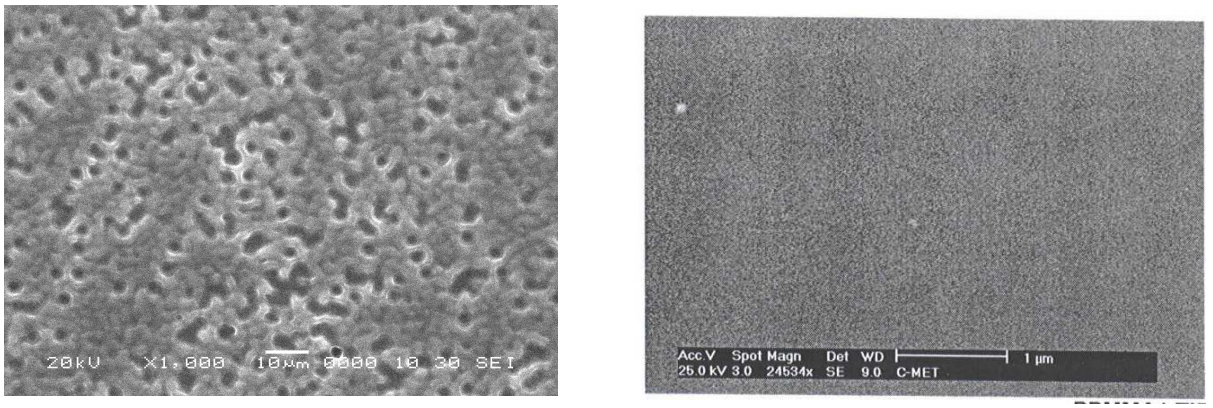

a **b**

Fig-3.3: SEM of spin coated film.

3.1.5: Humidity Response of the spin coated films:

Humidity response of the films was initially measured in terms of change in resistance. It was observed that the resistance value was in GΩ and the readings were not stable. Secondly it was also observed that change in resistance with humidity was very small, of the order of KΩ and therefore cannot be measured accurately. Therefore it was decided to use capacitance method. Next the voltage-divider or Wheatstone-bridge circuit is typically used for most resistive sensor applications. It is reported by Story et. al. [9] that the linearity of the humidity response depends on the relative values of the film resistance and external resistance selected. For small values of external resistances in relation with the film resistance the humidity response is nonlinear and for comparable values the relation is linear. The resistances of the films in the present work are found to be very high. Therefore high value of external resistance is required which will pose problems in stability of the readings. This circuit characteristic limits the ability of a resistive sensor to provide a linear response with high sensitivity at low RH levels, but can provide increased sensitivity at higher RH levels. This also prompted the use of capacitive measurements.

Films of various thicknesses in the range of 2.79µm to 6.11 µm were used for humidity sensing. Humidity response of the films in terms of capacitance was initially measured using continuous step method. No repeatable results were obtained. This may be because of the slow response of PMMA to comparatively fast variation of humidity. Further experiments were therefore carried out using step static method.

To take the readings of capacitance with changing humidity LCR meter (Agilent 4284A) was used. Here one other parameter was introduced and that was frequency. Readings of capacitance as a function of frequency (from 300Hz to 1MHz) at different humidity levels for all the films were taken. The responses were similar. A typical response for thickness 5.25µm is plotted in Fig. 3.4. It is observed that the capacitance is almost constant over the given frequency range except at 500Hz and 1MHz. At these two frequencies high capacitance value is observed. The reason of these high values is yet to be known. Therefore these frequencies are not used in further measurements.

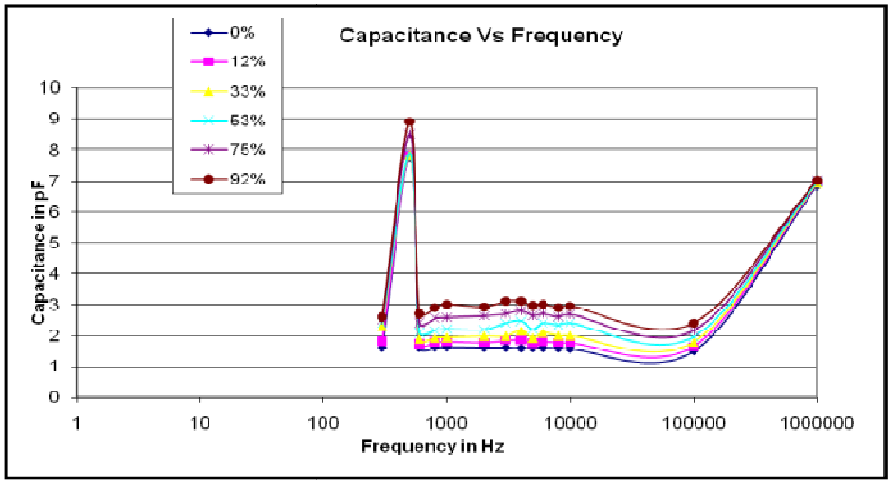

Fig-3.4: Capacitance Vs frequency variation for one sample.

It is also observed that the capacitance increases with humidity and the change in capacitance occurred for each frequency (including 500Hz and 1MHz) is not greater than 3pF. Humidity response is studied, at typical frequency of 5000Hz.

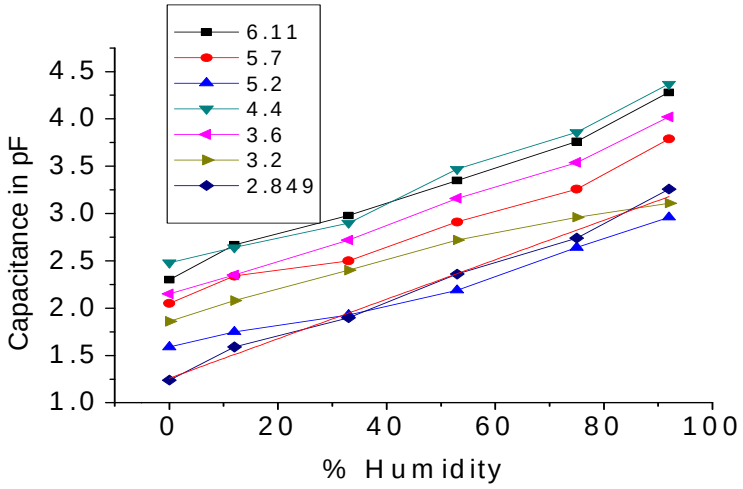

Fig-3.5: Capacitance Vs Humidity variation for different thicknesses.

Humidity response of the films of different thicknesses measured at frequency of 5000Hz is shown in Fig.3.5. It shows that as the thickness of film increases, its capacitance value also increases. This is as expected because the value of the capacitance is directly proportional to the cross-sectional area of the dielectric film. It may be noted that the electrodes of IDT are 33micron thick and inter electrode distance is 0.5mm. Further the PMMA film thickness varies from 2.85 to 6.11micron.

Therefore it is possible that the electric field between the electrodes is entirely through film. So films can work here as a dielectric material. So depending upon thickness we got the variations in the capacitance values [9].

Further the response of all the films of different thicknesses is linear. It may be noted that capacitive-type humidity sensors rely on a change in permittivity (ε) of a ceramic or polymer dielectric with relative humidity. PMMA adsorbs water. Water has permittivity of ~80 and therefore adsorption of water is increasing the permittivity of PMMA which is 2.6. Since amount of water adsorbed increases with increase in humidity and therefore the capacitance increases.

If thickness Vs sensitivity (slope) graph Fig.3.6 of these values is plotted, it shows a random variation. This may be attributed to the variation of the humidity affected thickness of the films. Since PMMA is hydrophobic whole of the thickness of the film may not absorb humidity. How much thickness will get affected is unpredictable.

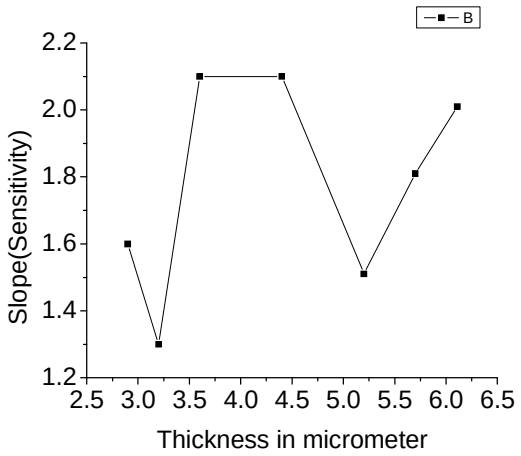

Fig-3.6: Thickness Vs sensitivity (slope) graph

The sensitivity of high thickness film is greater than films having low thickness. So graph indicates some variations accordingly.

3.1.6: Response and recovery time of the films:

Response and recovery time of spin coated film having 6.11µm thickness was taken. It was approximately 10 minutes and recovery time of 12 minutes which were better than reported value of 7-14 min [10] for the plasma treated films and 15 min [11] for different humidity values.

In spin coated films, thickness of the film is of the order of some microns. The adsorbed water do not get into the film, but it remains on the surface only. So the change in response time and recovery time is attributed to surface phenomena.

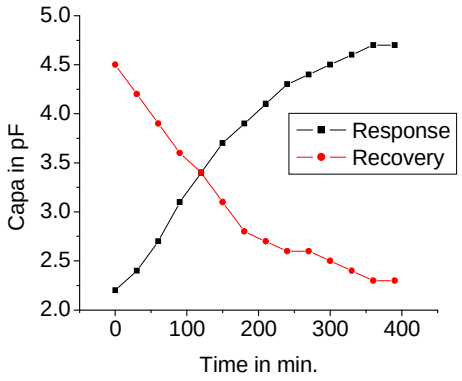

Fig-3.7: Response and recovery time of film.

3.1.7 Hysteresis of spin coated films:

Hysteresis is defined as the maximum difference in the response curves taken while increasing and decreasing the variable parameter, at the same value of parameter. The hysteresis curves (capacitance versus humidity) for 6.11µm thickness film is shown in fig.3.7. The hysteresis is found to be 1% for all RH values. For other films also hysteresis of same order was observed. The hysteresis in the response at lower RH is a result of slow desorption of the water from the surface of PMMA. At higher humidity, the condensation occurs and forms a cluster over the surface of the film, which attributes to hysteresis [10].

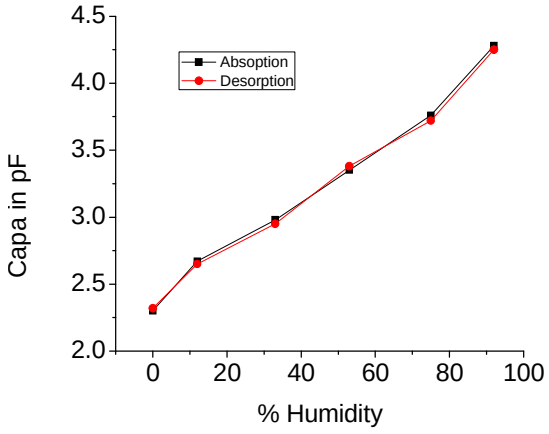

Fig-3.8: Hysteresis result for 6.11µm thickness film.

The sorption mechanism can be understood by considering a dry sample placed in certain humidity, and then the zone which is immediately adjacent to the surface takes up water both by filling of micro-voids and by a process of accumulation of water on the surface which results in small clusters on the surface. The accumulation continues to contribute to the uptake of water as a result there is

acceleration in the rate of sorption which continues until the accumulation in the surface zone of the samples reaches an equilibrium value. There after a constant rate of sorption is achieved [12]. The opposite will be the case in case of de-sorption.

3.2: Plasma treated PMMA as humidity sensor- Results and Discussion:

3.2.1: Introduction:

The hydrophilicity of polymers is one of the key factors that determine the surface properties of polymeric materials. It controls various properties of polymers, including wettability, adhesion, colorability, and anti-electrostaticity. Depending on the situation, sometimes more hydrophilicity or hydrophobicity of a polymer surface is desired. For modification of the surface properties of a polymer, a number of methods have been developed. Physical and chemical modifications are two main methods. The physical modifications include plasma, [13,14] corona, [15,16] flame [17] and ion beam treatments [18] while the chemical modifications comprise chemical reaction and wet treatment.[19,20]

As is observed from literature survey, surface modification of polymer surface is known to increase the wettability and surface energy of the polymer surface [21, 22]. It is thought that this technique may be able to give higher sensitivity and better response and recovery time. Secondly, as adsorption of humidity is a surface phenomenon and plasma treatment for a few minutes can easily change the surface structure, so the surface of the PMMA films is modified by plasma treatment and its effect is studied. For this purpose, Emitech K1050X Plasma Etcher/Asher/Cleaner system was used. Argon gas was introduced in the system. The flow of argon gas was 20sccm. PMMA solution of 0.1 concentrations was taken. Plasma treatment was done with the power of 20, 30 and 40watt for 2, 5 and 8 min. The system pressure was kept constant at 0.2 mbar. Power greater than 40 W and time larger than 8 min was not used as this lead to etching of the samples.

3.2.2: The plasma treatment process

Spin coating of PMMA on to IDT, glass and silicon substrates was carried out as stated in section 3.1.2.The concentration of PMMA used in the experiments was 0.1 g /10 c.c. $CHCl_3$. The spinning was carried out at the specific spin speed of 500 rpm for a constant time of 30 second. The samples prepared were plasma treated as explained in section 2.3.2 (check section number).The FTIR spectra were taken on one silicon sample for each condition.

3.2.3: Characterization of the plasma treated films:

3.2.3.1 FTIR analysis:

The IR spectra of the untreated PMMA film spin coated on to silicon substrates is given and discussed in detail in section 3.1.3.

Fig-3.9, 3.10 & 3.11 show the FTIR absorption spectrum of argon plasma treated samples on silicon with power variations (20,30,40watts) and time variation (2,5,8 min.) respectively. Peaks typical of PMMA shown in Table-1 are observed. In addition some new peaks are seen to be present and/or the intensity of the old peaks is observed to have changed.

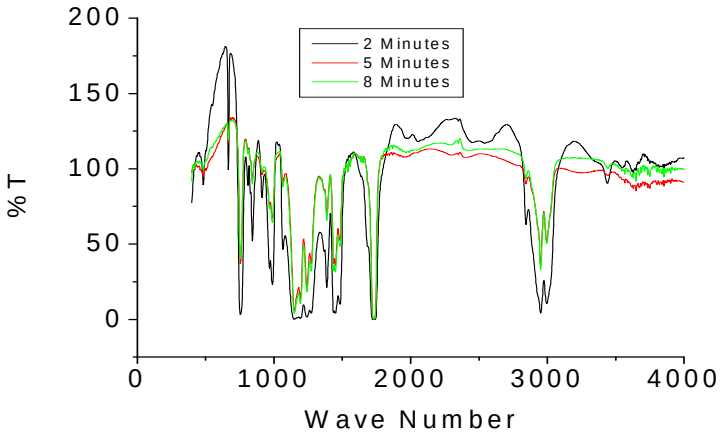

Fig-3.9: FTIR of samples plasma treated at 20watt for different time durations.

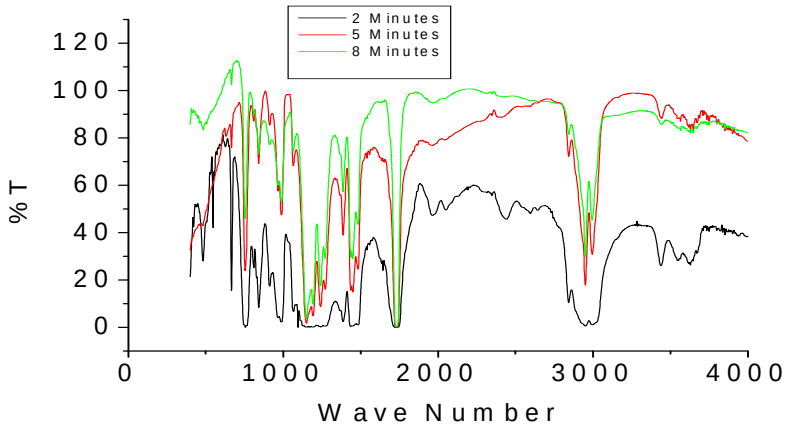

Fig-3.10: FTIR of samples plasma treated at 30watt for different time durations

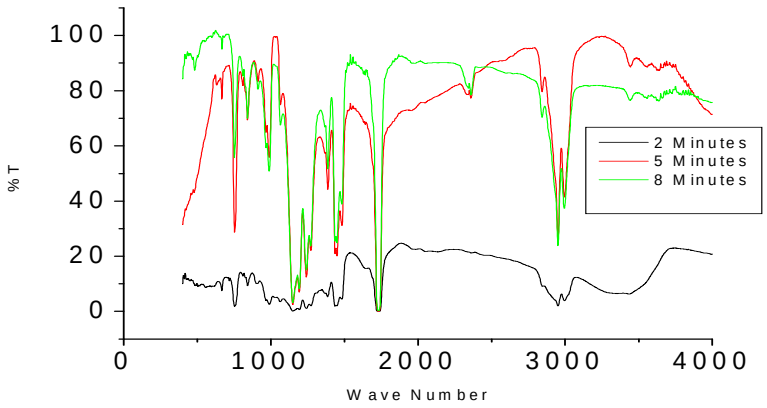

Fig-3.11: FTIR of samples plasma treated at 40watt for different time durations

The band due to ester C-O stretching mode at 1150 cm^{-1} is broad in modified samples which is characteristic of cross linked polymer system [23,24]. Comparison of the absorption peaks seen in the region between 3600-3900 cm^{-1} (attributed to -OH feature) shows newly formed and/or increased –OH functionality's after treatment which may be responsible for increase in the hydrophilic properties of the top surface[25]. The OH functionality varied from sample to sample sugges variation in the hydrophilic character of the topmost surface due to argon plasma treatment. For samples treated at a constant power at 40 W with time variation from 2 to 8 min are substantially reduced and not distinct(sentence incomplete what has reduced is not clear). For all the samples (except sample treated at 30watt for 2 min.) the carbonyl and the ester functionality's were visible and there was no notable shift in the peaks positions of C=O at 1730 cm^{-1} and C-O at 1149 cm^{-1} & 1241 cm^{-1} within ± 3 cm^{-1}. For that particular sample (treated at 30 W and 2 min??? mention so.) these peaks are shifted to 1720, 1154 cm^{-1} and 1241 peak is absent. This suggests that for other samples the C=O and C-O environment has remained more or less static even after the plasma treatment although their intensities varied considerably suggesting cross linking [26]. In the present case in PMMA C=C does not exist and C=O & C-O are responsible for cross linking of the samples.

M. Matsuguchi *et al* [26] have shown that with the increase in the photo irradiation time there was a rapid decrease in the absorbance at 1630 cm^{-1} of the C=C stretching vibration. They have attributed this fall in intensity of the C=C absorbance peak to the degree of cross linking due to photo irradiation. They have concluded that with photo irradiation time the degree of cross linking goes on increasing until it reaches a maximum after which it remains constant. The peaks at 1149 and 1241 are clearly observed, Ulrike *et al* [27] also observed those peaks at 1150 cm^{-1} and 1240 cm^{-1} separately and

with sufficient intensity. The %transmission peak intensity of C=O and C-O showed an overall decrease with increased power.

Choi *et al* [28] have studied chemical changes in PMMA caused by various irradiations like UV, X-ray, electron and proton beams. They have suggested that gaseous products like CO, CO_2, CH_4 and main chain scissions may have caused due to irradiation leading to formation of new bonds in the polymer chain, cross linking being one of them. They have further confirmed that the decrease in the carbonyl bond intensity is proportional to the incident dose of different radiations used.

The changes are also observed in the PMMA films exposed to plasma in the present work. The argument by Choi *et al* [28] that chain scission and the formation of new bonds due to irradiation by UV, X-ray, electron and proton beams can also be extended in case of the present work. This is because there are various species available in the plasma for interaction with matter, but the exact estimate of them is difficult.

The C=O and C-O absorption peaks(write peak values) in all the argon plasma treated samples (for power variation at constant time of 2/5/8 min) were narrow and distinct only their % absorption intensity changed. These results can therefore be compared with those of Ulrike et al [27]. The % absorption peak intensity of C=O and C-O showed an overall decrease with increased power at constant time.

In case of samples treated for 5 and 8 min at 20, 30 and 40 W it is interesting to note that there is an increase in C=O as well as C-O functionality. The increase in C-O can be due to formation of new C-O functionality as we had also observed loss of C-C 1640 cm^{-1} in the FTIR spectra. This could be attributed to the fact that at this power, time and pressure the oxygen present in the reactor (the reactor pressure was 0.2 mbar) could have got incorporated into the material. This is in good agreement with the work carried out by Vargo Gradilla [29]. They have studied the surface modification of PMMA by O_2/H_2O and H_2O RF glow discharge plasmas. They had observed an increase in the carbonyl functionality in PMMA after O_2/H_2O RF plasma treatment for 10 min.

3.2.3.2 The SEM of the Plasma Treated Samples:

To observe the surface roughness or the extent of micro-pore or cracks formation, the SEM was taken of all selected samples namely argon plasma treated with 20Watt power applied for 2,5,& 8 minutes, 30 Watt power applied for 2,5,&8 minutes, 40Watt power applied for 2,5,&8 minutes.

Micrographs are shown in Fig- 3.12. Micro pores were observed all over the sample surface at a low magnification X1000 and at higher magnification of X5000 these pores are found to be 1 to 3 μm wide. The micrographs shown for all the samples are taken at same magnification.

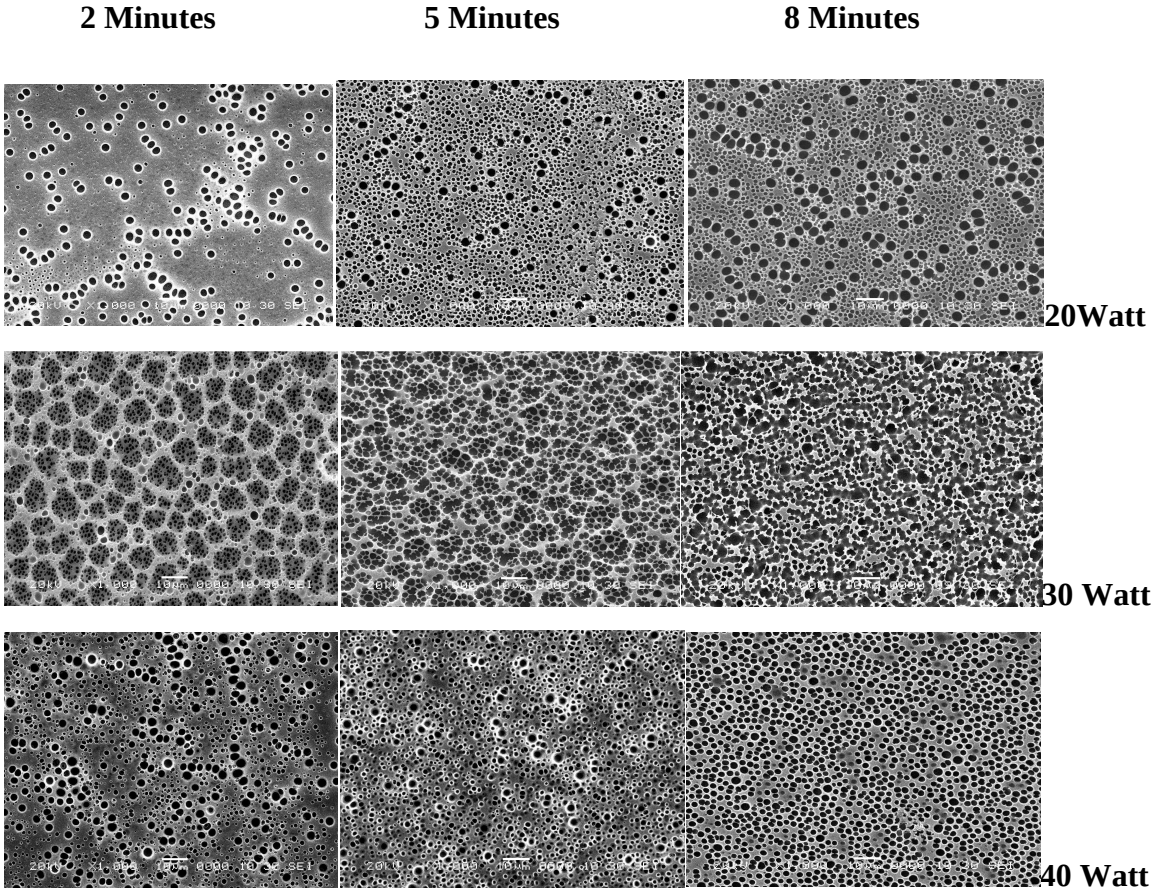

Fig-3.12: SEM of plasma treated samples

The pore density was low(20W/2 min. sample) compared with the samples treated at higher powers and longer times. When observed under the SEM, the untreated samples showed a very smooth surface at all magnifications and also at high resolutions. In the present work, it has been observed from the FTIR and SEM that plasma treatments have lead to various modifications in the polymer like cross linking, changes in molecular weight and free volume due to scissioning, introduction of hydrophilic sites (C=O) and increase in porosity leading to surface roughness. One or more of the parameters may be responsible for giving the observed response of films to humidity.

3.2.4. Humidity Response of the Argon plasma Treated Films:

Humidity response of the plasma treated films is measured in terms of change in capacitance at 5000 Hz using LCR meter (Agilent 4284A). Change in capacitance with respect to humidity of three samples plasma treated with the power at 20,30 and 40Watt for 2, 5, and 8 minutes are given in Fig.15(a-d) and their outputs are compared with the output obtained for spin coated films with different spin speeds.

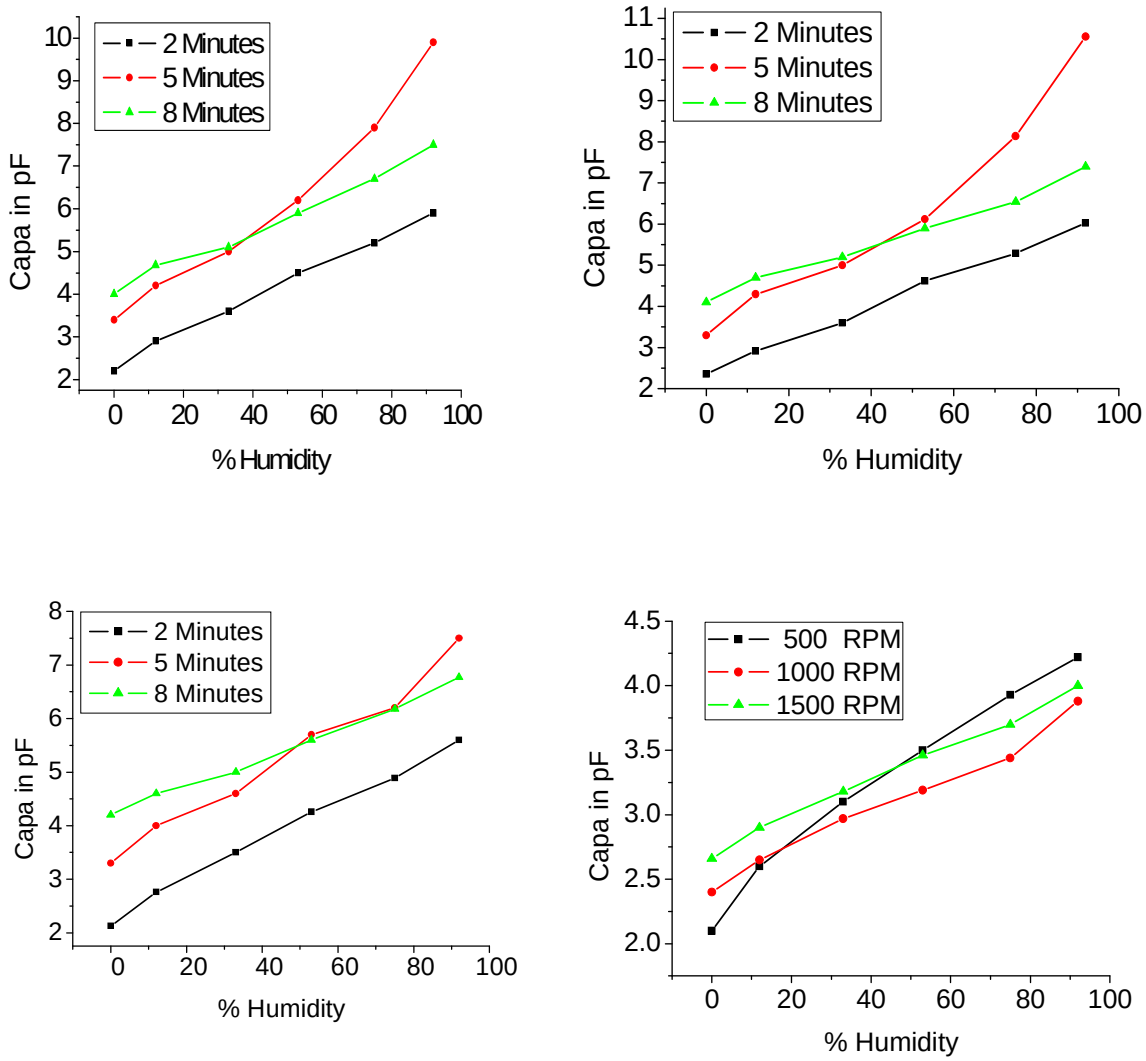

Fig-3.13.: Capacitance change w.r.t. humidity for plasma treated and spin coated samples a)20 W,b)-30W,c)40W, d) Spin Coated films.

Fig. 3.13(a-c) represent change in capacitance with humidity of plasma treated samples at 20 watt, 30watt, 40watt respectively and Fig 3.13(d) is for spin coated samples with different speeds.

These graphs indicate that at 5000Hz frequency due to plasma treatment, output increases in the linear fashion as the humidity was increased. The reasons for change in output for films treated for different time intervals may be surface roughness - pore size and pore density. As these films are treated at the powers of 20-40 W, surface roughening is quite possible. This change occurs due to surface modification. While for the spin coated sample, its output response is slowly increasing up to the humidity of 53%. Afterwards it increases in the linear fashion. The reason behind this behavior is in the spin coated samples water did not get absorbed in the material, but it remains on the surface only. So the change in capacitance occur is small initially and as humidity increases the output increases after 53% humidity.

It is also observed that the maximum change in capacitance in whole range of humidity for plasma treated samples is 7pF and that for spin coated sample it is 3pF. The dielectric constant of PMMA is 2.6 and that of water is 80, the uptake of water into the polymer leads to changes in the overall dielectric constant of the material hence leading to change in the capacitance of the sensor with %RH. Further plasma treatments have lead to various modifications in the polymer like, cross linking, changes in molecular weight, free volume due to scissioning, introduction of hydrophilic sites (C=O) and increase in porosity leading to surface roughness. One or more of the parameters may be responsible for giving the observed response of films to humidity.

The nature of the RH response curves follow specific trend over the entire range of RH that was measured. Overall it is noted that the slopes (pF/%RH) of the curves are different for different treatment time and different powers. Those values are tabulated below (Table 3.3).

Table -3.3: Slopes (sensitivity)(pF/%RH) of the plasma treated samples.

Power. / Treatment time	20W	30W	40W
2 Minutes	0.0375	0.03888	0.0355
5Minutes	0.07125	0.07825	0.04375
8 Minutes	0.03525	0.03375	0.02713

The sensitivity values obtained are low, probably due to the small thickness **(2-6µm)** of the films. Again water in that situation may not get into whole of the thickness of the material irrespective of microporosity of the surface. So change in capacitance occured is small w.r.t. change in humidity.

Surface roughness is another factor which is responsible for sensitivity changes. If SEM shown in the fig (3.12) are observed, it is noted that as time of treatment is increased, number of pores are increasing. It means that the samples treated for 8 minutes should show maximum sensitivity factor, but that is not observed. On the contrary for 8 minutes the sensitivity factors are less than other samples. This may be due to the pore size variations. The pore density is increasing but the pore size is decreasing with the increase in treatment time as well as with treatment power.

Therefore one can say that both surface roughness and hydrophilicity may in addition to some other factors contribute to the overall sensitivity of the sensor.

Other factors which have to be considered are cross linking and change in molecular weight and free volume of the polymer due to plasma treatment. Cross linking is evident in most samples but their degree is difficult to calculate as derived from FTIR analysis. The change in the molecular weight is difficult to predict. It has been proposed that increase in the molecular weight leads to increase in the water uptake whereas decrease in the molecular weight leads to closer molecular packing leading to decrease in the available free volume necessary for water uptake[30]

According to Andrew *et al* [30] the differences in the free volume in the polymer is mainly responsible for the observed differences in the sensitivity of the sensors. The dual–state model of gas sorption has been widely used in the interpretation of gas diffusion in amorphous polymers including PMMA. In this model, sorbed gas molecules are interpreted as being a part of one of two populations in the polymer, the Henrian population of molecules sorbed by ordinary dissolution mechanisms in the polymer, and the Langmuir population residing in the free volume within the polymer.

The concentration of water sorbed in the Henrian sites in these films will depend on the availability of hydrophilic sites like C=O in case of argon treated samples. The Langmuir population (dependent on the free volume available in the polymer) of the sorbed gas molecules on the other hand will depend on the available free volume which in turn will depend on the cross linking density and degree of packing porosity, and the presence and absence of side groups of the polymer backbone. Other factors which contribute to the water uptake are molecular weight and surface roughness.

Turner D.T. [30] has studied the sorption kinetics and volumetric changes in PMMA sheets, where by after the immersion of PMMA sheets in water for a week he observed that the total percentage increase in weight of the samples leveled off near 1.2% in which about one-half of the water was observed to be accommodated in micro voids. Further, Turner D.T. [31] studies on effect of molecular

weight suggest that samples of low molecular weight (Mw = 60600, Mn = 33200) take up only 1.2 % water as compared with the samples of high molecular weight ($Mw>10^6$) which take up water up to 2.0%. From the density changes which accompany water sorption it is estimated that a low molecular weight sample accommodated only 15% water in micro voids whereas about 50% of water was found in samples of high molecular weight. This suggests that lower molecular weight means closer molecular packing leading to lesser micro void formation.

If we once again observe the C=O intensity in these samples it is observed that the C=O absorption peak increases as we increase time of treatment. Once again it is to be noted here that these samples with well defined C=O absorption peaks did not give any improvements in the sensitivity, on the contrary these samples showed lesser sensitivity (treatment time of 8 min.) than the untreated sample suggesting the bulk properties of the polymer may have changed due to plasma treatment leading to changes in the free volume.

All the factors discussed above are responsible and play a crucial role in determining the uptake of water in the polymer. The percentage contribution of each factor in the water uptake is however not known but the availability of free volume and the presence of hydrophilic sites are major contributors in the water uptake mechanism.

As the degree of cross linking, scissioning (availability of free volume), changes in molecular weight, hydrophilic sites available, and porosity is different in all the samples due to various plasma parameters, the sensitivity shows wide variations. The sensitivity is also not uniform throughout the RH range being measured; this is due to the fact that the percentage of all these factors responsible for water uptake at various depths in the polymer could be different for different samples which in turn are plasma parameter dependent.

Response time of plasma treated films:

The time interval in min between 90% and 10% of the maximum capacitance (at saturation) value is defined as response time and is calculated from Capacitance Vs time graph. Fig 3.14 shows the response curves of the plasma treated films treated at 30 Watt for 5 min since this film gave maximum sensitivity.

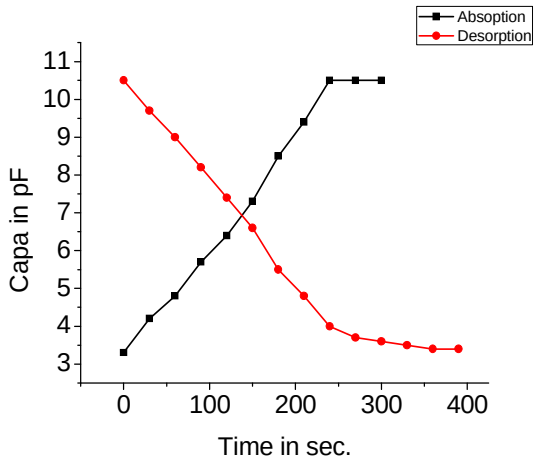

Fig-3.14: Response and recovery time of film.

The response time for sample plasma treated at 30watt for 5 minutes is 6 min and recovery time of same sample was 7 minutes which is better than 7 to 14 min. reported by Dabhade et.al.[10]. Kulwiki [11] has suggested that typical equilibration time for polymer based sensors to be around 15 min which he has further set as programmed time for sensor characterization measurement. The observed time in the present work 6 min and 7 minute is of similar order suggested by Kulwiki [11].

3.2.5 Hysteresis:

Hysteresis defined as the maximum difference in the two outputs (increasing and decreasing cycle) at the same RH level. It is observed to be nearly 4% for plasma treated sample at 30 watt. The hysteresis in the response at lower RH is a result of slow desorption of water from the surface of PMMA. At higher humidity, the condensation occurs and forms a cluster over the surface of the film, which attributes to hysteresis. Here, hysteresis for plasma treated sample at

30 watt for 5 minutes film is shown in fig.3.15. For other films also hysteresis of the order of 4 to 7% was observed.

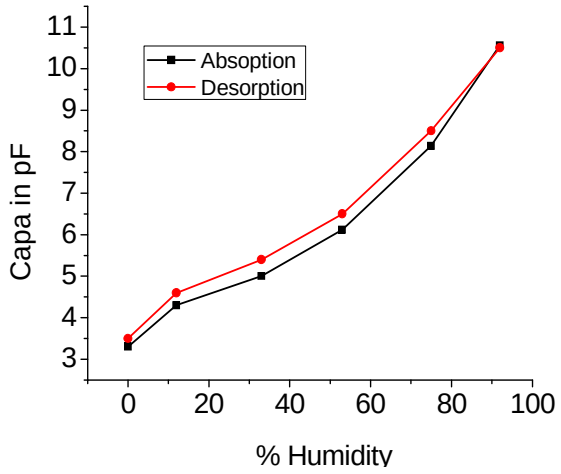

Fig-3.15: Hysteresis result for 30W/5 min. film

During increase in the %RH the response increase in RH is slow and the change in capacitance is not much as the humidity is also low. After 50 %RH the sensor starts to show the variation in capacitance gradually up to about 75 %RH when the sensor response is fast. The sensors do not show the initial capacitance as the sensors were removed from the RH chamber after the maximum RH was reached and as they require more to equilibrate the initial capacitance can only be retained after the sensor is kept at maximum RH for more than 15 min. Due to this cycle the sensor shows a large hysteresis in the static mode of RH sensing.

Hysteresis is related to film thickness, since measurements are performed using fixed time intervals and thin films equilibrate faster than thicker films. Other contributions to differences in capacitance include process variations which lead to differences in dielectric permittivity of the material and contact problem.

Another reason for large variation in hysteresis from sample to sample can also be attributed to the fact that the samples have a considerable response time therefore during the dynamic response the sensor does not immediately respond to the changes in humidity which leads to hysteresis. According to Andrew *et al* [23] hysteresis in polymer films is caused in part by the mechanical relaxation of the polymer when the water is sorbed. Relaxation to the low-RH state is not instantaneous, so removal of water lowers the cohesive energy density of the polymer, requiring a larger difference in chemical potential between water in the ambient and water in the polymer to remove the water. Addition of cross-links to the polymer will increase the dimensional stability by limiting the movement of polymer chains in any relaxation that occurs. Thus hysteresis is expected to be lower in the cross-linked PMMA.

3.3: Plasma Polymerized PMMA as humidity sensor- Results and Discussion

3.3.1: Introduction

This section describes the results on monomer purification, deposition of plasma polymerized MMA (PPMMA) films at various system parameters and characterization of the deposited films by SEM, FTIR and RH sensing. The results are discussed in view of the available literature.

3.3.2: IR Analysis of the Purified Monomer:

In the commercially available monomer (MMA) very small percentage of quinone (150 ppm) is added as inhibitor to prevent polymerization. The monomer was distilled using the procedure described in section 2.3.3. The IR spectra of undistilled and distilled MMA are shown in Fig. 3.16 (i) and (ii). Change observed in the spectrum indicates that the monomer is properly distilled. All the peaks observed in conventional PMMA (see section 3.1.3) are observed in distilled monomer. Standard IR spectrum is taken from Aldrich Library [32] and compared with the results obtained. It confirms the purification of the monomer. Further no peak is observed at 3450 cm^{-1} which corresponds to OH stretching, indicating the absence of moisture in the monomer.

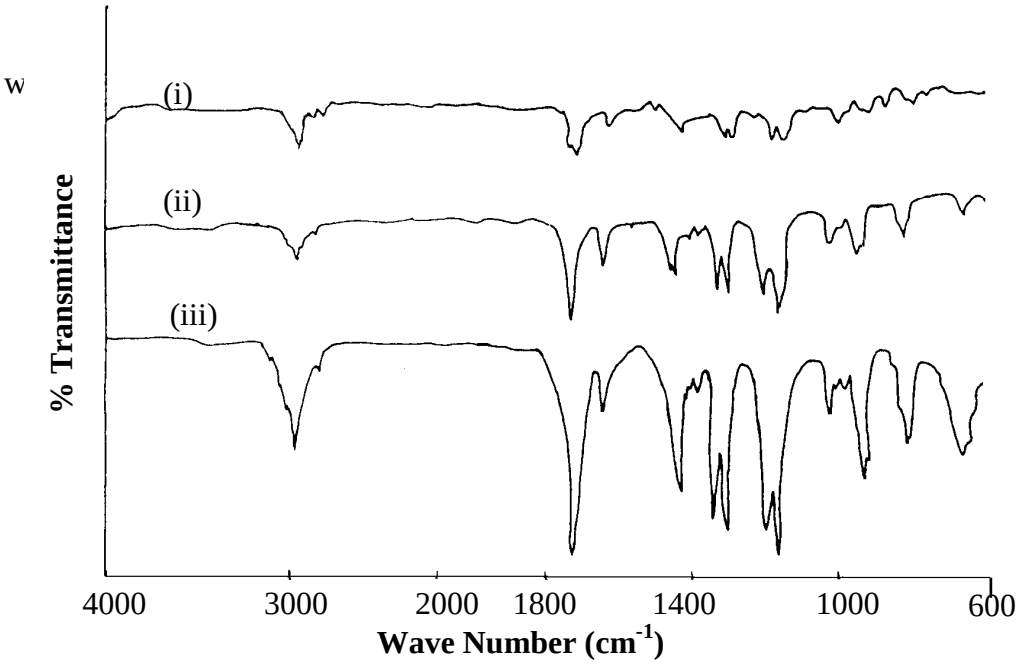

Fig-3.16: IR spectra of MMA (i) Un distilled (ii) Distilled (iii) Standard Aldrich

This purified monomer is then used as a starting material for the plasma polymerization of the methyl methacrylate [10].

3.3.3 Synthesis of Plasma Polymer Films

It is observed from the literature [33] that the main variable parameters for plasma polymerization are the monomer flow rate, carrier gas flow rate, system pressure, input RF power and reactor dimensions. Hattori *et al* [34] carried out plasma polymerization of MMA in an inductively coupled, tubular type reactor at system pressure of 1 Torr, argon flow rate of 40 cc/min., MMA flow rate of 3 cc/min and the input power of 20 W. Gangal *et al* [35] had carried out depositions of PPMMA in a reactor similar to the one used by Hattori where they varied the pressure from 0.2 Torr to about 1 Torr. The typical argon flow rate was 50cc/min and the monomer flow rate was varied between 10-50 cc/min. The input power used was from
30 to 60 W.

Using above parameters as guidelines, depositions in the present work were carried out in a similar inductively coupled tubular type reactor [33,34]. A large number of experiments were carried out in order to get deposition of plasma polymerized films having same chemical structure. Many experiments with various combinations of power, pressure and flow rates were carried out to deposit the films, for RH sensing.

The typical conditions used were in the ranges, argon flow rate between 5-15 cc/min, MMA flow rate 20-30 cc/min; pressure 0.1-0.4 mbar and the RF power 10-45 W. The time of deposition was kept constant at 1 hour to get sufficiently thick films. Plasma polymerized films were formed only at certain combinations inthe above givenranges of parameters.

The oily films were obtained at relatively high pressure (0.4 mbar). The RF power used during these depositions was also considerably higher i.e. 60 W. Such high power was necessary to obtain the glow in the polymerization region at high pressure. At lower discharge power and pressure of 0.4 mbar, the glow does not extend to the substrate holder, which is necessary for the polymer deposition on to the substrate. These were not used for further characterization.

Formations of oily films indicate that oligomers are formed at high system pressure and high RF power. This observation is similar to the one reported by Duval and Theoret [36], they suggest that at

high reaction pressure, (> 1 Torr) there is sufficient monomer on the surface of the substrate to dissolve the reaction chain and limits the degree of polymerization. This leads to the formation of low molecular weight oily products. This observation implies that fragmentation of the monomer may be taking place.

Liepins and Sakaoku [37] carried out plasma polymerization experiments in an inductively coupled plasma in the pressure range between 0.6 to 3 Torr. They have reported that polymeric powders are formed nearly exclusively in an inductively coupled RF reactor where organic vapor is introduced in the plasma of carrier gas. They have further reported that powdery film formation at higher pressures also depends upon the structure of the monomer used. Methyl methacrylate however lies in the list of monomers which do not form powdery films[37]. Formation of oily films and not powdery films at higher pressures in all our experiments is supported by this result. Duval and Theoret [36] found that high molecular weight is favored by low pressure and high power. They concluded that at low pressure the surfaces are monomer deficient and the reactive species continue to grow yielding high molecular weight solid products. These observations were later verified by Kobayashi *et al* [38].

Films formed at pressure 0.2 mbar, argon flow rate (5cc/min), MMA flow rate (25 cc/min) and time of deposition (1 h) are the fixed parameters with different RF power from 10 to 45watt were subjected for further investigations. All the films were reproducible when similar parameters given above were maintained.

3.3.4: Characterization of the plasma polymerized films:

3.3.4.1 FTIR:

Three samples (one silicon and two IDT substrates) were deposited at each power level in the range 10 to 45W. Samples deposited on silicon are used for FTIR measurement and remaining two samples were used for humidity measurement. Thickness was measured using talystep method (Taylor Hobson, Fukuoka, Japan). It was found to vary from 150 to 250nm in the power range used. The films deposited on the silicon substrates showed color striations on the surface, which is created because of the variations on the thickness deposited on the substrate. FTIR spectra of the films deposited under various power conditions are taken. The FTIR spectrum of conventional PMMA is used for comparison. All the absorption peaks of PMMA are also observed in the PPMMA.

The representative IR spectrum of the films is shown in Fig-3.17.

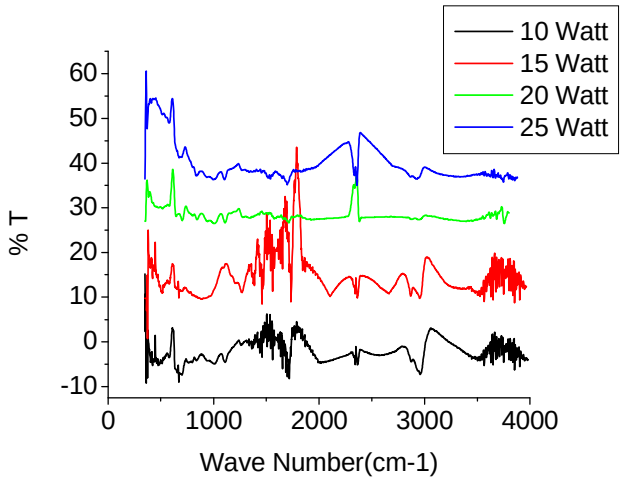

Fig-3.17: FTIR spectra of PPMMA samples

Table-3.4 IR absorption peaks for films at different RF power (10 to 45W)

Wave number conventional PMMA cm^{-1}	Peak assignments	Absorption peaks obtained for PPMMA films deposited at different power levels cm^{-1}							
		10 Watt	15 Watt	20 Watt	25 Watt	30 Watt	35 Watt	40 Watt	45 Watt
3450	O-H stretch	-	-	-	-	-	3475.5	3480	3454
2950	CH_2 stretch	2958	2949.8	2949.8	2951.6	2936.4	2951	2956	2962
1730	carbonyl group	1715	1742.3	1711	1710	1705	1724	1742	1729
1640	C=C stretch	1634	1646.4	1658	-	-	-	-	-
1430	CH bend in CH_2 group	1435	1460.7	1435	-	-	1456	1429.5	1454
1370	CH bend in CH_3 groups	1370	1384	1365.6	1377	1378	1377	1372	1378
1140	C-O stretch	1111.5	1154	1110	1104.5	1110	1124.5	1160	1161

The peak positions are shown in Table3.4. Column 1 of Table 1 gives the FTIR absorption peaks of conventional PMMA. Column 2 gives the corresponding assignments. Remaining 8 columns give the absorption peaks obtained of the films deposited under different power conditions. As can be seen from the table the peaks observed in PPMMA films are near to the ones in conventional PMMA but are different in films deposited under different power conditions.

As shown in the table, for 10W to 30W all the peaks are very close to the standard peak values of PMMA except the peak at 3450 cm^{-1}. As this peak is not present, it indicates absence of moisture in monomer at the time of distillation and so complete loss of the O-H stretch at 3450 cm^{-1}.

The IR spectrum shows absorption peaks at wave numbers 3450 cm^{-1} due to OH stretch, 2950 cm^{-1} due to CH_2 stretch, 1730 cm^{-1} due to carbonyl group, 1430 cm^{-1} for CH bend in CH_2 group, 1370 cm^{-1} for CH bend in CH_3 groups and 1140 cm^{-1} due to ester group. These peaks are all at similar wave numbers compared to conventional PMMA (refer to Table-(3.3.1). The only difference is that the absorption peaks are broader than the conventional PMMA and seem to be merged indicating the formation of cross linked polymer [23] The IR analysis thus confirms the formation of the polymer.

These results are well in agreement with the results of Tobin et al [39], wherein they have found that the index of refraction 'n' of PPMMA films is inversely proportional to the deposition pressure at constant plasma power. The density is presumed to increase with the increasing 'n'. They have inferred that films produced at higher pressures can be termed as 'low-density' and those deposited at lower pressures as 'high-density' films.

In the present case the films deposited at lower pressure of 0.2 mbar could also be of high density in nature as they showed broadening and merger of absorption peaks in the FITR spectra suggesting cross linking. Therefore we can further say that more cross linking may lead to higher density of the PPMMA.

It is reported by Suzuki *et al* [40], that the humidity sensor that contains well designed carbonyl group as adsorption sites will respond directly to RH. As is evident from the FTIR spectra, all the films deposited in the present work contain well defined carbonyl group at 1730 cm^{-1} and therefore are supposed to be sensitive to humidity. The intensity of the carbonyl peak is however varying depending on the polymerization conditions and degree of cross linking. For 35 and 45W films, the peaks obtained are very much close to the standard PMMA peak value.

From 25W to 45W, all the peaks are absent at 1640 cm^{-1} of the C=C stretching vibration, probably due to high wattage.

The absorption peaks of 15, 40 and 45W especially in the range 1000-1200 cm^{-1} are seen to be broader indicating the presence of cross links. The band due to ester C-O stretching mode at 1140 cm^{-1} is broad in 15, 40 and 45W samples which confirms characteristic of cross linked polymer. In the present work the decrease in the absorption peak followed by broadening for some samples is more attributed to cross linking and the extent of cross linking is different for different samples [10].

Summing up the work on variation in power at fixed time, one can say that in the present work the decrease in the absorption peak followed by broadening for samples 15W, 40W, and 45W is more attributed to cross linking. Out of these eight samples, from FTIR table it is observed that most of the peaks for 35W sample are close to standard peaks. But we are not getting peak near 1640 cm^{-1}. The reason is to be analyzed.

3.3.5: Humidity Response of the plasma polymerized Films:

Humidity response of the plasma polymerized films is measured in terms of change in capacitance at 5000 Hz using LCR meter (Agilent 4284A). Fig.3.3.3 shows the change in capacitance with respect to humidity of all samples formed from 10 watt to 45 watt power.

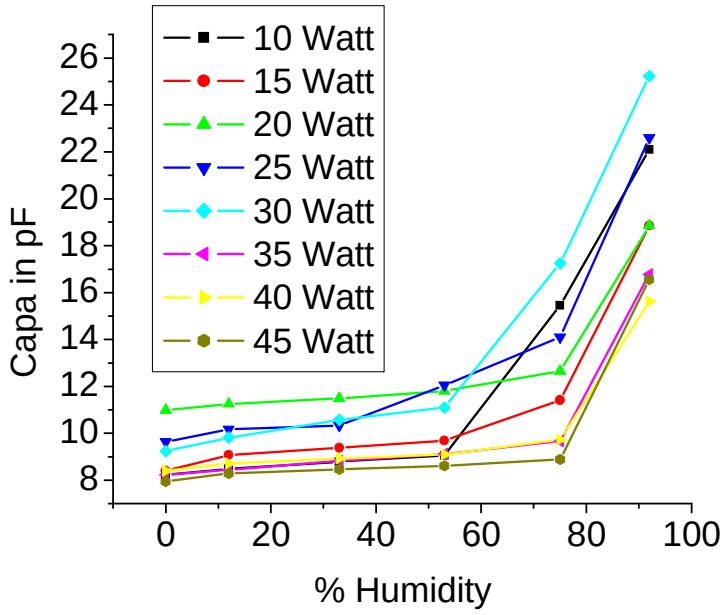

Fig- 3.18: Capacitance change w.r.t. humidity for plasma polymerized samples.

As seen from fig-3.18, the variation of capacitance is different in different humidity regions for a particular film and these humidity ranges vary from film to film. Broadly speaking there are two regions, in lower humidity region(around 12-53%) the sensitivity is low and at higher humidity region (above around 53%) the sensitivity increases suddenly. The reason of this increase probably lies in the structure of the films and the readings are taken at the room temperature and room environment. However the detailed investigation are yet to be done. Table 3.5 gives the values of sensitivities in two different humidity ranges for different films.

Table 3.5 Sensitivity of PPMMA films.

Plasma power	Low humidity region	High humidity region
10	0.016	0.335
15	0.024	0.235
20	0.015	0.181
25	0.045	0.27
30	0.035	0.362
35	0.017	0.196
40	0.013	0.167
45	0.013	0.204

Higher sensitivity of the PPMMA films is interpreted as a larger concentration of sorbed water caused by a higher free volume in the PPMMA film. In the present case the cross linked polymer can be regarded as a high molecular weight material accommodating more water in the network structure.
The variation of sensitivity from film to film is attributed to the difference in the free volume in the sensor films, presence and intensity of the carbonyl group and the molecular topology of the films [23].

While explaining the results obtained on PPMMA films deposited in parallel plate plasma system Andrew et al[23] have used a duel-state model of gas sorption. In this model, sorbed gas molecules are interpreted as being part of one of two populations in the polymer, a Henrian population of molecules sorbed by ordinary dissolution mechanisms in the polymer and Langmuir population residing in the free volume within the polymer. Because the PPMMA and PMMA films can be regarded as basically identical as PPMMA and PMMA have been formed from the same basic monomer-MMA, the concentration of water sorbed in the Henrian sites can be viewed as being the same in these films. The difference in the sensitivity of PPMMA films compared to PMMA films is regarded to be due to the adsorbed water in the Langmuir population. Higher sensitivity of the PPMMA films relative to the PMMA films is interpreted as a larger concentration of sorbed water caused by a higher free volume in the PPMMA film. The PPMMA films thus have low density, though they are cross-linked, which varies as the deposition conditions. The films deposited under different deposition conditions have shown

different sensitivity to RH. The differences in the dielectric behavior of the PMMA and PPMMA films reveal details of the difference in structures between the two materials.

Andrew et al [23] have reported the sensitivity of PPMMA films to relative humidity. The films were deposited in parallel plate reactor. However, their work show sensitivity lower than PMMA which is reported to be due to the high density of cross linking implying less free volume within which water will be adsorbed in Langmuir population.

Turner D. T. [31] has reported that samples of PMMA of low molecular weight may take up less water than samples of normally high molecular weight. Turner has also concluded that, from the density changes accompanying water sorption it is estimated that a low molecular weight sample accommodated only 15% water in microvoids, as compared with 50% for samples of high molecular weight. In the present case the cross linked polymer can be regarded as a high molecular weight material accommodating more water in the network structure. In linear glassy polymers closer molecular packing may be the cause of the material accommodating lesser amount of water.

The difference in the obtained density of cross-linking in the present work as compared to the reported work by Andrew et al [23] may also be attributed to the difference in the reactor used. In the present study we have used an inductively coupled reactor.

3.3.6 Response and recovery Time of plasma polymerized films film:

To determine the response and recovery time of the sensor, the graph of change in resistance Vs time is plotted. (Fig. 3.19) From this graph the response and recovery time is calculated. Response time of the film is 118 sec and recovery time is 63 sec which is slower than reported value of 30sec [23]**.** The reason of this increase probably lies in the structure of the films. Here we tried all the films but we got good result for 35W film.

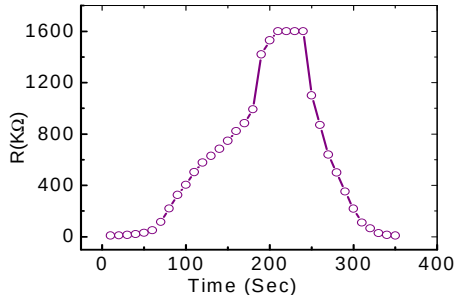

Fig-3.19: Variation of Resistance with time for 75% humidity

3.3.7 Hysteresis of plasma polymerized films:

Hysteresis defined as the maximum difference in the two outputs (increasing and decreasing cycle) at the same RH level. It is observed to be nearly 2% for plasma polymerized samples at 35 watt. The hysteresis in the response at lower RH is a result of slow desorption of the water from the surface of PMMA. At higher humidity, the condensation occurs and forms a cluster over the surface of the film, which attributes to hysteresis. Here, hysteresis for plasma polymerized sample at 35 watt film is shown in fig-3.20. For other films also hysteresis of the order of 2 to 5% was observed. Representative graph of only one sample is given.

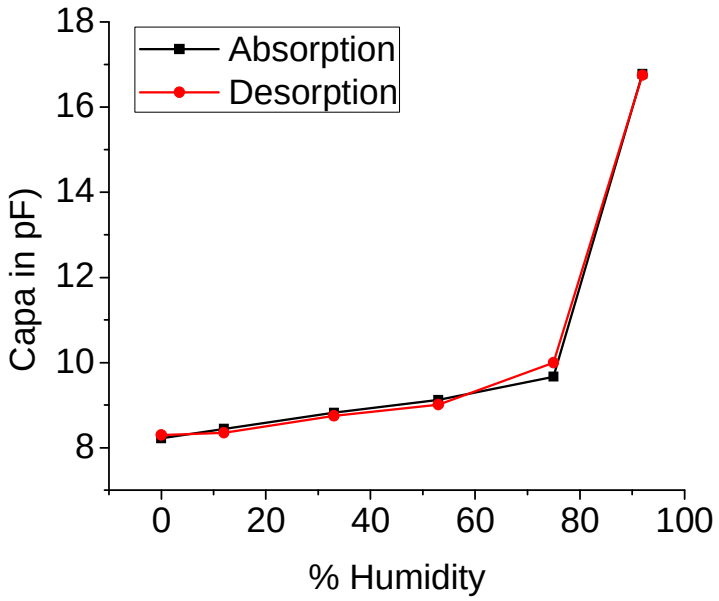

Fig-3.20: Hysteresis result for 30W film

3.4 Conclusion:

Comparative study of spin coated, plasma treated and plasma polymerization films as humidity sensor

Parameters	Spin Coated Film	Plasma Treated Film	Plasma Polymerized Film
Response time	10 minutes	6 minutes	118 sec
Recovery Time	12 minutes	7 minutes	63 sec
Hysteresis	1%	4%	2%
Repeatability	Good	Good	Good
Reproducibility	Good	Good	Not good
Ease of Construction	Very easy	Easy	Depends on system

From above table, it is observed that plasma polymerization system can be preferred as the sensor formed by that system has the minimum response and recovery time. But on the other side to form a film of 2000 Angstrom thickness, the system requires minimum one hour. Also depending upon the type of system, its reproducibility also changes. So it is better to use a method by virtue of which good sensor can be built in minimum time interval. So spin coating is preferred. Its response time is large but by using some surface modification method it is possible to modify its surface to get quick response of the film. One of the methods is plasma treatment.

References:

1. W. W. Flack, D. S. Soong, A. T. Bell, D. W. Hess, J. Appl. Phys. **56**, 1199**(1984).**
2. A. G. Emslie, F. T. Bonner, L. G. Peck, J. Appl. Phys. **29**, 858**(1957).**
3. D. J. Meyerhofer, Appl. Phys. **49** 3993**(1978).**
4. C. Walsh, E. I. Franses, Thin Solid Films 429, 71**(2003).**
5. D. E. Bornside, C. W. Macosco, L. E. Scriven, J. Appl. Phys. 66, 5185**(1989).**
6. D. E. Bornside, R. A. Brown, P. W. Ackmann J. R. Frank, A. A. Tryb, F. T. Geyling, J .Appl.

1. Phys.,73**,** 585**(1993).**

7. Silversteen RM and Webster FX, Spectroscopic Identification of organic compounds,Wiley,

2. New York, (**2002**).

8. B. Schneider; J. Stokr; P. Schmidt; M. Mihailov; S. Dirlikov; and N. Peeva; *Polym* .20 705**(1979)**.
9. P.R. Story, D.W. Galipeau, R.D. Mileham, Sensors and Actuators B 24-25 681-685**(1995)**.
10. R.V.Dabhade, Ph.D. Thesis, University of Pune; **(2002).**
11. B. Kulwicki, J. Am. Ceram. Soc., 74 -4 **(1991)** 697.
12. D. T. Turner; *Polym.*, 28 **(1987)** 293.
13. Flamm, D. L.; Donnelly, V. M. Plasma Chem Plasma Process (1981), 1, 317.
14. Gerenser, L. J. J Adhes Sci Technol (1987), 1, 303.
15. Occhiello, E.; Garbassi F. In International Encyclopedia of Composites; Lee, S. M., Ed.; Wiley: New York, (1991); Vol.5, p 390.
16. Onyiriuka, E. C.; Hersh, L. S.; Hertel, W. J. Colloid Interface Sci (1991), 144, 98.
17. Sutherland, I.; Brewis, D. M.; Heath, R. J.; Sheng, E. Surf Interface Anal (1991), 17, 507.
18. Bather, K. H.; Hermann, U. Surf Coat Technol (1995), 74, 670.
19. Astumian, R. D.; Schelly, Z. A. J Am Chem Soc (1984), 106, 304.
20. Dwight, D. W.; Riggs, W. M. J Colloid Interface Sci (1974), 47, 650.
21. A. Grill; Cold plasma in Materials Fabrication- from Fundamentals to Applications; IEEE Press, New York; (1994).
22. F. Denes; R. A. Young; M. Sarmadi; J. of Photopolymer Sci. and Technol. 10 (1997) 112.
23. R. K. Andrew; Ralston; J. A. Tobin; S. S. Bajikar; D. D. Denton; *Sens. & Actu. B* 22 ,(1994), 139.
24. B. A. Kuruvilla; M. Zambare; S. Gosavi; S. Gorwadkar; A. Datta; S. A. Gangal; and S. K. Kulkarni; J. of Polym. Sci. Polym. Chem. Ed. 32 (1994) 2275.

25. T. G. Vargo; and J. A. Gardella; *J. of Polym. Sci. Polym Chem. Ed.* 27 (1989) 1267.
26. M. Matsuguchi; M. Shinmoto; Y. Sadaoka; T. Kuroiwa; Y. Sakai; *Sens. & Actu. B* 34 (1996) 349.
27. U. Schulz; P. Munzert; and N. Kaiser; *Surf. & Coatings Technol.* 142-144 (2001) 507.
28. J. O. Choi; and J. C. Corelli; J. P. Silverman; and H. Bakhrun; *J. Vac. Sci. Technol.* B-6 **(1988)** 2286.

29. T. G. Vargo; and J. A. Gardella; *J. of Polym. Sci. Polym Chem. Ed.* 27 **(1989)** 1267.
30. D. T. Turner; *Polym.* 23 **(1982)** 197.
31. D. T. Turner; *Polym.* 28 **(1987)** 293.
32. C. J. Poucher; The Aldrich Library of IR Spectra; Aldrich Chemicals Company Inc., Milwaukee, US.
33. M. Zambare; "Plasma Synthesis of electron beam resist, their Characterization and Plasma Diagnostic by Langmuir probe" Ph.D. Thesis, University of Pune; (1996).
34. S. Hattori; J. Tamano; m. yamada; M. Ieda;S. Morita; K. Yoneda and S. Ishibashi; *Thin Solid Films* 83 (1981) 189.
35. S.A. Gangal; M. Hori; S. Morita; and S. Hattori; *Thin Solid Films* 149 (1987) 341.
36. Duval; and Theoret; *J. Appl. Polym. Sci.* 17 (1973) 527.
37. L. R. Sakaoku; *J. Appl. Polym. Sci.* 16 (1973) 2633.
38. Kobayashi *et al J. Appl. Polym. Sci.* 18 (1973) 885.
39. J. Tobin; and D. D. Denton; *Appl. Phys. Lett.* 60-21 (1992) 2595.
40. K. Suzuki; Y. Nabeta; and T. Inuzuka; Tech Digest, 10^{th} Sensor Symp Tokyo, Japan; pp 61-64(1991).

Chapter-IV

Humidity Sensing Properties of Drop Casted PMMA Films Using Direct Optical Transmission Method

4.1 Introduction

The electrical response for humidity variations has been attributed to both chemi-sorption and capillary condensation of water molecules [1]. Over the years, different sensing methods have been developed by measuring a variety of humidity-related parameters [2]. Each of these has unique advantages and limitations and is suitable only in certain applications. The range of applications in which humidity measurements are needed is endless and is increasing with time because with the advancement of technology new information is required on the effects of humidity on quality and cost the product as well as safety, comfort, and health of the human beings. The conventional materials used for sensing humidity are electrolytic metal oxides, alumina thin films, and ceramics. [3] However, polymers are identified as good candidates for practical applications because High sensitivity, Low cost, Simple fabrication technique. There is a wide choice of molecular structures for improving their properties. However there are shortcomings of polymer's e.g. low stability at high humidity, too high impedance at low humidity and drafting etc. To overcome these problems some techniques are developed such as grafting, cross linking and embedding of nanoparticles etc.

Polymers are having two main properties; they (i) act as surface capping agents & (ii) provides matrix to disperse nanoparticles. They are compatible with oxides and ceramics, because of their low cost, flexibility, light weight, and easy processibility. They can be used at room temperature. [4, 5] Various polymers have been used to fabricate humidity sensors. From their basic principles, they are classified into two categories based on (1) changes in the electrical properties of the materials due to the absorption of water vapor and (2) gravimetric changes in the materials after absorption of water vapor. The first category is divided into two types: -resistive type and capacitive type. Generally hydrophilic polymers are used for resistance type humidity sensors, whereas hydrophobic polymers are preferred for the capacitance type [6]. Nowadays, a variety of polymers doped with suitable molecules or dyes

are being used in optical humidity sensing applications [7]. Based on the changes in electrical or optical properties, different humidity sensors are popularly studied.

Different polymers like PANI, PVA, PVP and PPMMA in neat or doped with various acids or mNA and with nano-metal polymer composites are reported for humidity sensing [8-14]. Sensors based on evanescent waves are well reported [15-20]. In those planar optical wave guide based and plastic optical wave guide based are well studied. Another simple but the most sensitive optical method reported is direct transmission of laser beam through the humidity sensitive film [5,18] The method is applicable only for the materials which are optically transparent to the laser beam used unlike that of optical waveguides, which are applicable to any material, that can be in the form of a film and works as an optical clad .

PMMA is reported as a humidity sensitive material based on its electrical properties. [21].To the best of our knowledge it is for the first time is evaluated in the form of drop casted films for their Humidity sensitive behavior using Direct Optical Transmission Method. Characterization of the deposited films is done by SEM, FTIR.

4.2.Characterization of Material :

The drop casted films having 1, 2,3 and 4 drops denoted as A, B, C, and D respectively, were characterized by SEM and FTIR in the presence of different percentage of Relative Humidity**.**

4.2.1 SEM:

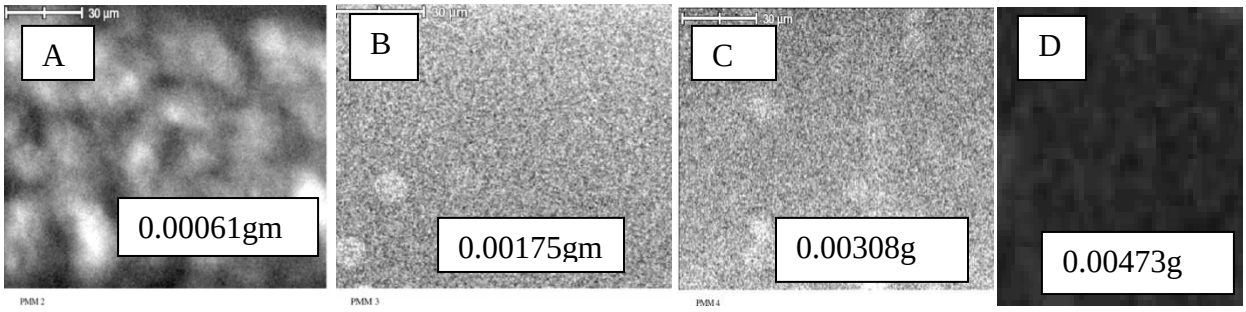

Fig. 4.1 SEM pictures of A,B,C,D films.

The SEM pictures show uniformity of the film surface. For the layer one (A Type), there are bigger voids. The number of surface sites appears to be small in number. One can expect small contribution from surface and intra grain sites. The B type sensors show large number of grains with micro voids. The C type have more number of micro voids than those in type B while the D type has agglomerated grains with bigger voids. The same is reflected in the sensitivity curves. The results summarized in table 4.1 are supported by SEM pictures.

4.2.2FTIR:

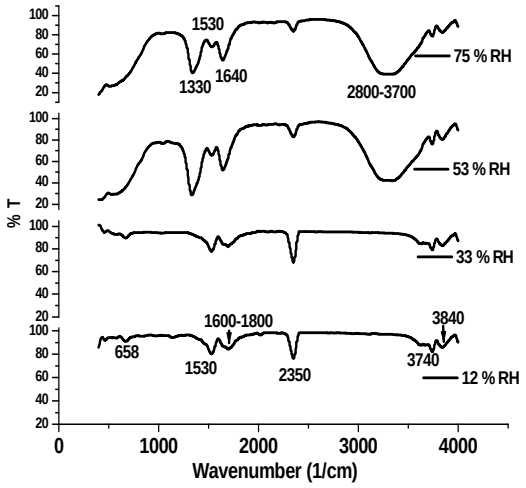

Fig.4.2 FTIR spectra with variable Relative Humidity

The FTIR spectra show the effect of humidity. With increase in humidity, the % transmission decreases and new peaks are introduced. At low humidity of about 12 % RH and 33 % RH, PMMA samples show peaks at 1530 cm^{-1} 2350 cm^{-1}, 3740 and 3840 cm^{-1} and broad band at about 1600-1800 cm^{-1}. The bond in the region 1600-1800 is due to C=O stretching. The peak at 2350 cm^{-1} is attributed to gaseous CO_2 that represents asymmetrical stretching [22, 23]. This bond is instrumental error. The weak bonds at higher wave number i.e. 3840 and 3740 might be due to attachment of OH bond with surface [24].

With increase in humidity the broad band in the region 1600-1800 cm^{-1} becomes sharp at 1640^{-1}. The broad band is introduced at $1240\text{-}1470^{-1}$ which is centered at 1330^{-1}. A strong peak in the region $1240\text{-}1470^{-1}$ is associated with the asymmetric stretching vibration of the carbonate anions [25] due to bonding between carbon and two -OH groups [26]. The strong and broad absorption band at a higher wave number $(2800\text{-}3700)^{-1}$ in the FT-IR spectra is attributed to the O-H stretching.

4.3.Optical response of PMMA:

After depositing PMMA solution on 1.0 cm x 1.0 cm borosilicate glass, film thickness was measured by using following equation,

$$P = (M/V) = (M/A*t)\ldots. (1)$$

Where ρ is the density of the PMMA (1.17 g/cc), It is assumed that the density of PMMA films is constant irrespective of the film thickness. M is the weight of the film in gm, V is the total

volume of the PMMA film in CC which is equal to the area A of the film covered (1.0cmx1.0cm size glass samples were used) and‘t’ thickness of the PMMA film.

The characteristic response of PMMA as a function of relative humidity is shown in Fig. 4.3.

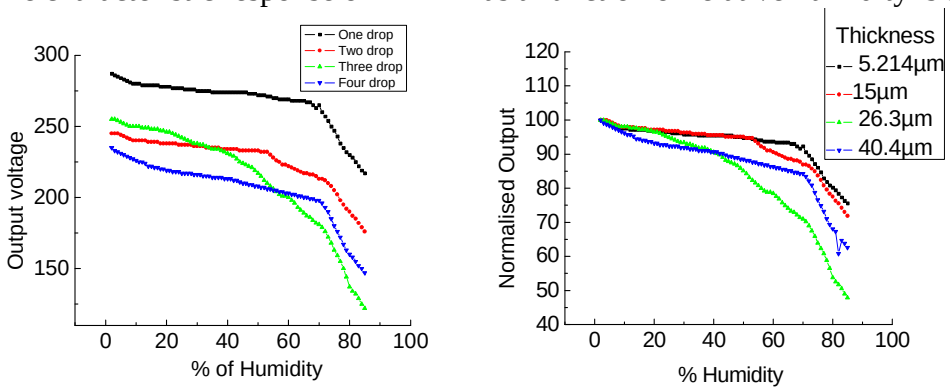

(a) **(b)**

Fig.4.3. Variation in transmitted output Vs Relative humidity for different thicknesses. (a) output (b) Normalized output

Fig. 4.3. (a) shows the typical response, i.e. the change in transmitted light intensity measured in mili volts (mv) with RH% variation for various thicknesses of PMMA films whereas (b) shows normalized response normalized with respect to the output at the lowest humidity for inter comparison. It is observed that, in general, the transmitted intensity of light decreases which effectively decreases the output voltage with increase in RH%. It is also seen that all the sensors roughly exhibit three to four regions of sensitivity. The sensitivity is lowest in region 2 for sensors A and B, in region 1 they exhibit higher sensitivity than in region 2. In the region 1 the sensitivity comes from the surface sites, whereas in region 2, it is contributed by the surface sites as well as intra grain boundaries The higher sensitivity in region 1 means that surface sites are more dominating than surface sites plus intra grain occupation of water molecules.. Sensors of A type exhibit 3 regions in their response against the Relative Humidity; third region is because of capillary condensation. The sensors of B, C, and D type exhibit 4 regions. The last region is because of capillary condensation, the second region is because of combination of surface sites plus intra grain sites. The third region is attributed to intra grain surface sites as well as capillary condensation. At the thickness of 26.3µm (C type) the maximum response is seen for regions 2, 3 and 4. The highest sensitivity is exhibited in the first region by sensors D. The region wise sensitivity is tabulated in table 4.1

Table 4.1 Sensitivity as a function of film thickness (region wise)

Layer No	Region1 %RH	sensitivity mV/RH	Region 2 %RH	Sensitivity mV/RH	Region3 %RH	sensitivity mV/RH	Region 4 %RH	Sensitivity mV/RH
1 (A)	2-9	0.43	9-67	0.22	67-85	2.77	--	--
2(B)	2-7	0.4	7-50	0.24	50-68	1	68-85	1.99
3(C)	2-28	0.5	28-45	0.81	45-69	1.95	69-85	3.12
4(D)	2-15	1	15-41	0.5	41-69	0.54	69-85	3.2

The results can be explained as follows. At a lower humidity, first region of the sensitivity spectra, water gets chemisorbed on the surface sites for few mono-layers. The thickness of these mono-layers is negligibly small in comparison with the wave length of used light used for study. Therefore the change in transmitted light intensity is negligibly small. The amount of sorbed water increases with an increase in RH. At higher humidity (second region) the water molecules get adsorbed on the surface of the already chemisorbed water layers, the water molecules are loosely bound on the film surface. Therefore they occupy intra grain sites. With the increase in number of micro-pores, the amount of sorbed water also increases. This reduces the transmitted intensity of light more than that in the first region. In the third and fourth region, because of the contribution from capillary condensation, the refractive index of the film increases with adsorption of water, the transmitted intensity is absorbed by the condensed water and light also gets scattered at higher humidity as condensed water forms a water forms a meniscus [27].

The weight of the film at room humidity and at highest humidity was measured. The gravimetric change in these weights is given as an inset in SEM pictures. The change in the weight is a measure of the porosity of the film. The porosity of the film goes on increasing as a function of thickness.

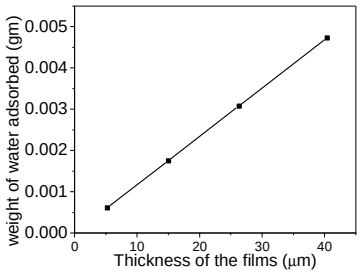

Fig. 4.4. Adsorbed water as a function of thickness of the film

The model to describe the water absorption process is explained by a model given in Figure 4.5.

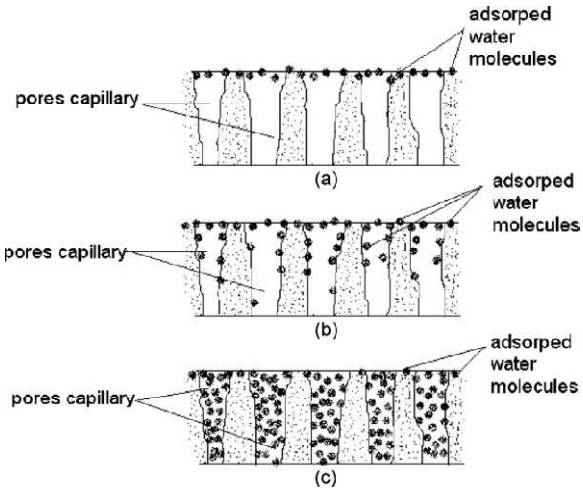

Fig. 4.5. The adsorption phenomena of water molecules on film (a) at lower humidity (surface adsorption); (b) at intermediate humidity (adsorption on capillary walls) surface sites plus intra – grain adsorption (c) at higher humidity (full capillary condensation).

The response time of the sensor is 10s and recovery time of the sensor is 20 s which are faster than the reported values of 30 seconds [28] for PMMA Fig.4.6.

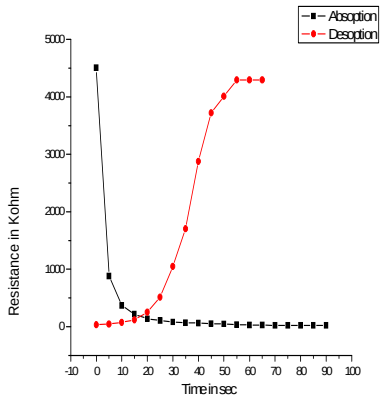

Fig.4.6 Response and Recovery Time of C film.

The fast response of the sensors can be attributed to the fast penetration of water molecules into the film. The slow recovery in the response is a result of the slow desorption process and capillary forces [29]. The maximum response is evidenced for thickness of 26.3µm which gives the maximum output voltage change (133mv) for the whole humidity range (2 to 85%RH).

The thickness of 26.3 µm gives a maximum sensitivity (109.01mV/%RH).

To understand the role of thickness of the films the percentage moisture content was measured by weighing the samples at room humidity and at highest humidity and using following equation, [30], the moisture content was calculated..

$$\textbf{Moisture (\%) =[(Wx-W}_0\textbf{)/W}_0\textbf{]*100 ….(2)}$$

The sample was exposed to 85% RH for around 10 min. and then immediately weighed (Wx). The weight of the sample was .44944gm. Then the same sample was vacuum dried and weighed again at room humidity (42%RH). The weight of the sample was 0.44931gm. The percentage moisture content was calculated using equation (2). The weight change obtained for A, B, C and D type films is shown in Fig. 4.7. The plot is linear. However the humidity sensitivity is not increasing proportionately. This is because number of sites, number of voids, their sizes are different. The height of the capillaries is also different.

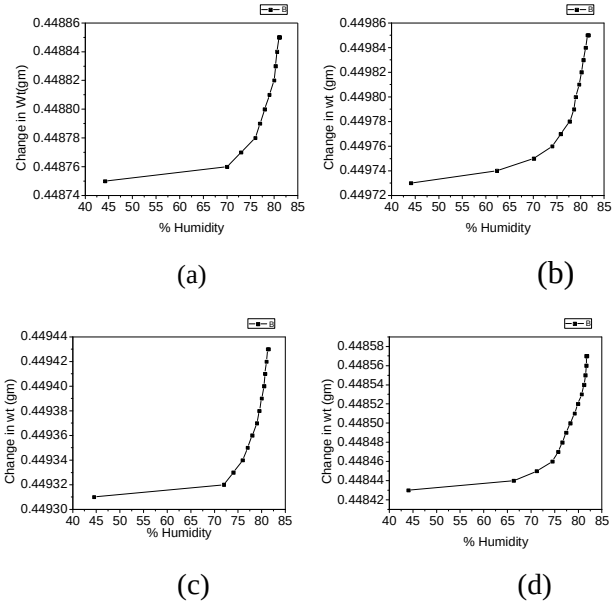

Fig 4.7 Change in weight with humidity for sample : a) A b) B c) C d) D.

It is observed that water content increases with the film thickness, which also indicates that, the porosity of the films increase with thickness. The weight is saturated with increase in humidity. By using this change of weight values, it is possible to calculate percentage moisture content in each film. The association of water increases the refractive index and effectively dielectric permittivity of the film as free air is replaced by adsorbed water [13]. This also indicated that losses at higher humidity are due to absorption as well as scattering on input intensity.

Conclusions:

In conclusion, drop casted films of PMMA were evaluated for their thickness dependent relative humidity sensing properties using direct transmission of laser light. The films show response to wide range of humidity (2 to 85%RH). The C type films show the highest sensitivity.

References

1. V.K. Khanna and R.K. Nahar ,Applied Surface Science 28 (1987) 247.
2. M. V. Fuke, Ph. D. Thesis, Submitted to Pune University, India, 2010
3. G V. Kunte, S. A Shivashankar and A M. Umarji Bull. Mater. Sci., Vol. 31, No. 6, November 2008, pp. 835.
4. Nguyen Duc Nghia and Ngo Trinh Tung Journal of Physics: Conference Series 187 (2009) 012050.
5. Kaushi Mallick,Michael J. Witcomb3, and Andre M. Strydom **,**Phys. Status Solidi A 206, No. 10 (2009) 2245.
6. John J. Steele, Michael T. Taschuk, and Michael J. Brett, IEEE SENSORS JOURNAL, vol. 8, no. 8, August 2008.
7. Prakash R. Somani, A. K, Viswanath, R. C. Aiyer, and S. Radhakrishnan. Sensors and Actuators B, 80, (2001) 141.
8. Milind Kulkarni, Annamraju Kasi Viswanath, R. C. Aiyer and P.K. Khanna: Journal of Polymer Science: Part B: Polymer Physics 43,16 (2005) 2161.
9. Madhavi V. Fuke, Anu Vijayan, Milind Kulkarni, Ranjit Hawaldar, R. C. Aiyer Talanta, 76(5) (2008) 1035.
10. Madhavi V. Fuke, Anu Vijayan, Prajakta Kanitkar. IEEE Sensors journal, 9 (6) (2009) 648.
11. Madhavi V. Fuke, Anu Vijayan, Prajakta Kanitkar, Milind Kulkarni, B. B. Kale, R. C. Journal of Materials Science: Materials in Electronics, 20 (2009), 695.
12. Madhavi V. Fuke, P.V. Adhyapak, U.P. Mulikb, D.P. Amalnerkarb, R.C. Aiyer Talanta 78 (2009) 590.
13. Y. S. Sonawane, Milind Kulkarni, B. B. Kale, R. C. Aiyer Polymers for Advanced Technology.; 18 (2007) 1.
14. Shilpa Jain, Narsimha Parvatikar, Shilpa Jain, C.M. Kanamadi, B.K.Chougule, S.V.Bhoraskar, M. V. N. Ambika Prasad. Journal of Applied Polymer Science ;103(2), (2007) 653.
15. Z.A. Ansari, R.N. Karekar, and R.C. Aiyer, Thin Solid Films 305 (1997) 330.
16. Madhavi Fuke, Ranjeet Hawaldar, D. Amalnerkar, Milind Kulkarni Sensors and Actuators B, Chemical ,129 (2008) 106.
17. Anu Vijayan, Madhavi V. Fuke, Prajakta Kanitkar, R. N. Karekar, R. C. Aiyer Sensors and Transducers, Vol. 92(5) (2008) 43.
18. Madhavi Fuke, Milind Kulkarni, B. B. Akle, R. C. Aiyer. Talanta 81(2010) 320.
19. P. V. Adhyapak, A. Vijayan, R C. Aiyer, P. K. Khanna, U. P. Mulik, D. P. Amalnerkar Int. J. Nanotech,Vol. 7 Nos. 9-12 (2010) 1054-1064
20. Parag Adhyapak, Poonam Mahapure, Rohini Aiyer, Suresh Gosavi, Uttamrao Mulik, Dinesh Amalnerkar J. Appl. Poly. Sci (In press) (2011).
21. R.V.Dabhade. Ph. D. Thesis, Submitted to Pune University, India, 2001.
22. Robert M. Silverstein, Francis X.Webster and David J.Kiemle, Spectometric identification of Organic Compound, seventh edition.
23. Erno Pretsch, Philippe Buhlmann, Martin Badertsch, Structure Determination of Organic Compounds (Tables of Spectral Data), fourth edition.

24. Valdeilson S. Braga, Jose´ A. Dias, Sı´lvia C. L. Dias and Julio L. de Macedo, Chem. Mater., 17 (2005) 690.
25. Guo-An Wang, Cheng-Chien Wang, Chuh-Yung Chen, Polymer 46 (2005) 5065**.**
26. Sanjai J. Parikh, James D. Kubicki, C. M. Johnson, Christopher L. Johnson, R. M. Hazen, D. A. Sverjensky and D. L. Sparks, Langmuir 27(5) (2011)1778.
27. S.G. Ansari, Z.A. Ansari, M.R. Kadam, R.N. Karekar, and R.C. Aiyer, Sensors & Actuators B 21, 159 (1994).
28. A. R.K. Ralston, J. A. Tobin, S. S. Bajikar, D. D. Denton**,** Sensors and Actuators B 22 , (1994) 139.
29. B. Kulwicki; J. Am. Ceram. Soc. 74 (1991) 697**.**
30. Yang M R and Chen K S, Sens. Actuators B 49 (1998) 240.

Chapter- V
Future Scope

We would like to emphasis that plasma treated polymers can be used as alternative materials for RH sensing, where the desired characteristics can be imparted to the polymer surface by setting the optimum power and treatment time. We feel a lot of work in this area needs to be taken up for example various gases can be tried for this purpose including oxygen as the C/O ratio is and important factor in determining the sensitivity of the PMMA to RH.

In the plasma polymerization process to the variation in the carrier gas for example oxygen, could be tried for the incorporation of certain species in the polymer chain and then the RH response could be studied.

Thus we feel synthesis of polymers with varied properties via plasma polymerization route using various gases or plasma treatments of polymers using various gases for RH sensing or for any other purpose for that matter remains to be an exciting field for future investigations.

Surface study of the material using different characterization techniques should be done. Accordingly its sensitivity to RH should be determined.

Publications

International Journal

1. **"Comparative study of Irradiated and Annealed ZnO Thin Films for Room Temperature Ammonia Gas Sensing."**Abhijeet Kshirsagar, Jagdish Deshpande, D. K. Avasthi, T. M. Bhave, S.A. Gangal; Journal of Sensors and Transducers; Special issue on Chemical Sensors and Biosensors, Vol. 88, Issue 2, February 2008, pp.40-46..

Papers presented in conference

1. **"Ammonia Gas Sensor using ZnO Thin Films."**
   Abhijeet Kshirsagar, A. B. Joshi, J. D. Deshpande, S. A. Gangal; National seminar on Interdisciplinary Applications of Electronics, 28th – 29th Jan 06.
2. **"Comparative Study of Irradiated and Annealed ZnO Thin Films for Room Temperature Ammonia Gas Sensing."**
   Abhijeet Kshirsagar, J. D. Deshpande, A. C. Joshi, A. B. Joshi, T. Seth, D. K.Avasthi, T. M. Bhave, S. A. Gangal; NSPTS – 11, Dept. of Electronic Science, University of Pune, 27th Feb to 1st Mar 06.
3. **"Development of Relative Humidity Sensor Using PMMA".**
   J. D. Deshpande, Jamkar P.P, Adhi A.A, Gangal S.A. NSPTS – 12, B.A.R.C.,Mumbai, 7th Mar to 9th Mar 07.
4. **"Micro- Sensor Fabrication Using Silicon Bulk-Micromachining"**.
   A.B. Joshi, J.D. Deshpande, K.Natarajan, S.A. Gangal. NSPTS–13, University of Pune, 3rd Mar 08 to 5th Mar 08.
5. **"Application of etched latent tracks in flexible polyimide foils for Humidity sensing".**
   Kale S.P, J. D. Deshpande, Bhave T.M, Gangal S.A. NSPTS–13, University of Pune, 3rd Mar 08 to 5th Mar 08.
6. **"Ammonia Gas Sensing Properties of Polypyrrole Thin Film at Room Temperature."**
   Joshi A.C., Padma N., Aswal D. K., J. D. Deshpande, Kshirsagar A. V., Gangal S.A., Gupta S. K. NSPTS – 13, University of Pune, 28thFeb 08 to 5th Mar 08.
7. **"Relative Humidity Sensor Using Plasma Polymerized Methyl Methacrylate (PPMMA)."**
   J. D. Deshpande, Kshirsagar A. V., Joshi A. B., Gosavi S. W, Gangal S.A. NSPTS–13, University of Pune, 3rd Mar 08 to 5th Mar 08.